MICROCOPY RESOLUTION TEST CHART
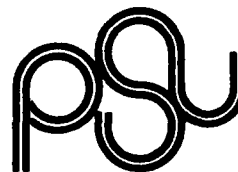
NATIONAL BUREAU OF STANDARDS-1963-A

January 24, 1983

PORTLAND
STATE
UNIVERSITY
p o. box 751
portland, oregon
97207
503/229-4290

school of
engineering
and applied
science

department of
mechanical
engineering

Dr. H. S. Pilloff
Office of Naval Research
Physics Program (Code 421)
800 N. Quincy St.
Arlington, VA 22217

Dear Dr. Pilloff:

Enclosed is a final report concerning my research on a "Fast Discharge Excitation Source for Ultraviolet/Visible Lasers." It summarizes the work and results obtained to date in the original and renewal contract phases of the study.

In the second phase we proposed incorporating our excitation source into an excimer laser. As our work progressed in that phase, it became clear that much more development and optimization study was necessary on the pulser circuit itself before incorporation into an actual laser. Some of the needs for further modification and testing of the pulser prototype before use in a laser are noted in the recommendations section of Part I of the Final Report. Of special importance is the need for better switching to pulse charge the transmission line and also a need for a better current measurement method. Both were studied in detail in the second contractual phase of this project, and it was recognized that even further study and testing was necessary.
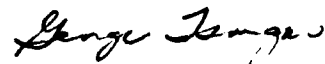
Furthermore, examination of the test results suggested the need for computer modeling of the excitation system and its operation to determine its capabilities, limitations, and further research needs prior to full scale use in a laser. Thus, preliminary modeling was undertaken with good success. It became obvious that the modeling should be continued and expanded, but that was beyond the scope of the present study. The excitation system was, therefore, not incorporated into an actual laser as originally proposed.

Because of the way the project developed, the results are presented in the Final Report in two parts. Part I presents the background on the study as well as the details of the laboratory experiments. Part II describes the computer modeling. Any further future work along these lines should involve concurrent expansion of both aspects of this project.

Finally, let me thank you for your willingness to fund this project. I still believe it has worthwhile potential, although much more study is clearly needed prior to actual use in a laser. I also want to apologize for the incredible delay in finalizing this report. I appreciate your patience.

Sincerely,

George A. Tsongas
Professor of Mechanical Engineering

wh
Enclosures

LIQUID TRANSMISSION LINE PULSER CIRCUIT

FOR LASER EXCITATION

Final Report

for

the Office of Naval Research

under

Contract N00014-77-C-0589

Submitted by

by

George A. Tsongas

Mechanical Engineering Department

Portland State University

Portland, OR 97207

January 1983

ABSTRACT

The subject of this report is the study of liquid dielectric
transmission lines and their potential application as a reliable
excitation source in high power, high repetition rate laser designs.
The design problems associated with the construction of high repetition
rate (khz), short wavelength lasers have been reviewed and the major
shortcomings of conventional electrical driving circuits identified.
The identification of these shortcomings and a review of the available
literature on electrical circuits for various types of lasers suggested
that liquid dielectrics and transmission lines could potentially have
significant advantages over more conventional circuitry used in high
repetition rate, short wavelength lasers. Use of this excitation source
for laser pumping is expected to result in major performance improvements
with regard to high average power, high repetition rate operation, high
wall-plug efficiency, and high reliability.

The pump source consists essentially of a fast and highly reliable
electrical driving or pulse forming network coupled either to a series of
sparks for optical pumping or to a simple discharge for direct gas
excitation. The key component is a liquid-filled transmission line which
operates at high repetition rates ($\sim 10^3$ Hz) and provides reliable energy
storage and pulse forming. Unlike capacitor discharge systems, liquid-
filled transmission lines characteristically provide a rectangular current
pulse whose duration is selectable. With proper design the transmission
line impedance can be varied to match that of the gas load and hence

ii

provide excellent energy transfer efficiency. The fast risetime of the
rectangular current pulse also reduces the energy wasted prior to achieving
threshold current levels; moreover, it provides a constant excitation
rate which is clearly desirable for maintaining temporal gain uniformity.
In addition, liquid-filled transmission lines are self-healing and
rugged, thus providing longer lifetimes than capacitors during highly-
stressed fast pulse operation. Further, using the system under development
at PSU, extremely high repetition rates (>1 kHz) appear possible, thus
greatly facilitating the achievement of high average power lasers.

In Part I of this Final Report background on the project is given,
including a review of pulsed excitation schemes. Development of the
liquid dielectric transmission line scheme and its design is described
in detail, Laboratory tests and their results for a prototype pulser.
device are also presented. Results showed that the electrical driving
network was capable of reliably delivering high voltage, 50 nsec square
wave current pulses at repetition rates exceeding one khz. Recommendations
for further study are presented.

In Part II background and results are presented of preliminary
computer modeling of the excitation system and its operation. The purpose
of this part of the study was to help more clearly determine the pulser's
capabilities, limitations, and further research needs prior to incorporation
into an actual laser.

ACKNOWLEDGEMENT

PREFACE

The research effort presented in this report originated out of the need identified by Los Alamos Scientific Laboratories and others for a reliable, long lived, high repetition rate electrical driving network for use in various short wavelength laser excitation schemes. This work was initiated in the fall of 1975 with an extensive literature search on the electrical circuits used in electric discharge and flashlamp pumped lasers.

Initial efforts in the design stage centered on improving flashlamps used to pump dye lasers. Later these efforts were expanded to include direct electrical discharge excitation schemes as well. Review of conventional circuitry used in these types of systems identified the energy-storage capacitor as the weak-link precluding long lived, high repetition operation. Typical lifetimes for the low-inductance, high energy density capacitors used in these circuits varied from a low of 10,000 to a high of several million discharge cycles. At 1 khz repetition rates the lifetimes of these type capacitors are quickly extinguished.

A literature review of various types of gas, liquid and solid dielectrics use in capacitive energy storage schemes identified several liquids, notably glycerine, water and oil, whose electrical properties appeared favorable to the design of an electrical driving network with the desired characteristics. Liquid dielectrics were chosen due to their high energy-density storage capabilities for short duration pulses, and because they are self-healing in case an internal fault

v

condition occurs. Transmission type pulse lines were used to provide square wave approximation pulse shapes for potential laser applications.

The actual transmission lines were constructed in the summer of 1976 with funds obtained through an internal grant from the PSU Research and Publications Committee. The initial experimental work with this system began in late 1976. Due to the lack of a suitable power supply, repetition rates of only 10 to 10 hz were attainable.

In the fall of 1977 a small grant was obtained from the Office of Naval Research to further study the liquid-dielectric transmission line concept. A high voltage power supply was purchased, and the equipment and measurement capability was refined in order to extend the operating range of the liquid-dielectric pulser circuit to as high as 2 khz repetition rates. A renewal contract continued the project for a second year. Experiments continued along with further development of the concept. In addition, preliminary computer modeling was undertaken. Thus, the project results are presented in two parts: Part I, Background and Laboratory Testing of Pulser Circuit, and Part II, Pulser Circuit Computer Modeling.

TABLE OF CONTENTS

PART I

BACKGROUND AND LABORATORY TESTING

OF PULSER CIRCUIT

LIST OF TABLES

x

LIST OF FIGURES

LIST OF SYMBOLS

A:	Electrode Area
α :	Proportionality Constant
c:	Speed of Light in a Vacuum
C:	Capacitance
C_s:	Source Capacitance
C_{TL}:	Transmission Line Capacitance
ς :	Dielectric Loss Coefficient
$\in$:	Dielectric Permittivity
$\in_o$:	Permittivity of Free Space
f:	Repetition Date
f_o:	Resonant Frequency
I:	Current
I_o:	Output or Load Current
J:	Joules
K:	Dielectric Constant
ℓ :	Electrode Length
L:	Inductance
L_o:	Outp t Inductance
t:	Time Variable
T:	Time Period or Pulse Duration (i.e., Pulse Length)
T_c:	Pulse length for a critically damped capacitive discharge
T_R:	Resonant Charging Time

T_{TL}:	Pulse Length for a Transmission Line Storage Element
ν :	Frequency
V:	Voltage
V_c:	Capacitor Voltage
V_s:	Source Voltage
V_o:	Output or Load Voltage
V_{TL}:	Transmission Line Voltage
w:	Electrode Width
ω :	Angular Frequency
z:	Reactive Impedance
z_{TL}:	Transmission Line Impedance
L_T:	Total Discharge Loop Inductance
η :	Electrical Energy Transfer Efficiency
N:	Inversion Density
N_2:	Molecular Nitrogen
nsec:	nanoseconds (10^{-9} seconds)
P:	Excitation Power
P_{ave}:	Average Electrical Power
P_o:	Output Power or Load Power
Q:	Electric Charge
Q_f:	Quality Factor
R:	Resistance
R_L:	Load Resistance
R_c:	Resistance in a Critically Damped Circuit
s:	Electrode Separation Distance
S:	Dielectric Working Stress Level
S_{max}:	Dielectric Strength

1. INTRODUCTION

Background

In recent years there has evolved considerable interest in the development of lasers operating in the ultra-violet region of the spectrum. It is here that many of the electronic transitions in atoms and molecules occur[1] and a tunable, narrow band source of coherent radiation would greatly facilitate the study of the electronic structure of atoms and molecules. Ultraviolet sources are also urgently needed for a wide variety of photochemical processes, most notably that of isotope separation.[2] These two applications alone have warranted the growth of extensive research programs throughout the world to develop UV (ultra-violet) lasers of various types. The present lack of suitable lasers in this region as compared to the proliferation of sources that has appeared in the visible and infrared portions of the spectrum can best be understood by a review of the fundamental considerations in obtaining laser action. The basic difficulty in obtaining lasing in this region of the spectrum was first noted by Schalow and Townes[3] in their original analysis on infrared and optical lasers. They showed that the required excitation power needed to establish useful inversion densities was strongly frequency dependent. The results of their analysis shows that the dependence of inversion density N on excitation power P and lasing frequency ν is

$$\Delta N \propto P \, \nu^{-4} \tag{1}$$

This clearly shows the difficulties encountered in achieving useful inversion densities and laser action at short wavelengths or high frequencies.

Scope of Study

It is the partial intention of this study to review the present* methods for attaining the high levels of power needed to successfully pump a UV laser. It has been found in a review of the literature that only too often lasers have been designed with respect to the convenience of available components and simplicity of construction. This design procedure is entirely justifiable in many instances, but applications such as isotope separation require an especially efficient use of the available power. In particular, a unique electrical driving network has been designed, constructed and tested to verify that it could not only deliver the necessary input powers for obtaining UV laser action, but show needed improvement in performance with respect to reliable, high power capabilities. These characteristics are of special interest to laser systems destined for isotope separation and other wavelength selective chemical synthesis techniques because of their possible application to commercial processes.

A review of the literature on the electrical driving networks used in many short wavelength laser schemes showed that the weakest link precluding reliable, high repetition rate operation was the energy storage capacitor used in the high speed discharge circuits. The high speed requirements were met by using very high voltage, low inductance capacitors. The low inductance in these type of capacitors was partially achieved by minimizing the positive-negative electrode

---

*See Preface

separation distance which also maximizes the dielectric stress. Maximizing the dielectric stresses of a capacitor almost invariably leads to short capacitor lifetimes because sooner or later an internal fault or breakdown will occur in the dielectric itself.

It was for this reason that another literature search was made on various types of dielectrics including gases, liquids and solids in order to find one with electrical characteristics more favorable to the design of a long lived, low inductance capacitive storage system. The literature search revealed that several liquids, most notably transformer oil, water and glycerin had many of the desired electrical characteristics. A electrical circuit was then designed to take advantage of the properties of liquid dielectrics.

Thus, the design of the driving network used in the present research effort centers around the use of liquid filled transmission lines which generate rectangular shaped output pulses when discharged into matched resistive loads. Liquid dielectrics were used in preference to solids because of their self-healing characteristics under fault conditions. Of all the liquids considered, glycerine appeared to be the best choice because of its high dielectric constant ($k = 44$), good breakdown strength (> 20 kv/mm), and electrical stability under no flow conditions. Pure water was initially selected for use, but subsequent experimentation revealed that ionization products degraded the electrical properties so fast that only continuous deionization would render it usable in the prototype system. Because the selected dielectric also suffered significant losses when left charged for more

than a few usecs due to internal bleedoff, it was necessary to pulse charge it to make effective use of the available power. In this context two different types of pulse charging networks were constructed and used in the various experimentation phases of the research project. The first consisted of a low inductance, two stage Marx bank resistively charged by a 17 kv, 100 watt power supply. The second pulse charging network was based on a voltage doubling, resonant charging scheme utilizing a capacitor discharge. This second network was constructed in order to increase the power transfer efficiencies from the electrical mains to the transmission line storage elements. The latter circuit realized transfer efficiencies approximately 10 times greater than those obtainable with the Marx bank.

Initially, testing of the glycerine filled transmission lines was aimed at determining the practical attainable working stresses. Later experiments explored fault conditions, healing times and charging voltage waveforms. After the proper range of working conditions were determined, the experimentation was directed toward measurements of the current and voltage output waveforms under varying conditions of load impedence and inductance. Later work included extending the repetition rates from single shot experiments to high repetition rates in the low khz range.

During the course of the experimental work, a continuing study of potential laser applications was being made. This study, which was mainly an extensive literature search and review, revolved around trying to categorize that group of applications including

laser mediums which might benefit from the characteristics of this particular type of electrical driving network. A list of these potential applications including further work that should be performed with liquid dielectric energy storage systems is discussed in the recommendation section of this study. In addition, because it was recognized that the next major step should involve incorporation of the excitation system into an actual laser, that was an expected follow-on project. Simultaneous analytical modeling of the transmission line was also anticipated.

2. REVIEW

General Pumping Techniques

Two of the more prominent pumping schemes used today are that of electrical and optical pumping. The former is the most efficient theoretically because the latter introduces an intermediate conversion step (electrical to optical) which can only decrease total conversion efficiencies. Since both of the pumping techniques impact a wide variety of ultraviolet lasing mediums, both will be considered briefly with respect to their general operating characteristics. It is not the purpose of this investigation to address these techniques in their totality but to focus on the process of taking electrical energy from the utilities distribution system and delivering it to an appropriate load, whether it be a flashlamp or laser gas. Therefore, flashlamps and lasing mediums will be addressed only with respect to their effects on the driving network used and detailed laser and gas discharge kinetics will be avoided.

Optical pumping is presently the only practical method for attaining laser action in the various liquid and solid laser mediums discovered to date. The most well known liquid laser is the dye laser whose wide tuning capability has elevated it to a prominent place in many research laboratories. There are a number of dyes which operate in the ultraviolet with the lower end extending down to 340 nm in paraterphenyl.[4] Solid state lasers on the other hand do not presently operate directly in the ultraviolet, but must rely on nonlinear upconversion techniques for obtaining coherent UV radiation.

- 6 -

Since this method involves not only electrical to optical to lasing conversion steps, but the additional one of a nonlinear nature it will be addressed no further because of its inherent overall inefficiency and inability to be scaled to high average powers.[5]

One of the most widely used pulsed light sources is that produced by a spark discharge in a high pressure gas.[6] The radiation is caused by the retardation of electrons in the field of positive ions (free-free transitions), electron-ion recombinations (free-bound transitions), and finally the radiation broadened lines of bound electron transitions (bound-bound transitions). To produce these high brightness light sources it is common to use a high voltage, low inductance discharge circuit and a high pressure flashlamp. It should be pointed out that high voltage, low inductance discharge circuits are also used in direct electrical pumping schemes as well. This common link is very important to the latter systems because of the wealth of information available on high intensity light sources. Long before the advent of the laser, considerable amounts of data were amassed concerning high power spark discharges. Much of this information is related to the complex interactions between driving source and gas load. Detailed studies have also been made of the spectral output of various types of discharges. This latter information is an excellent indicator of energy level populations and by correlating the spectral output with the circuit parameters used in these studies it is possible to size relevant circuit parameters when designing various types of gas lasers, UV or otherwise. It is because of this common

connection that spark discharges are so important to the development of efficient gas lasers. It is also the reason why many of the design criterion used in this investigation on fast discharge pumping schemes were derived from spark discharge studies.

High Intensity Spark Discharge Circuits

High brightness, ultraviolet rich spark discharges are generally produced from high voltage, low inductance discharge circuits. The high voltage, low inductance requirements insure the maximum possible speed of energy input from the capacitor to the discharge channel. An idea of how these parameters actually affect the power input can be gained by analyzing the current-time dependency of a damped RLC oscillation. It is well known that the RLC discharge current is given by the expression[7]

$$I(t) = \frac{V_c e^{-(Rt/2L)}}{\left[\frac{L}{C} - \frac{R^2}{4}\right]^{1/2}} \; SIN\left[\frac{1}{LC} - \frac{R^2}{4L^2}\right]^{1/2} t \qquad (2)$$

For the case of an underdamped oscillation (i.e. $1/LC \gg R^2/4L^2$) expression (2) reduces at the beginning of the discharge to

$$I(t) = \frac{V_c}{(L/C)^{1/2}} \; SIN \, (1/LC)^{1/2} t \qquad (3)$$

where Vo is the initial capacitor voltage, C the capacitance and L the total loop inductance of the discharge circuit. Inspection of

- 8 -

equation (3) will show that $(L/C)^{1/2}$ has the units of ohms and is usually termed the reactive impedance (Z) of the discharge circuit. $(1/LC)^{1/2}$ on the other hand has the units of frequency and represents the angular oscillation frequency ( ) of the discharge. The rate of power input to a resistive load is to a first approximation given by the time rate of current buildup dI/dt in the channel. Differentiation of (3) shows that initially this time rate of change dI/dt depends only on the voltage and inductance of the discharge circuit.

$$(dI/dt)_{t=0} = V_c/L \tag{4}$$

The maximum value of the current and hence power input is given in an underdamped circuit by

$$I_{max} = V_c/Z \tag{5}$$

where Z represents the reactive impedance $(L/C)^{1/2}$ of the discharge circuit.

Based on the above considerations the rate of power input to a high pressure spark discharge can be increased by raising the voltage, lowering the circuit inductance or both. In order to construct high intensity spark light sources it becomes necessary to use high voltage, low inductance capacitors coupled with the proper busing network for connecting the capacitors to the discharge gap. To reduce the inductance of the discharge circuit to a minimum possible value the arrangement of the circuit elements should be such that the magnetic field formed by the current is contained in the smallest possible

volume. It should be noted that with a given set of circuit components the maximum power input occurs under critically damped conditions. That is all of the energy stored in the capacitor is delivered to the spark load in approximately the first half period of oscillation instead of being spread out over many periods as in the underdamped case. The energy stored in a capacitor is

$$E = 1/2 \ CV_c^2 \qquad (6)$$

where V is the charging voltage and C the capacitance. The first half period is given by

$$T = \pi (LC)^{1/2} \qquad (7)$$

with L being the total discharge circuit inductance. The _average_ power input during the discharge pulse is then

$$P_{ave} = V_c^2/2\pi \ Z \qquad (8)$$

where Z is again just the reactive part of the total discharge impedance. The total discharge impedance is the sum of the reactive and resistive parts. It happens that for the critically damped case the reactive component is one-half the resistive part.[8]

$$R_c = 2(L/C)^{1/2} \qquad (9)$$

Therefore, the average power could alternatively be given as

$$P_{ave} = V^2/\pi \ R_c \qquad (10)$$

It should be clarified that these results are only first approximations because the actual energy delivery during a critically damped pulse extends somewhat beyond the first-half period. Even so this analysis does show the relative effect that various circuit parameters have on the power input to a spark discharge. It should also be realized that because of the changing discharge impedance with respect to time during breakdown, exact matching between the reactive and resistive parts of the circuit is not entirely possible. It is known that the spark impedance during breakdown goes from a very high value to a small fraction of an ohm.[9] Because of this changing impedance, discharge circuits are usually designed to deliver maximum power after the discharge has leveled off to its low impedance level. A critically damped discharge pulse is also, because of its limited length, the most efficient pulse shape for transferring electrical energy from a source to a coherent optical output. This second characteristic is the result of temporal changes in the populations of various energy levels of the lasing medium of interest.*

Self-Terminating Laser Candidate Systems

The following is a discussion of three particular types of lasing systems which benefit from using a critically damped discharge pulse (i.e., one of a limited length) in the excitation scheme used to achieve lasing conditions. These three systems all lase at short wavelengths and are potential candidates for use in high repetition rate, chemical process oriented applications.

---

*This may also apply to mediums not directly involved in the lasing process such as dye solvents or host mediums in solid state lasers.

- 11 -

There are many types of lasers whose outputs terminate prematurely before the conclusion of the pumping pulse. The molecular nitrogen laser operating at 3371 Å in the ultraviolet is one of the most well known of these self-terminating lasers. The reason for this self-termination in the nitrogen laser is due to the fact that the lower laser level ($B^3\Pi g$) has a lifetime of about 6 usecs, more than two magnitudes greater than the 40 nsec lifetime of the upper level ($C^3\Pi g$).[10] Population inversion can be achieved because the excitation cross section of the upper level is about twice as large as the lower one, so using a very fast discharge the system can be inverted. The long lifetime of the lower level as compared to the upper is the reason for the self-terminating nature of this laser. The lower level bottlenecks the electronic flow, effectively destroying the inversion condition and lasing. It is for this reason that the discharge pulse lengths necessary to efficiently pump the N_2 laser should be no longer than the upper state lifetime or about 40 nsec. For a discharge pulse longer than this much of the energy will be needlessly wasted.

The flashlamp pumped dye laser also has a type of self-terminating characteristic associated with it. The operating principle of a dye laser is much the same as for other lasers. The dye molecules are raised to the lowest singlet state directly or more often by relaxation from some higher lying singlet state. Lasing involves a return to a lower level by stimulated emission. These processes are further complicated by nonradiative transitions to the lower level, singletstate absorption of the lasing wavelength and more importantly,

- 12 -

intersystem crossing from the upper singlet level to a long-lived triplet state which can also absorb at the lasing wavelength.[11] These processes are not as detrimental to lasing as in the N_2 bottle-necking case, but intersystem crossing and subsequent absorption at the lasing wavelength severely restricts the levels of wall plug conversion length severely restricts the levels of wall plug conversion efficiences obtainable for times longer than that required for intersystem crossing to occur (100 nsec or more). Even though there exists quenching agents that do prevent a large accumulation of molecules in the triplet state,[12] any molecules that do cross over represent a loss in efficiency. Therefore, here too, the maximum overall wall plug conversion efficiencies should be attained with short high power pump pulses.

The last system to be discussed concerning self-termination and probably the most promising today regarding the development of a high power, efficient, ultraviolet laser is the rare gas mono-halide group. This group of lasers is based on gaseous excimers. An excimer is a molecule which only exists in the excited state and dissociates when it reaches the ground state. This is because the ground state is weakly bound or even repulsive and the only stable state is the excited one. Since the terminal state is very unstable it exists only for about 10^{-13} second (i.e. that time required for molecular vibration). This extremely fast depopulation prevents the terminal state bottle-necking problem of the nitrogen laser. The fact that the ground state is also the lower laser level is one of the reasons for the high quantum efficiencies of this laser. There are other factors which

- 13 -

contribute to this laser group's high overall efficiency, but what we are concerned with here is the the self-termination characteristic that also shows up in the rare-gas mono halides.[13] All of the reasons are as yet unclear, but present evidence seems to indicate that both gas clean-up and discharge runaway (arcing) are major causes for premature laser pulse termination. Whatever the reason it appears that efficient operation of UV wavelength rare gas halides may also require short pulse length electrical discharges.

These previous three cases of self-terminating laser action have been used to illustrate the fact that the efficient transfer of energy from a source to a coherent optical output may not only require a high rate of power input in accordance with equation (1), but should also satisfy a temporal requirement as well. The most efficient pulse shape or duration for exciting many types of UV lasers has been found to be of a very limited length usually much less than a usec. This additional requirement of short pulse length poses a very serious reliability problem with respect to the components that make up the discharge circuit. This reliability problem arises because a short pulse length is achieved by using very low inductance circuit elements including the primary energy storage element, the capacitor. As mentioned earlier, low inductance capacitors have very limited life-times in high voltage, fast discharge (i.e., short pulse length) applications. See the section on capacitors for a more detailed explanation of this problem.

3. FAST ELECTRICAL DISCHARGE EXCITATION TECHNIQUES

Introduction

The discharge circuits used to directly pump various UV laser mediums must at least satisfy equation (1) and should have a short pulse length for maximizing transfer efficiencies. The actual pulse length will be determined primarily by the lasing medium selected because of the need for the pulse excitation length or time to be less than that required for self-termination to occur in the selected lasing system.

Figure 3.1 shows a schematic diagram of the usual arrangement of electrical components in a fast, high power discharge circuit.
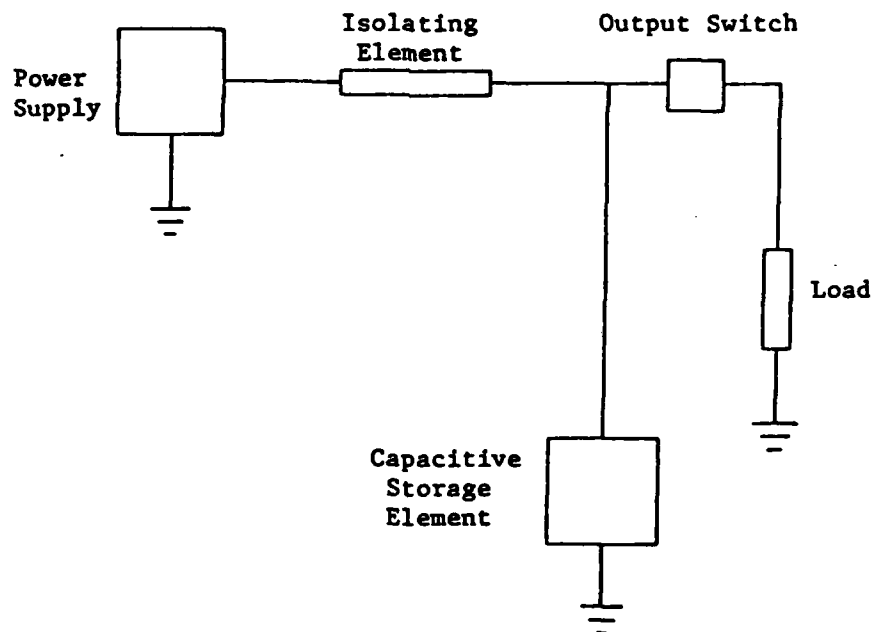
Fig 3.1. Block diagram for a high speed discharge circuit

The discharge circuit proper usually consists of an energy storage element, an output switch and of course an appropriate load, be it a flashlamp or laser gas medium. In reality any practical high power electrical driving circuit not only includes a discharge circuit but also a circuit to charge the energy storage element as shown in Figure 3.1. Notice that the storage element is common to both the charging and discharging sections of this circuit. There are many different varieties of these two circuits, each with its advantages and disadvantages. The following sections are a review of the various methods and components used in these types of circuits.

Energy Storage Elements

The two most general ways of storing and subsequently retrieving electrical energy are the capacitor which stores energy in an electric field and the inductor which utilizes a magnetic field for storage purposes. The latter form of storage has not yet been developed to the extent that capacitive storage has because of the lack of a suitable switch. For high energy systems (kilojoules) capacitive energy storage costs between $.10 and $1.00 per joule depending on the complexity of the switching and energy transmission systems. The economics of an inductive system on the other hand is estimated to be at least an order of magnitude lower. Moreover, including the switch, an inductive system will be far more compact than a comparable capacitive system. Therefore, inductor storage switch development is underway at various laboratories around the world, but presently the capacitor is far easier to energize and switch across a load than an

inductor. It is not then unexpected that present high power electrical discharge systems are designed around the capacitor with all its advantages and unfortunately, faults.

The Capacitor

The capacitor is one of the oldest forms of electrical energy storage devices for pulsed power requirements. Capacitance exists between any two electrical conductors. Basically a capacitor consists of two parallel conductors separated by a dielectric material. The actual energy storage occurs in the dielectric, and thus it plays a major role in the operation of a capacitor. When a direct voltage is applied to a capacitor, the electric field is distorted and the bound electric charges are polarized or displaced from their normal position of equilibrium. If the voltage per unit length (i.e. electric field strength) is increased beyond a certain point, the dielectric may break down, resulting in a short and failure in the capacitor. This factor is important in determining the applicability of any one dielectric towards capacitor construction and is characterized by the measurable quantity of dielectric strength which can be given in kv/mm. The total energy stored in a capacitor (V/s) is given by equation (6) to be

$$E = 1/2 \ CV_c^2 \tag{6}$$

For a parallel plate capacitor the capacitance is given by reference (8) to be

$$C = \epsilon \ A/s \tag{11}$$

- 17 -

With ϵ being the permittivity of the dielectric, A the plate area and s the plate separation or dielectric thickness. Therefore, for a given ϵ , A, and s which determine the capacitance of an electrical element, if the dielectric strength of the material used in the element is increased, then the applied voltage that can be used on this element can also be increased. Referring back to equation (6), an increase in the usable voltage will lead to an increased energy storage capability for a given size capacitive element. This fact is more properly represented by an increase in energy density, which is the energy stored per unit volume of dielectric material. The only other parameter that can increase the energy density is the dielectric permittivity. It is the permittivity and the dielectric strength which affect the construction of high energy density capacitors. The delivery ability of any capacitor with respect to speed is reflected by the system's inherent inductance. Low inductance is required for fast energy delivery because during discharge of a capacitor the impulse current branches off energy to the magnetic field equal to $1/2 \ LI^2$ (see reference 9) which reduces the first peak value of the impulse current; L is the inductance of the discharge loop and I the impulse loop current. The energy absorbed by the magnetic field is not lost but becomes effective during the latter part of the discharge. With proper circuit design most of the inductance found in the discharge circuit will be the self-inductance of the capacitor itself.

The optimum pulse shape for maximizing transfer efficiencies has been shown to be a critically damped one. The pulse width for the

critically damped case is given by equation (7), as follows:

$$T = \pi (LC)^{1/2} \qquad (7)$$

This expression shows that critically damped discharge pulse lengths are proportional to the square root of the inductance–capacitance product. The average power delivered during the time of this pulse is given by:[8]

$$P_{ave} = V_c^2/2\pi Z \qquad (8)$$

Inspection of these two equations will show that for a given voltage and capacitance the pulse length can be reduced and the power increased by lowering the total inductance in the discharge loop. The difficulty in p ractically accomplishing this is the strong interdependence between the inductance and capacitance of an energy storage capacitor. The inductance of a simple parallel plate is equal to:[14]

$$L = \mu s \ell/w \qquad (12)$$

where μ is the permeability of the dielectric, s the plate separation, l the plate length and w the plate width. Using equations (11) and (12), we can rewrite the expressions for the pulse length and average power.

$$T = \pi (\mu\epsilon)^{1/2} \qquad (13)$$

$$P_{ave} = (V^2 w/2\pi s) (\epsilon/\mu)^{1/2} \qquad (14)$$

Equation (14) shows the desired result for discharge pulse lengths.

For a given dielectric, and   will be constant and the length of the
plates will determine the pulse length. Likewise for a set of plates
of a given length, the pulse length can be changed by using dielectrics
with varying permittivities (i.e. dielectric constant). Equation (15)
is slightly more complex and requires an additional modification before
certain characteristics can be highlighted. It has been shown pre-
viously that the energy density of a capacitor is directly proportional
to both the dielectric strength and the permittivity. The dielectric
stress is equal to V/s and this factor appears in (15) as well as the
square root of the permittivity. Rewriting equation (15) we introduce
the dielectric working stress level S which is equal to V/s. The
dielectric strength is just S_{max} which is the maximum stress that be
applied to a dielectric above which dielectric breakdown will occur.

$$P_{ave} = (VSw/2\pi) \ (\epsilon/\mu)^{1/2} \tag{15}$$

From electromagnetic field theory we can obtain identities for the
various forms that the combinations of the permittivity and permea-
bility have taken. The term $(\epsilon/\mu)^{1/2}$ is the inverse of the speed
of light in the dielectric and equals $(K)^{1/2}c$ where K is the dielec-
tric constant of the medium, whereas $(C/L)^{1/2}$ is the reciprocal of the
impedance of the dielectric. The ratio of the voltage V to the
impedance Z is by Ohm's Law the short-circuit current I. Rearranging
equation (14) and (15)

$$T = (\pi/c) \ (k)^{1/2} \ell \tag{16}$$

$$P_{ave} = ISw/2 \tag{17}$$

_____

*The impedance of a capacitor is equal to $(L/C)^{1/2}$.

The last expression shows that for a simple strip line geometry the average power output of the device can be raised by increasing the short-circuit current, the width of the lines or by maximizing the dielectric stress. It should be realized that all these parameters are not independent of each other. For a given dielectric and strip line geometry and hence impedance, the maximum current occurs when the dielectric is stressed to its maximum value without failing (i.e., $I_o \rightarrow I_{max}$ when $S \rightarrow S_{max}$). If one stresses a dielectric to such high levels in order to maximize the current it severely limits the lifetime of the dielectric under repetitively pulsed conditions. It has been found empirically that most high energy density capacitors follow the well known "fifth power law."[15] This empirical derived law shows that the lifetime (T_L) of these types of capacitors are inversely proportional to the fifth power of the dielectric stress.

$$T_L \propto S^{-5} \qquad (18)$$

As an example of the effect that these relationships have on the lifetime of a capacitor, assume that two identical capacitors are charged up. The first capacitor is charged to the maximum voltage corresponding to S_{max}. Following equation (19), its lifetime will be inversely proportional to the fifth power of S_{max}. If the second capacitor is charged up to only one-half the voltage of the first, its lifetime will be inversely proportional to the fifth power of 1/2 S_{max}. A simple calculation shows that the second capacitor will have a lifetime of 32 (i.e., 2 raised to the fifth power) times that of the first.

Some of the more promising dielectrics developed for use in high energy density capacitors such as the polyester films have shown an even poorer dependency of dielectric lifetimes to dielectric stress levels when stressed to high levels of electric fields.[16] For the mylar polyester films

$$T_L \propto S^{-7} \tag{19}$$

This means that for a given stress level polyester dielectrics have much shorter lifetimes than those types whose lifetimes follow equation (19).

Present high energy density capacitors are limited to energy densities of about 50 joules/lb with dielectric strengths not exceeding 150 kv/mm.[19] Commercially available, low inductance units usually have lifetimes of not much more than 100,000 shots.[17] At a repetition rate of 100 Hertz the useful lifetime would be used up in less than 2 minutes, necessitating complete replacement of the burned out capacitor.

This problem of limited lifetime in high density, low inductance capacitors has been a stumbling block in the development of reliable and compact short pulse length, high power, high repetition rate electrical driving networks for UV laser excitation.

Liquid Dielectrics

One possible solution to the limited lifetimes in highly stressed solid dielectrics is found in the use of self-healing liquid dielectrics such as water, glycerine and transformer oils. All three

Pulse Shape

Energy storage elements are not only sources of energy in a discharge circuit but also serve to help shape the output pulse. The storage element itself does not solely shape the output pulse but does so in conjunction with the load it sees on its output terminals. Capacitors are essentially made up of series and parallel combinations of either strip (i.e., parallel plate) or coaxial electrodes. There are three distinct types of pulse shapes that can be realized from such a network depending on the conditions that exist at the output of the storage element. Figure 3.2 shows the three voltage or current pulse shapes with the corresponding relationship between the R, L, and C components of the circuit that must be met in order to achieve these pulse shapes.

Figure 3.2A shows the pulse shapes obtained when the electrical energy storage element acts as a conventional capacitive discharge system (lumped parameter networks). Figure 3.2B indicates the pulse shapes obtained using transmission lines for storage elements (distributed parameter networks). The difference between these two pulse shapes lies in the risetime of the discharge into the load as compared to the pulse length. A capacitive discharge has a risetime into the load of:[19]

$$T_r = 2.2 L_T / R \tag{20}$$

where T_r is the risetime (10 to 90%) into the load, L_T the total

A. LUMPED PARAMETER NETWORK
(most capacitive discharge systems)

Overdamped

L << R²C/4

Critically Damped

L = R²C/4

Underdamped

L >> R²C/4
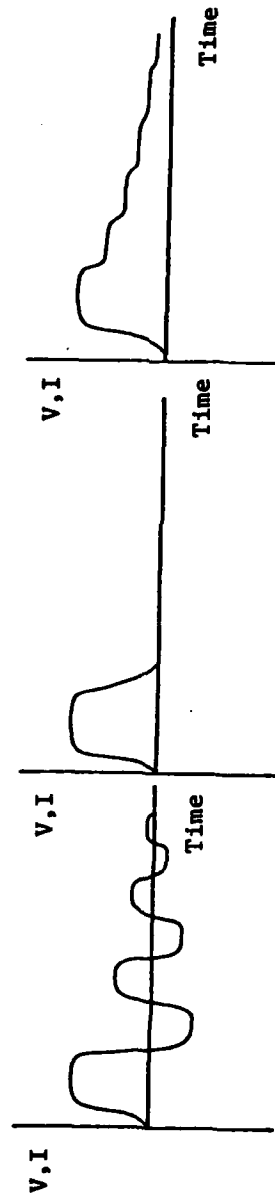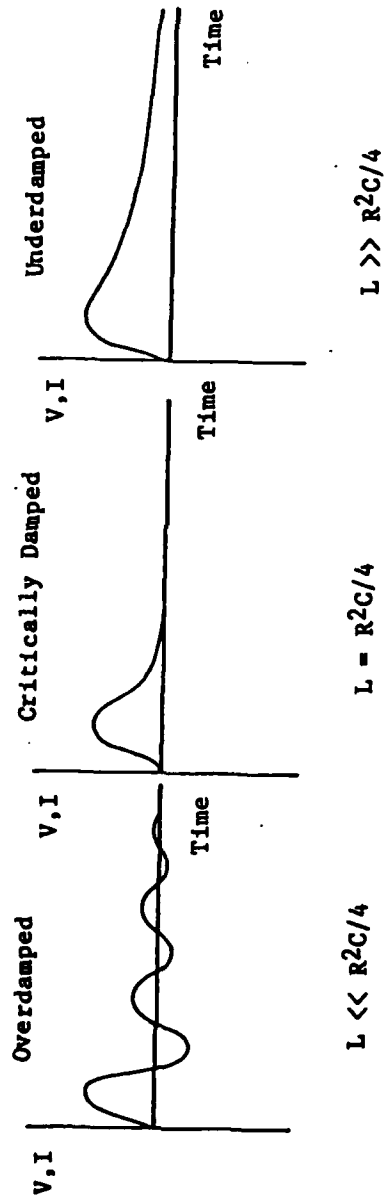
B. Distributed Parameter Network
(Transmission Lines)

Fig 3.2. Pulse shapes for lumped and distributed parameter networks

- 25 -

discharge loop inductance and R is the load resistance. A transmission line has a risetime equal to [19].

$$T_r = L_0/Z_{TL} \qquad (21)$$

with L_0 being the output inductance and Z_0 the transmission line impedance. Comparing these two expressions, it should be noted that the risetime of a transmission line is proportional to the output inductance and not the total inductance of the discharge loop as in the capacitive system. The difference in these two expressions can be traced back to the pulse lengths obtained with these two types of networks. If the risetime of the network into the load is much less than half the one way transit time of the network, then the transmission line pulse shape will be observed (Figure 3.2B). On the other hand, if the risetime is much greater than the one way transit time of the network, then the lumped parameter pulse shape will be observed (Figure 3.2A). The one way transit time of a transmission line is the time it takes for a light pulse to travel from one end of the transmission line to the other through the dielectric. This pulse length versus risetime criterion distinguishes whether an energy storage element will act as a transmission line or a capacitor when discharged into some load. For a given output inductance the pulse shape of a transmission line approaches that of a capacitive system as its impedance is reduced. Theoretically, a transmission line discharged into an impedance-matched and completely resistive load should yield a perfectly rectangular pulse with no risetime associated with it. The inherent inductance in the bus work connecting the transmission line

- 26 -

to the load and in the load itself modifies this ideal wave shape into one with a finite risetime.

Fast risetime, rectangular shaped pulses are highly desirable for driving many lasing gas mediums. If the driving or excitation pulse has a long risetime there is a significant amount of energy delivered to the load before lasing threshold is reached. This also holds true for the tail end of the pulse. Therefore, a rectangular wave shape would be ideal for maximizing the energy transfer between source and load during the lasing process. A fast risetime pulse is also desirable for systems that exhibit bottlenecking and self-terminating characteristics. A pulse with too slow a risetime can prevent lasing from occuring altogether in these types of system, so that it is imperative to use a fast risetime pulse for their excitation. The flat top characteristic of transmission lines also simplifies the conditions under which the lasing process takes place. This simplifies the study of not only kinetics but gain parameters as well because of the constant driving force that exists during much of the time that lasing does occur.

A transmission line discharged into a matched resistive load delivers a voltage pulse of magnitude equal to one-half the charging voltage Vo. The current pulse is given by

$$I = V_{TL}/(R + Z_{TL}) = V_{TL}/2Z_{TL} \qquad (22)$$

$$V_o = (V_{TL}R)/(R + Z_{TL}) \qquad (23)$$

The power delivered to the load is by circuit theory.

- 27 -

In general, $$P_0 = V_0 I_0 \qquad (24)$$

Substituting (23) and (24) in (25)

$$P_0 = V_{TL}^2 / 4Z_{TL} \qquad (25)$$

and using the expression $E = 1/2 \; CV_0^2$ from equation (6) for the energy stored in the transmission line, the pulse length can be solved for using the fact that $P_{out} = E/T$, $\qquad (26)$

where T is the pulse length.

Thus $$T_{TL} = (C_{TL}V_{TL}^2/2)/(V^2/4Z_{TL}) = 2C_{TL}Z_{TL} \qquad (27)$$

Using the fact that $Z_{TL} = (L/C)^{1/2}$ (see footnote on page 18)

$$T_{TL} = 2 \; C_{TL}(L_{TL}/C_{TL})^{1/2} = 2(L_{TL}C_{TL})^{1/2} \qquad (28)$$

Note that this is always less than the time period of a critically damped capacitive discharge $T_c = \pi \; (LC)^{1/2}$. This is a natural result of the fact that a transmission line discharge only degrades into a capacitive shaped discharge pulse when the output inductance increases beyond a certain point. This increase in the output inductance not only changes the shape of the pulse but also increases the time period in which energy flows to the load. Therefore, one of the primary design criterion in the selection of the liquid dielectric and electrode structure was that the resulting electrical energy storage element act as a transmission line in the electrical discharge circuit.

4. CHARGING CIRCUITRY

Introduction

After the decision was made to design and construct a liquid dielectric energy storage element that would act as a transmission line when discharged into an appropriate load, it was also necessary to design a charging circuit that would transfer energy from the laboratory power supply to the energy storage elements of the high speed circuit itself. The three types of charging networks that will be discussed in the next section include resistive, inductive and inductive-diode charging circuits.

In any fast discharge circuit there always exists an element for isolating the power supply from the energy storage element during the fast discharge phase of operation. The necessity of this element evolves out of the fact that most laboratory power supplies cannot furnish on a continuous basis the extremely high levels of power needed to pump many types of UV lasers. Therefore, these types of devices are usually operated in the pulsed mode for this and other reasons (i.e. self-termination). Figure (3.1) previously showed the conventional arrangement of components in such a circuit.* In this instance, a capacitor is charged up until the output switch closes and connects the capacitor directly across the load. The output switch can operate in either a triggered or self-breakdown mode. When switch closure does

---

*Notice that in all the circuits used, at least one side of the high-voltage network is always grounded. This reduces the number of points in the circuit that are at high voltage and is a typical safety precaution in high-voltage systems.

occur, the capacitor delivers its energy to the load very quickly in any properly designed circuit. After delivery, the capacitor voltage returns to zero so that point A <u>without</u> the isolating element would present a short-circuit to the power supply causing either serious damage to the supply by overloading or decoupling by protective fuse or relay openings. At a given voltage the isolating element must always present an effective impedance to the supply such that the maximum current drawn does not exceed the supply capabilities.

Resistive Charging

Resistive charging is probably the most widely used charging technique because of its simplicity, low cost and availability of components. Figure 4.1a show the conventional arrangements of components in the charging circuit while Figure 4.1b shows the operational waveforms. Initially, the capacitor is fully discharged and the switch is open. The subsequent capacitor voltage and current will then be[8]

$$v(t) = V[1 - e^{-(t/RC)}] \qquad (29)$$

$$i(t) = (V/R)[e^{-(t/RC)}] \qquad (30)$$

The energy delivered by the power supply (E_s) during a time period T is just

$$E_s = V\int_0^T i(t)dt \qquad (31)$$

Substituting (30) in (31) and integrating

$$E_s = CV^2[1 - e^{-(T/RC)}] \qquad (32)$$

The energy stored in the capacitor (E_c) at this time T is

$$E_c = 1/2 \ Cv(T)^2 \tag{33}$$

Substituting (29) in (33), the energy stored in the capacitor at time T becomes

$$E_c = 1/2 \ CV^2[1 - e^{-(T/RC)}] \tag{34}$$

The energy transfer efficiency between source and capacitor is just the ratio of the energy stored in the capacitor to that delivered by the source in the same time period, or

$$= 1/2 \ [1-e^{-(T/RC)}]2 \tag{35}$$

Clearly the maximum efficiency for resistive charging is only 50% and this occurs only when $T \longrightarrow \infty$ or RC $\longrightarrow$ 0. These two conditions are never met in any practical situation and especially those cases pertaining to high repetition rate operation. Because high repetition rates are a desired goal, equation (35) must be evaluated in order to determine the practical working efficiencies attainable under high repetiion rate conditions. Since it is also desired to maximize the power transfer from the source to the load, expression (34) should be manipulated in such a fashion as to yield the condition under which maximum power transfer occurs. This yields the following equation:

$$E_c = 1/2 \ CV^2[1-e^{-(T/RC)}]2 \tag{36}$$

For a given supply voltage V and repetition rate, T and R will remain
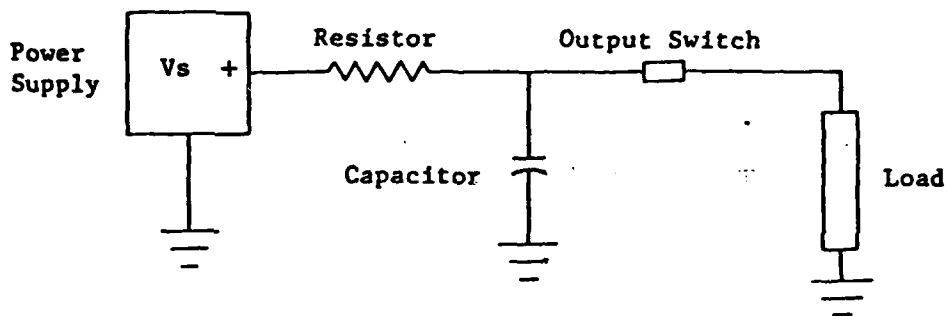
Fig 4.1a. Resistively charged circuit
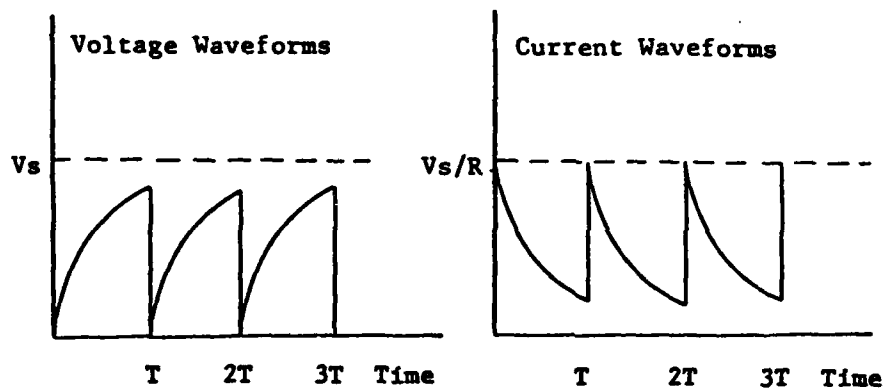
Fig 4.1b. Capacitor voltage and current waveforms in a resistively charged circuit

Therefore, with high repetition rates and resistive charging almost two-thirds of the source power is unavailable at the load. This clearly demonstrates the need for alternate and more efficient methods for charging the energy storage element in high pulse rate circuits. In fact, the most efficient types of charging networks are those which utilize resonance techniques.[20] Rather than using a resistive isolating element, they employ an inductive element. This technique minimizes the resistances of the charging circuit with the result that high transfer efficiencies are possible between source and storage element than can be achieved with resistive charging schemes.

Resonant Inductive Charging

Figure 4.2a illustrates the inductive charging circuit and Figure 4.2b, the waveforms of a circuit utilizing an inductive charging element. In order to maximize transfer efficiencies, the resistive component of such a circuit should be as small as possible (i.e. the circuit should operate in an underdamped or oscillatory mode).* The condition for this is defined by

$$R \ll 2\pi(L/C)^{1/2} \qquad (41)$$

Also to prevent significant voltage droop during charging, the source capacitance should be at least 10 times larger than that of the storage element. The series resistance in the charging circuit (see Figure 4.4)

_____

*Note that this criterion is different for a system charging a capacitive load than one charging a resistive load in which a critically damped oscillation is the optimum one.

fixed. R has to remain fixed because for a given supply voltage the maximum current drawn has to be within the supply range. Therefore, the only remaining variable is the capacitance C. To find the maximum of the power that could potentially be transferred to the load P_L, it is simply a matter of differentiating (34) with respect to C, setting the resulting equation to zero and then solving for the relationship between the independent (C) and dependent (R,T) variables. Letting $(P_L)_{max}$ equal the maximum power that could be transferred to the load and using this procedure yields the following equation*.

$$C = (R/2T)[e^{(T/RC)} - 1]^{-1} \qquad (37)$$

Inspection of this equation will show that it is transcendental in nature and an exact solution does not exist. Nevertheless, an approximate solution can be found*.

$$C = .73T/R \qquad (38)$$

Substitution of (37) in (33) and (34) yield an expression for the maximum transfer efficiencies attainable using a resistive charging network under high repetition rate conditions.

$$(P_o)_{max} = TV^2/5R \qquad (39)$$

$$\eta = 37\% \qquad (40)$$

---

*Appendix 1

- 33 -

is usually just the inherent or series resistance in the coil windings of the inductor. In commercially available inductors, this resistance is of low enough magnitude that transfer efficiencies greater than 90% are common. If the triggering sequence of the output switch is such that it keeps in step with the resonant transfer of energy from the source to storage element, the following condition holds true.

$$T_R = \pi (L_c C_s)^{1/2} \qquad (42)$$

Where L is the charging inductance, C the storage element capacitance and T_R is the resonant charging time.

It is useful to develop several design equations by which the average current capability of the power supply (I_{ave}) can be related to the usable values of the charging inductance, energy storage capacitance and desired repetition rate. Consider first the average current drawn from the source.

$$I_{ave} = Q/T \qquad (43)$$

where Q is the total charge transferred during the charging period T.

$$Q = CV_c \qquad (44)$$

with V_c being the capacitor voltage and C the storage element capacitance.

During resonant charging a voltage doubling occurs.[18] This is an important attribute of resonant charging in that for a

- 35 -

given output voltage only half as much supply voltage is required. Therefore

$$Q = 2CV_s \qquad (45)$$

where V_s is the supply voltage. Therefore

$$I_{ave} = 2CV_s/T \qquad (46)$$

Solving for the capacitance, we arrive at one design equation that is

$$C = I_{ave}T/2V_s \qquad (47)$$

Eliminating C in (47) by using equation (42) and solving for the inductance, we find

$$L = 2TV_s/\pi^2 I_{ave} \qquad (48)$$

The energy stored in the pulse forming network after charging is

$$E = 2CV_s^2 \qquad (49)$$

It should be noticed that in Figure 4.5 the pulse forming network (PFN) or energy storage element is discharged at the time of peak voltage. If the system was not discharged at this time, the flow of energy would reverse itself and flow backwards from the PFN to the source. Therefore, the PFN should be discharged at or near the peak system voltage in order to optimize energy transfer from source to PFN. This mode of operation with a given charging inductor and PFN capacitance will necessarily limit the repetition rate to a single frequency determined by the resonant frequency of the charging circuit.

A wider range of operational frequencies can be obtained by triggering the discharge on the rising portion of the PFN voltage voltage. This is the so called "linear" charging range ir that the wave front is approximately linearly increasing with time.[26] The cost of operating in the linear charging range as opposed to resonant charging is illustrated in Figure 4.7. It should be evident that for a given amount of switch jitter the possible variations in output voltage are much larger in linear charging because of the difference in the slope of the wavefront at the time of discharge. It also should be added that the transfer efficiency will be lower in the linear case thus detracting from its advantage of having a wider range of repetition rates than resonant charging. One simple, inexpensive modification that can significantly widen the operational frequencies of a resonant charging circuit is the addition of a high voltage chain of diodes in series with the charging inductor as shown in Figure 4.6. The high-voltage chain of diodes prevents the PFN from discharging back into the source during the course of a normal resonant charging cycle. Figure 4.8 illustrates the waveforms attained with this type of resonant charging circuit. T is the time period between discharge pulses while T_R is just the resonant charging time. It can be seen from the above figures that T, the time between discharges can be extended out to infinity if desired limited only by the leakage in the diode chain and dielectric. Since the pulse recurrence frequency or repetition rate is inversely proportional to this time (PRF T^{-1}) the repetition rate can span a range from zero pps (pulses per second) all the way up to twice the resonant charging frequency (i.e. $f = 2fo$)

and beyond if linear charging is acceptable. This technique of inductor-diode charging is probably the most commonly used because of the wide range of repetition rates available as well as the high transfer efficiencies attainable.

The actual transfer efficiency is given by the expression[21]

$$\eta = 1 - \pi/4Q \tag{50}$$

where Q is the quality factor of the charging circuit. The quality factor is given by

$$Q = \omega L/R \tag{51}$$

where ω is the angular oscillation frequency, and R is the total series resistance in the charging circuit.

Quality factors from ten to twenty are common in such circuits with efficiencies from 92% to 95% being readily achieved.

In summary, of all the charging schemes, resonant inductor charging with a series diode represents one of the most efficient charging techniques which also encompasses a fairly wide range of operational frequencies.[21] Another important characteristic of resonant charging is in its ability to double the input voltage. This relaxes the requirements of the power supply for a given output voltage. Resistive charging which has been shown to be highly inefficient under high repetition rate conditions should only be used in low power circuit and applications in which inefficiencies are unimportant.
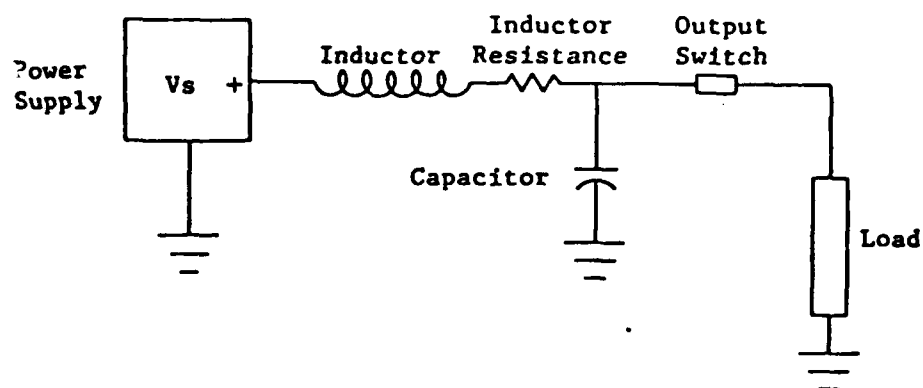
Fig 4.2a. Inductively charged circuit
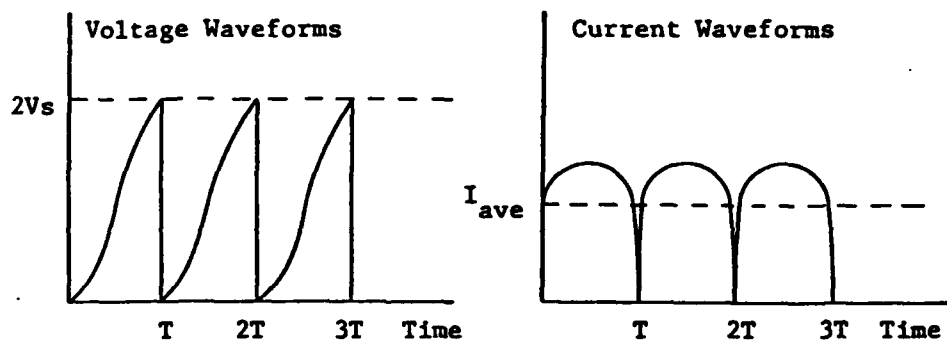
Fig 4.2b. Capacitor voltage and current waveforms in an inductively charged circuit
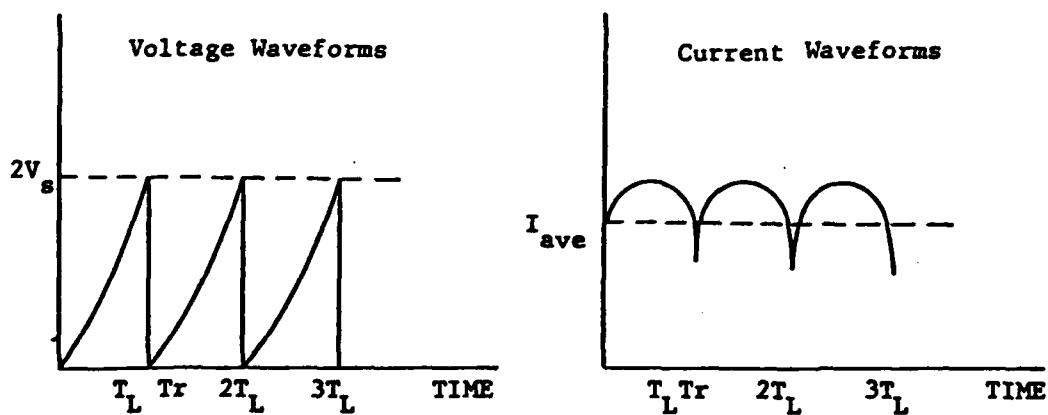
Fig 4.3. Capacitor voltage and current waveforms in the linear charging range
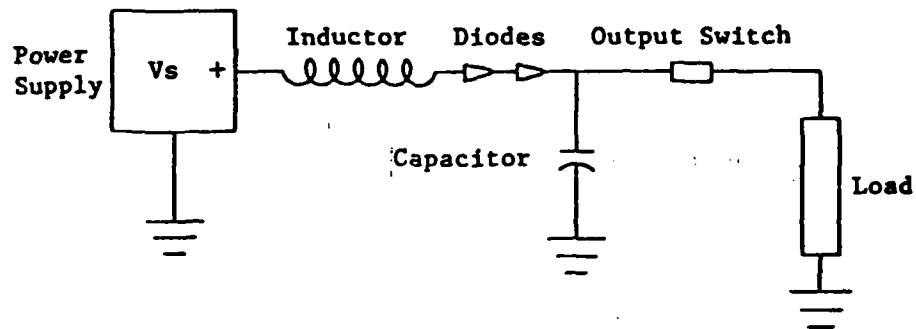
Fig 4.4. Inductor-diode charged circuit
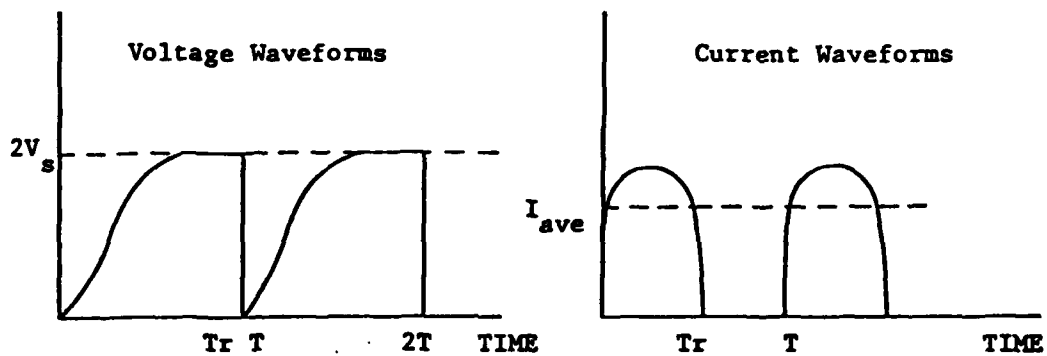
Fig 4.5. Capacitor voltage and current waveforms in an inductor-diode charged circuit

5. HIGH POWER PULSER DESIGN

Transmission Line Geometry and Power Transfer

The design of the present high power pulser electrical discharge circuit is based on the use of liquid filled transmission lines (LTL). Glycerine was selected for use because of its dielectric constant ($K = 44$), dielectric strength (> 20 kv/mm) and its electrical stability under no flow conditions. In any fast discharge circuit there are several design parameters that must be considered before the circuit is constructed. These are output energy, pulse shape and length, and load impedance. The first and the third parameters determine the maximum power input to the load when the source and load impedance are matched. In order to optimize conversion efficiencies, as well as reduce the variation in the driving force during the course of the discharge, it was decided to generate rectangular shaped pulses by the use of transmission lines. The pulse length was selected to be approximately 50 nsec because it represents a fairly optimal pulse length for many self-terminating UV lasers as well as keeping the length of the apparatus down to a reasonable size. The actual length will depend upon the speed of light in the dielectric medium used in the transmission lines. The speed of light in glycerine is given by the expression

$$c_k = c_v/K^{1/2} \tag{52}$$

Where c_k is the speed of light in a medium of dielectric constant K and c_v is the speed of light in a vacuum. Solving for c_k

$$c_k = (3 \times 10^{10} \text{ cm/sec})/(44)^{1/2} = 4.52 \times 10^9 \text{cm/sec}$$

Since the pulse length is the two-way transit time in the medium of interest[19]

$$c_{pk} = 2.26 \times 10^9 \text{ cm/sec}$$

where c_{pk} is the pulse velocity in a medium of dielectric constant k. Solving for the desired transmission line length using 50 nsec as the desired pulse length.

$$L_t = (c_{pk})(50 \text{ nsec}) = 113 \text{ cm} = 1.13 \text{ m}$$

The actual length of the constructed transmission lines is 122 cm., which gives an output pulse length (T_p) of

$$T_p = (1.22 \times 10^2 \text{ cm})/(2.26 \times 10^9 \text{ cm/sec}) = 54 \text{ nsec}$$

It should be apparent that for pulse lengths approaching, say a usec the device length would be over 74 feet. A device this size would have serious construction problems associated with it, especially those concerned with keeping a constant impedance over its entire length. It would be far simpler to utilize lumped parameter networks for pulse lengths this long.

The next parameter to be established is the output pulse energy. A value of 1 joule was initially chosen as a design point for several reasons. First, this represents enough energy to successfully drive many types of UV lasers.[22] Second, 1-joule per discharge

would minimize the electrode loading hopefully extending their useful lifetimes at high repetition rates. With this in mind, recall that the energy stored in a transmission line is by (6) equal to

$$E_{TL} = 1/2 \ CV^2$$

The capacitance C_{TL} of the transmission line is given by (11)

$$C_{TL} = \varepsilon \ wL/s = 44 \ \varepsilon_o wLo/s$$

The device length has already been determined by the output pulse length and is equal to 122 cm. Therefore

$$C = (5368 \ \varepsilon_o)w/s$$

For practical purposes of material selection, an electrode width of 1/2-inch was used.

$$C = (6817 \ \varepsilon_o)/s \tag{53}$$

The only remaining parameter is the separation distances. The last parameter's value can be determined from consideration of the load impedance. In order to maximize power transfer, the source impedance should be matched to the load impedance. It was determined from available data that a load impedance of 1 ohm was a realistic value for many types of discharges.[9] The impedance of a transmission line (Z_{TL}) is given by the expression[21]

$$Z_{TL} = 377s/\gamma^{1/2}w \qquad\qquad (54)$$

Using a value of 1 ohm for the load and transmission line impedances, the separation distance can be solved for because all the remaining variables, including the dielectric constant K and line width w are given. Therefore

$$s = Z_{TL}k^{1/2}w/377$$

$$s = (1\,\Omega)(44)^{1/2}(1.27 \text{ cm})/(377\,\Omega)$$

$$s = .02\text{cm}$$

Substituting this value in (53) and solving for the capacitance C.

$$C = 6817\,\epsilon_0/.02\text{cm}$$

$$C = (6817)(8.85 \text{ uf/cm})/(.02 \text{ cm})(10^8) = .03 \text{ uf}$$

or $\qquad C = 30 \text{ nf}$

Solving now for the voltage required to produce a 1 joule output pulse.

$$E = 1/2 \ CV^2$$

or $V = (2E/C)^{1/2}$ $\qquad\qquad (55)$

$$V = (2j/30\text{nf})^{1/2} = 8165 \text{ volts}$$

A quick check of the dielectric stress at these voltage levels for the prescribed separation distances will show that it exceeds the dielectric breakdown strength of glycerine. Therefore, it was necessary to increase the total capacitance of the transmission line by paralleling the three transmission lines in the present apparatus and operate into

a slightly mismatched mode in order to obtain 1 joule in the primary output pulse*. From a power delivering standpoint, a certain amount of mismatch can be tolerated without delivering a significant part of the stored energy after the main output pulse. Recall that the power output P_O is

$$P_O = I_O V_O \tag{56}$$

$$\text{where} \quad I_O = \frac{V_{TL}}{Z_{TL} + R}$$

$$\text{and} \quad V_O = \frac{V_{TL} R_L}{Z_{TL} + R_L}$$

Operating into a matched load, these expressions reduce to

$$I_O = V_O/2Z_{TL} \text{ and } V_O = V_{TL}/2$$

Therefore the maximum power output will be

$$(P_O)_{max} = \left(\frac{V_{TL}}{2Z_{TL}}\right)\left(\frac{V_{TL}}{2Z_{TL}}\right) = \frac{V_{TL}^2}{4Z_{TL}} \tag{57}$$

The power output into a mismatched load will be

$$P_O = \left(\frac{V_{TL}}{Z_{TL} + R_L}\right)\left(\frac{Z_{TL} R_L}{Z_{TL} + R_L}\right) = \frac{V_{TL}^2 R_L}{Z_{TL} + R_L} \tag{58}$$

---

*Increasing the capacitance allowed the separation distanced to be increase thereby increasing the effective breakdown strength while still keeping the impedance constant.

Taking the ratios of these two power outputs

$$Po/Po_{max} = \left(\frac{V_{TL}^2 R}{Z_{TL} + R}\right)^2 \quad \frac{V_{TL}^2}{4Z_{TL}} = \frac{4Z_{TL}R_L}{Z_{TL} + R_L} 2 \tag{59}$$

Let the load impedance R_L be given as a fraction x of the transmission line impedance

$$i.e. \ x = R_L/Z_{TL} \ or \ R_L = x \ Z_{TL}$$

Substituting this expression in (59) and reducing

$$Po/Po_{max} = \frac{4Z_{TL}(xZ_{TL})}{Z_{TL} + (xZ_{TL})^2} = \frac{4xZ_{TL}^2}{(1 + x)Z_{TL}^2} \tag{60}$$

$$P_o/Po_{max} = \frac{4 \ x}{(1 + x)^2} \quad with \ x = R_L/Z_{TL} \tag{61}$$

As an example, assume that it is desired to deliver at least 75 percent of the total available energy in the main pulse. Enter this value for P_o/P_{omax} and solve for x:

$$x = .33 \ or \ x = 2.80$$

If the load impedance is 1 ohm, then a transmission line impedance of either 3.3 or .36 ohms could be used with only a 25 percent loss of energy during the main pulse. It is always advisable to operate in a high to low impedance mode because more energy can be stored in the higher impedance line (almost two magnitudes more). This is a result of the fact that as the impedance increases for a given TL geometry,

- 46 -

the plate separation and the hold-off voltage also increases in the same ratio. On the other hand, the energy storage increases in quadrature with the hold-off voltage. Therefore, a doubling of the impedance and hold-off voltage will lead to a four-fold increase in the energy storage capability of the TL. Another advantage of using the higher impedance line is that since the pulse risetime is inversely proportional to the line impedance, a 3.3 ohm line can not only deliver more energy in the first pulse, but its risetime will be 30 percent of what could be achieved under a matched load situation. The only trade-off is a reduction in primary pulse transfer efficiency. Figure 5.1 is a graph of power transfer efficiencies versus load-line ratio. Figure 5.2 shows a diagram of the transmission lines constructed on the basis of the previous analysis. Copper straps were used to bus the three upper electrodes together to form an effective electrode width of one and one-half inches.

Pulse Charging Circuits

Liquid dielectrics such as glycerine and water while possessing characteristics favorable to their use in energy storage schemes do suffer from the effects of non-zero electrical conductivities. Because of the finite conductivities associated with all dielectrics, there always exists a certain amount of internal bleed-off charge occurring once the dielectric has been energized. The speed by which this bleed-off occurs is usually expressed by the internal RC decay constant of the dielectric. At one time constant only 40 percent of the
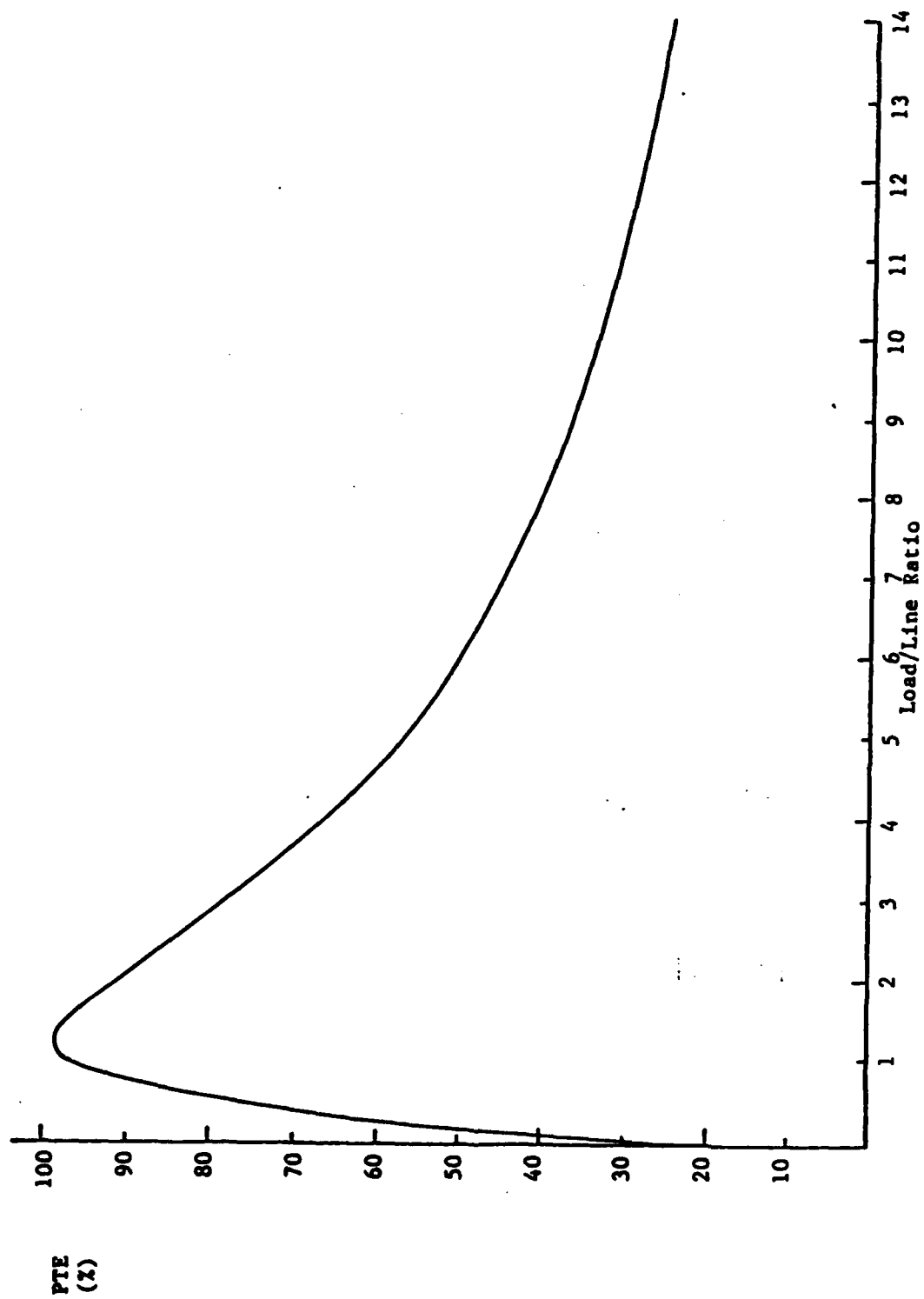
Fig 5.1. Power transfer efficiency versus the load/line ratio

- 48 -

Fig 5.2. Liquid dielectric transmission line

Lower Transmission Line Electrode

Upper Transmission Line Electrode

127 cm

Micrometers

15.2 cm

Dielectric Filled Space

Steel Support Structures

Plexiglass Support Structures
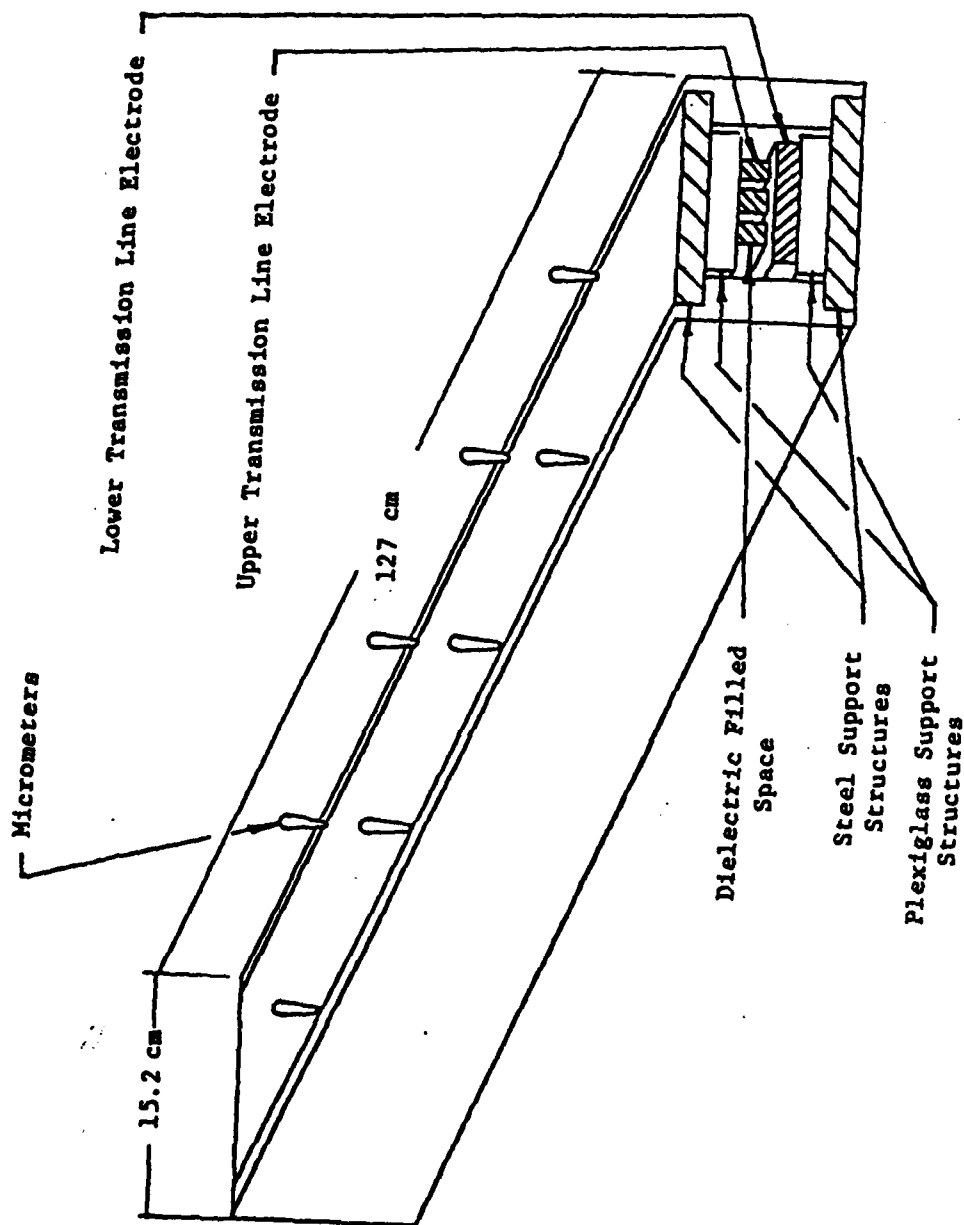
original amount of energy is left. The shorter the decay constant the faster bleed-off is occurring. The RC decay constant is equal to , the product of the resistivity and the dielectric permittivity.[11]* As an example of the time frames involved, consider the case of reasonably pure water having a typical resistivity of 1 MΩ-cm and a permittivity of 80 ϵ_o. The RC decay time in this instance will then be about 7.8 usecs. It should be clear that optimal energy use requires fast pulse charging of the liquid filled transmission lines. If one desires that losses during charging amount to no more than 10 percent, then the required charging time can be determined.

$$V(t) = V_o e^{-t/RC} \tag{62}$$

$$E \propto V(t)^2 \tag{63}$$

Letting RC = 7.8 usecs and $\left(V(t)/V_o\right)^2$ = .9 then the RC decay constant can be determined to be .41 usec. Therefore, the charging time should be no more than 1/2 usec in order to minimize losses during the charging cycle, hence the need for fast pulse charging circuits. A typical charging circuit utilizing a conventional solid dielectric capacitor only has to be charged a little faster than its discharge repetition rate. At a repetitive rate of 1 khz the necessary charging time is only 1 msec and is about 2,000 times slower than those required in liquid dielectric charging circuits.

The above case has been used to show the need for a fast pulse charging circuit in order to energize the liquid dielectric storage elements in the proper time frame. To this end there were two

pulse charging circuits built and tested to verify that they could meet the above criterion. The first consisted of a two-stage Marx Bank, shown in Figure 5.3. A Marx Bank consists of a number of capacitors charged in parallel and discharged in series. Because of this parallel-series mode of operation, a Marx-Bank realizes an output voltage which is equal to the charging voltage V_{in} multiplied by the number of stages N discharged in series (i.e. $V_{out} = NV_{in}$).[19] A two-stage Marx Bank will then be a voltage doubling circuit with an output capacitance equal to one-half the stage capacitance. The reduced capacitance on the output stage is a result of the conservation of energy and because capacitors discharged in series must acquire the same amount of charge.[7] The present Marx Bank has an output capacitance of about 53 nf with a maximum output voltage of 34 kv. This circuit was resistively charged because of the lack of an appropriate power supply and charging inductor. Later, funding allowed purchase of a 20 kv, 250 ma, 5 kw, power supply along with a 5 hy charging inductor. This allowed the use of a resonant charging technique to charge a single low inductance capacitor which was then switched in series with the liquid transmission lines by a jet blown spark gap. (Figure 5.3).[9] As discussed earlier, resonant techniques are very efficient energy users. This is the main reason for replacing the Marx Bank by a resonant scheme resulting in almost a ten-fold increase in efficiency. Most of this increase is related to the resonant versus resistive charging losses under high repetition rate conditions (7 percent for the resonant scheme and 64 percent for the resistive one). A second contributing factor is the ratio of the

source capacitance to the line capacitance for any charging configuration. If the source capacitance is too large (ratio > 1) there will be a late and inefficient flow of energy through the load after the passage of the main pulse. If this capacitance is too small (ratio < 1) there will be a significant voltage droop occurring during charging of the transmission lines. The most optimal ratio exists when source and line capacitances are approximately equal (i.e. ratio = 1).[23] In the case of the Marx Bank it was the voltage droop during charging that was minimized by the use of a large capacitance ratio (53 nf versus 5 to 15 nf). In the resonant scheme only one 15 nf capacitor was used allowing capacitances to be matched and thereby minimizing late and undesirable energy delivery. Even undesirable energy delivery. Even though some voltage droop does occur it is more important to make the best use of the available power than to achieve the highest output voltage. The amount of voltage droop occurring during such a charging cycle is:[23]

$$\Delta V/V = \Delta E/2E \qquad (64)$$

Therefore, a 50 percent energy removal from the capacitor will result in a transmission line voltage of 75 percent the original voltage on the charging capacitor.

Charging Network

The equations derived in the section on pulse charging circuits will be used here to size various circuit components given the

Power
Supply
(0 to 17 kV)

V_s +

R_1

R_3

A

Switch

B

R_4

Output Loop

R_2

R_1 = 3.43 M
R_2 = R_3 = R_4 = 112K
C_1^2 = C_2^3 = 105 nf (7, 15 mf capacitors in parallel)
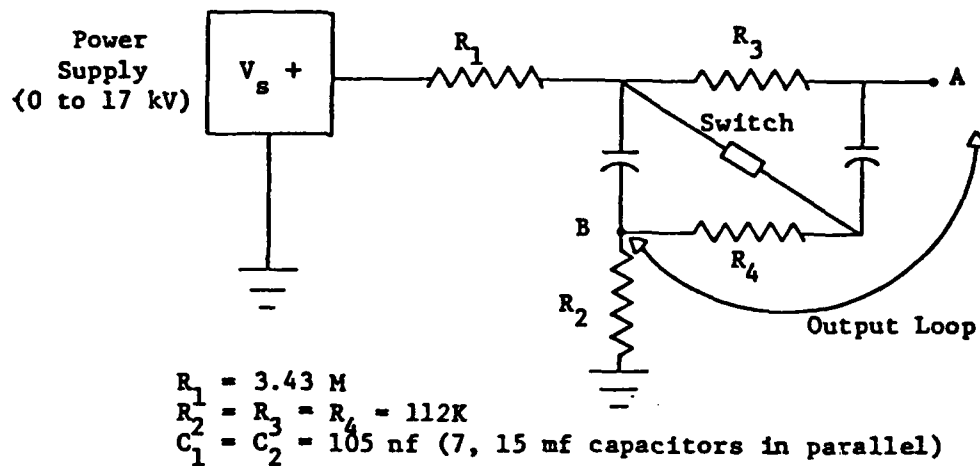
Fig. 5.3. Marx-Bank and charging circuit schematic

Power
Supply
(0 to 20 kV)

V_s +

L_1

D_1

Output Switch

Load
3 LTLS in
Parallel

L_1 = 5 hy
D_1 = 10, 5 kV diodes in series
C_1 = 15 nf
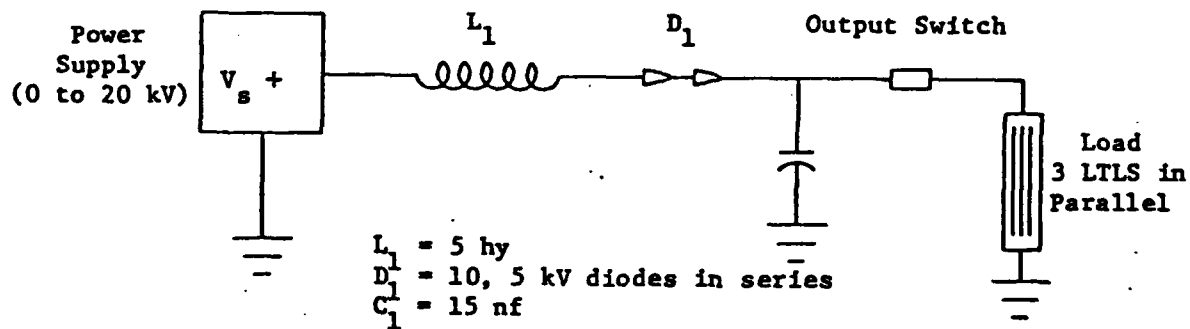
Fig. 5.4. Resonant charging circuit

- 53 -

charging circuit type and certain dependent system parameters. The dependent circuit parameters will be the average supply current and the pulse recurrence frequency (i.e., repetition rate). Since it has already been shown that inductor-diode resonant charging circuits are superior to ence frequency (i.e., repetition rate). Since it has already been shown that inductor-diode resonant charging circuits are superior to most others with regards to transfer efficiencies and range of operating frequencies, it is only logical that this is the type of circuit utilized. Figure 5.4 illustrates the configuration of the charging circuit including the values of some of the components. The power supply is a 20 kv, 250 ma, 5 kw unit (Hippotronics Model). The discharge capacitor is a 50 kv, 15 nf low inductance discharge capacitor rated at 360 pps (pulses per second). Since this capacitor is to be operated at only a fraction of the rated voltage, its operating range with respect to repetition rate may be correspondingly increased. The rated power output of this capacitor is 6,750 watts at 50 kv and 360 pps with a certain percentage of this power appearing as internal heat. At an operating voltage of say 10 kv, the repetition may be increased to $(50/10)^{1/2}(360$ pps$)$ = 9000 Hertz without increasing the internal losses of the capacitor. One of the most common modes of failure in this type of capacitor are thermal instabilities caused by overheating of the dielectric. Therefore, at 10 kv, the usable repetition rate of this capacitor can be well into the kilohertz range without reducing its useful lifetime. One of the primary design criterion for this charging circuit was that the operating frequency should extend into the kilohertz range. With this in mind, recall that

This is about 23 percent of the total power available. A high voltage diode chain has also been added to this circuit to allow operation below the resonant frequency. If it was desired to use all of the available power, a much larger inductor would be needed. This would necessarily mean a reduction in the repetition rate possible. The size of this inductor is determined by the maximum voltage and average current needed. This would necessarily mean a reduction in the repetition rate possible. The size of this inductor is determined by the maximum voltage and average current capabilities of the supply.

$$Z_{TL} = (20 \text{ kv})/(.25A) = 80,000 \text{ ohm}$$

$$\text{with } Z_{TL} = (L/C)^{1/2} \text{ with } C = 15 \text{ nf}$$

$$\text{Therefore } L = Z_{TL}^2 C = (80,000 \Omega)^2 (15 \times 10^{-9} \text{nf}) = 96 \text{ hy}$$

The repetition rate corresponding to this size inductor would be only 265 Hertz. The pulse energy available from the charged capacitor can be determined from the voltage doubling that occurs along with a measurement of the dissipation factor of the charging inductor. The dissipation factor (D.F.) was measured on an impedance bridge* to be 7 percent Referring back to equation (50), the quality factor Q of this circuit can be determined to have a value slightly greater than 11. Using the measured value of the dissipation factor, the maximum charging voltage on the capacitor can be calculated by consideration of

---

*ESI Impedance Bridge Model 252

the repetition rate f is equal to twice the natural resonant frequency of the charging circuit. The resonant frequency of the circuit is given by T_R^{-1}. Therefore

$$f_o = 1/2\pi (LC)^{1/2} \quad \text{or} \quad f = 1/\pi (LC)^{1/2}$$

Using 1 kiloherz as a design point the required size of the inductor may be determined

$$L = 1/\pi^2 f^2 2C = 1/(3.14)^2 (1000 \text{ sec}^{-1})^2 (15 \times 10^{-9} \text{nf}) = 6.75 \text{ hy}$$

In selecting a commercially available charging inductor, a 10 kw, 5 hy model was finally chosen. This allows a repetition rate of 1162 herz to be reached in the normal resonant range of operation.* The maximum voltage that can be used is determined by the product of the average supply current and the effective impedance presented to supply by the charging inductor (i.e. $V_{max} = Z_{TL}I_{ave}$ with $Z_{TL} = L$).

Since $= 2\pi f_o$ then $Z_{TL} = (2)(3.14)(581 \text{ sec}^{-1})(5 \text{ hy}) = 18.25 \text{ k}\Omega$

$$\text{and } V_{max} = (18,250 \Omega)(.25A) = 4562 \text{ volts}$$

From this operating voltage the maximum power drawn from the supply may be determined.

$$P_{out} = V_{max}I_{max} = (4562V)(.25A) = 1140 \text{ watts}$$

---

*The charging cycle may be operated above this point into the linear range but at a sacrifice in output voltage and decreased pulse to pulse reproducibility.

the energy flow from the supply to the capacitor.

$$(V_s)_{max} = 4562 \text{ volts}$$

$$(E_c) \text{ theoretical} = 2C(V_s)_{max}^2 = 1/2(C)(V_c)^2_{max}$$

$$(E_c) \text{ practical} = (1 - D.F.)(E_c) \text{ theoretical}$$

Solving for $(V_c)_{max}$

$$(V_c)_{max} = 2 (V_s)_{max} [1 - D.F.]^{1/2}$$

$$(V_c)_{max} = (2)(4562V)(1-.07)^{1/2} = 8799 \text{ volts}$$

The maximum energy available from the pulse charging network will then be

$$E_c = 1/2 \ CV^2 = (1/2)(15 \times 10^{-9} nf)(8799V)^2$$

$$E_c = .58 \text{ joules}$$

This value of 1/2 joule is only half of the stored energy necessary to realize 1 joule on the output end of the transmission lines. This situation was born out of the need to select an all around power supply for the laboratory and still operate in the kilohertz range. This naturally resulted in a sacrifice in pulse energy on the ouput. If the repetition rate is reduced, then the output pulse energy can be increased up to almost 12 joules per shot.* Thus an extended range of output pulse energies is available by varying the size of the charging inductor and the corresponding repetition rate for a given size discharge capacitor.

---

*This assumes that only 90 percent of the energy appearing at the discharge capacitor will be available at the load.

6. EXPERIMENTATION

Testing Overview

The testing phases of the present research effort consisted of several parts. The first part revolved around the selection and testing of the liquid dielectrics considered most suitable for incorporating into a liquid filled transmission line (LTL). The two primary candidates were water and glycerine. The most important electrical properties and energy storage capabilities of these two liquids have already been given in Table 1. Referring back to that table, both liquids appear to have suitable energy storage capabilities with water having the ability to deliver a longer pulse for a given transmission line length. Glycerine on the other hand, with its higher dielectric strength, can deliver more power to the load, again for a certain size transmission line. Since each one of these dielectrics possessed certain characteristics favorable to their use, both were tested to determine whether or not there were any operational differences between them. A Marx-Bank was first used to pulse charge a single liquid transmission line filled with either glycerine or water. These two dielectrics were tested in order to determine their maximum practical working voltages as well as their healing times under fault conditions. It was established during this series of experiments that glycerine was more electrically stable than water under no flow conditions. This was evidenced by the fact that water failed to achieve the expected hold-off voltage of 15 kv/mm.

Experimentation then turned towards measurements of the LTL's charging times with glycerine as the dielectric. Subsequent experiments were aimed at measurements of the risetimes and rates of rise of the current pulses under varying conditions of output inductance and impedance. These latter experiments shed considerable light on the transition region between a lumped parameter and distributed parameter network. The final product of all the above experiments was the gaining of an in-depth understanding of the operating characteristics of LTLs.

During the experiments involved with understanding the characteristics of the transmission lines there was a parallel development of fast pulse charging circuits used to energize the LTLs. The first circuit, a Marx-Bank while fast was deemed far too inefficient because it resistively draws its energy from the power supply. Therefore, this circuit was later replaced with resonant charging network that increased the total overall power transfer efficiency by almost a factor of 10. Final testing was undertaken with this latter system.

Marx Bank Testing

The first pulse charging circuit constructed was a 34 kv, 53 nf two-stage Marx-Bank. The capacitors used in the Marx-Bank are 50 kv, 15 nf capacitors from Sangamo. Figure 6.1 shows the entire Bank which consisted of two stages of seven capacitors per stage. It was necessary to parallel this number of capacitors in order to increase the output capacitance of the Marx-Bank (53 nf) to a value high enough so as to prevent significant voltage droop from occurring during

- 59 -

charging of the transmission lines. The bank was resistively charged
as shown in Figure 5.2. Erection of the Marx-Bank occurred via a
standard air-filled spark gap shown in Figure 6.2. One of the elec-
trodes was threaded and moveable, enabling the gap spacing to be varied
thereby changing its breakdown voltage and the output voltage of the
Marx-Bank. Operating characteristics of the spark gap and supply
limited this range to from several kv to almost 35 kv. A typical open
circuited output voltage waveform of the Marx-Bank is shown in Figures
6.3 through 6.4.

The output voltage has a 10-90% risetime of about 23 nsec
(Figure 6.4). The speed of the Bank was therefore deemed fast enough
to pulse charge the TLs in the time frames of interest (i.e. less
than several μsecs). The actual charging of the TLs was accomplished
by way of an isolating gap (Figure 6.5) set to be statically triggered
on the erection peak of the Marx-Bank. This gap's static breakdown
voltage was also variable in the same manner as the Marx-Bank gap.
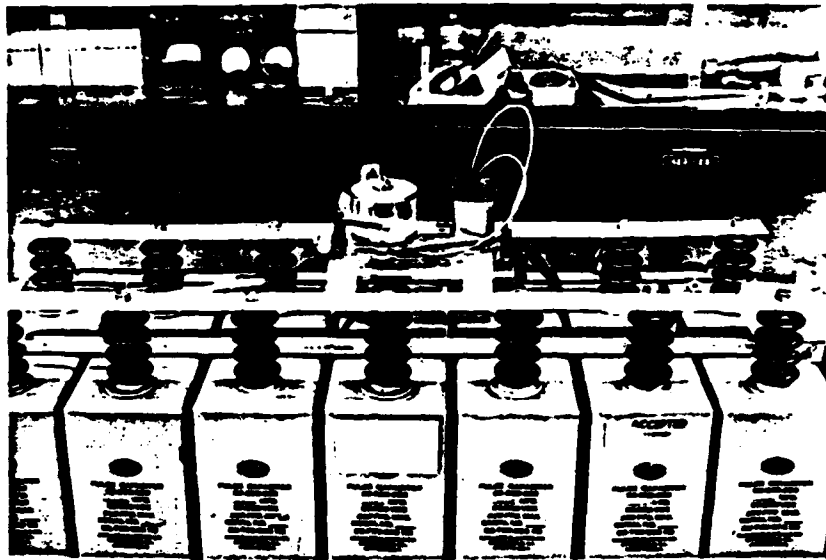
Fig. 6.1. High Voltage Marx-Bank and Transmission Lines
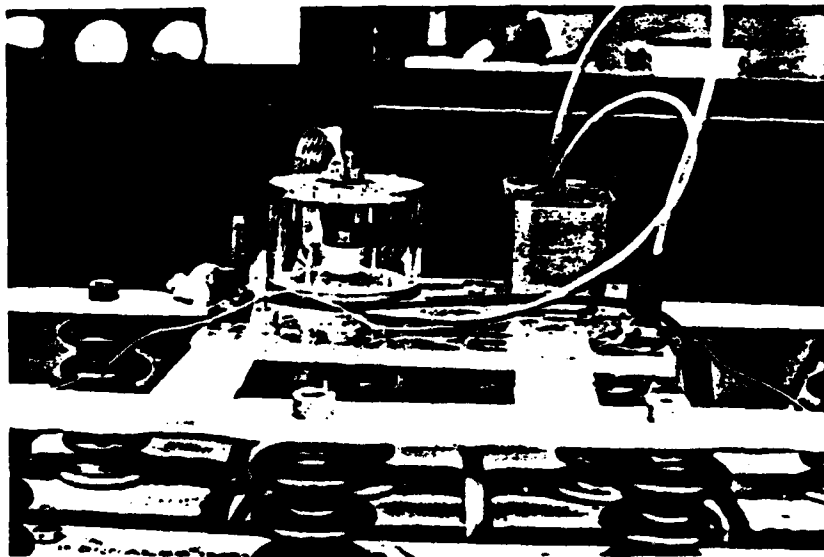
Fig. 6.2. Marx-Bank erection spark gap

Water Tests

Water was selected first for testing because it was available in a very pure form.* The basic procedure was to prepare the TL structure by thoroughly cleaning the interior with alcohol, enter the water as quickly as possible and then immediately begin testing. The quickness with which each of these latter two tasks was accomplished was deemed necessary in order to minimize the diffusion of ion products and contaminants into the high field regions of the TLs. The ion products and contaminants were assumed to be forming at the mild steel-water interface by the dissolving action of the water. Initially, tests at a 1 mm electrode separation were very negative. Supposedly the maximum practical working stresses on a negative electrode in water should be about 15 kv/mm. The first tests were at 14 kv/mm and breakdown through the TLs occurred on every charging cycle. The TLs were then drained and inspected for damage. The internal discharges had caused the appearance of small pits on the line structures. It was encouraging that these pits were not localized near the edges or ends of the lines. Both of these areas had been radiused to prevent field enhancement and premature breakdown. Nor were these pits localized at any certain point on the lines but were distributed rather evenly over the midsection of the line. From this evidence it was concluded that even though the expected field strengths were not reached, the electric field region of the TL structure was of a fairly uniform quality and the breakdowns occurring were statistically

---

*Distilled in a two-stage all quartz condensing unit.
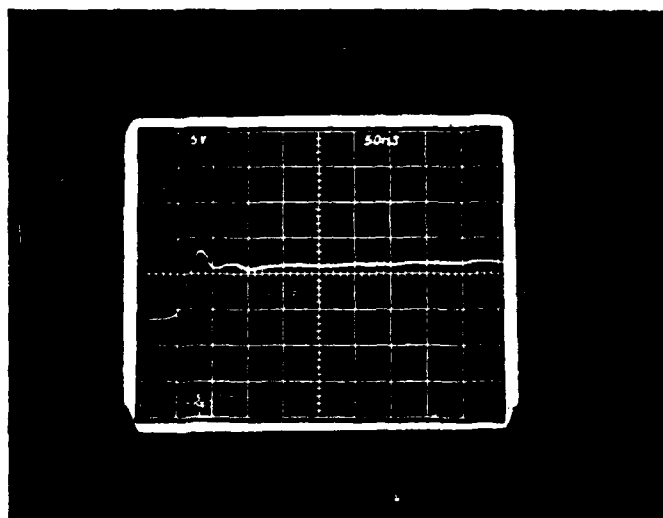
Fig. 6.3. Marx-Bank output voltage waveform
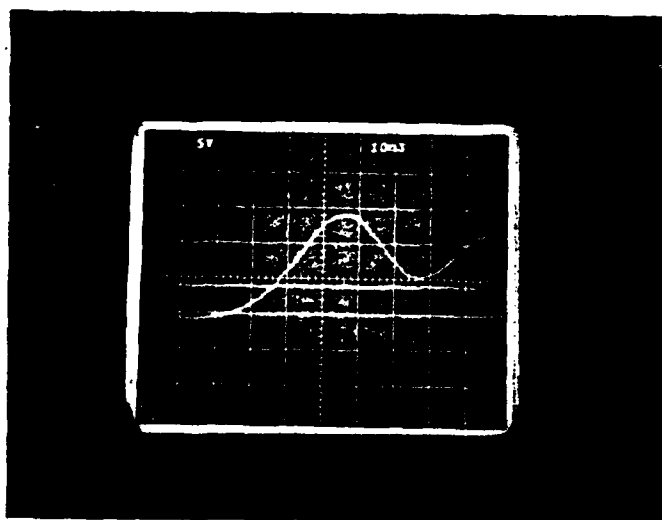
Fig. 6.4. Marx-Bank output voltage waveform (22 nsec risetime, 10-90%)

- 63 -

located. This simply means that the breakdowns were occurring at those instances in time at which the right conditions just happen to exist. Subsequent field strength testing of water occurred by lowering the voltage in 2 kv increments from the original 14 kv test voltage. In each of these tests only one TL was used with a constant spacing of 1 mm. After each test the system was drained, dismantled and painstakingly cleaned. All of the discharge pits from the previous experiment were smoothed off with very fine emery cloth. The test voltage steadily decreased downward from 12 kv to 10 kv to 8 kv, and finally, at 6,000 volts, hold-off occurred and sparking took place on the output gaps of the TLs. The output gaps consisted of opposing 1/8-inch diameter stainless steel pin electrodes of variable spacing. Testing proceeded around the 6 kv hold-off voltage and it was determined experimentally that the maximum stress obtainable with water under static or no flow conditions was no more than 7 kv/mm. This reduced the storage capabilities of water by more than a factor of four. The reason for this poor performance by water is probably related to the ionization products being produced through contact with the mild-steel box structure in which the three stainless steel TLs are housed. From conversations with several knowledgeable individuals as well as documentation found in several articles it was concluded that without continual flow and deionization, water would only be a substandard energy storage medium.[18,23] For the lack of a suitable deionizing and filtering system, it was decided to abandon the use of water and turn to glycerine instead.

Glycerine Tests

Reagent grade glycerine was obtained from the Chemistry Department and used to replace water as the TL medium. The results of the change were very positive. At two different spacings, 1/2 and 1 mm, breakdown strengths of 21 and 23 kv per mm were achieved with 200 to 300 nsec charging times. This is an average of 22 kv/mm and not too much different from the 25 kv/mm referenced in Table 1. All subsequent experimentation in this research program was with glycerine and no other liquid dielectrics were tested.

Self-Healing Times

One of the most important properties of liquid dielectrics is their ability to heal themselves once an internal discharge through them has occurred. In this respect it was decided to visually observe breakdown and then reapply system voltage with a varying time lag between breakdown and voltage application. This same experiment had been run earlier with water with the following results. The self-healing time of water was found to be fairly fast. After breakdown had occurred, the voltage was reapplied at a reduced level by varying the input voltage from the power supply. It was found that most of the time the system voltage could not be reapplied fast enough to cause premature or anomalous breakdown. No visual change in the medium was observed. Glycerine on the other hand reacted somewhat different. Every time an internal breakdown occurred there appeared a black cloud of ionization products along the trail of the discharge. If the voltage was reapplied too fast, anomalous breakdown occurred usually

- 65 -

very close to the region of the last breakdown. It took anywhere from 10-30 seconds for glycerine to heal depending upon the severity of the breakdown and the number of times that it occurred at any one location. Visually it could be seen that the black ionization products would slowly rise to the surface of the liquid. It might be that once the chain of ionization products from one electrode to the other has been sufficiently broken, the hold-off voltage will reappear.

These experiments showed that water clearly holds an edge over the more viscous glycerine regarding healing times. If glycerine is to be used in a highly stressed, high repetition rate mode there should be some sort of fault indicator and relay network used to interrupt the flow of energy for a time period sufficiently long enough for the dielectric to heal itself. In this respect it would also be very desirable to circulate the fluid and filter any contaminants from it. With water this can be accomplished rather easily, while with glycerine it presents a problem because of its higher viscosity.

TL Charging Voltage Waveforms

Since efficient use of the energy storage capabilities of liquids require the systems to be pulse-charged, it would be instructive to measure the actual charging times involved in the present system and determine the relative magnitude of the internal losses caused by bleed-off during the charging cycle. During the charging cycle a TL acts as a capacitor with a time constant of $_c$. The waveforms in Figures 6.6 through 6.10 are representative of the charging waveforms on the TL when pulse charged from the Marx Bank. The

voltage risetime from zero to 95% full charge ($5\tau_c$) varies from 100 nsec in Figure 6.6 to 250 usec in Figure 6.9. Comparison of the waveforms shows that there is a distinct difference between them with respect to the waveshape at the time of breakdown. It should be remembered that the discharge is operating in a self-breakdown mode. A tesla coil arc was applied to the lower electrode to provide the discharge gap with some initial ionization which reduced the static breakdown voltage for a given gap separation. The optimum breakdown mode occurred when the peak charging voltage was just enough to cause breakdown. If the voltage is insufficient to cause breakdown, no discharge will take place and the TL's entire supply of stored charge will bleed-off internally, resulting in an efficiency factor of zero for that particular pulse. If on the other hand the peak charging voltage is much greater than that required for breakdown, discharge of the TLs will take place on the rising portion of the wavefront. Since the risetime of the charging voltage on the TLs is <u>independent</u> of the final peak voltage,* premature breakdown will occur with a concomitant reduction in risetime. That is exactly what occurs in the above photographs. In Figure 6.6 the input charging voltage is clearly much more than is required to initiate conduction. Close inspection of Figure 6.6 will reveal that after initial breakdown takes place at Point A, the voltage levels off from A and B and then proceeds to fall toward zero. This leveling off is the result of an interaction between the charging and discharging voltage pulses. The discharge pulse can

---

*See Equation 40 - 67 -

- 67 -
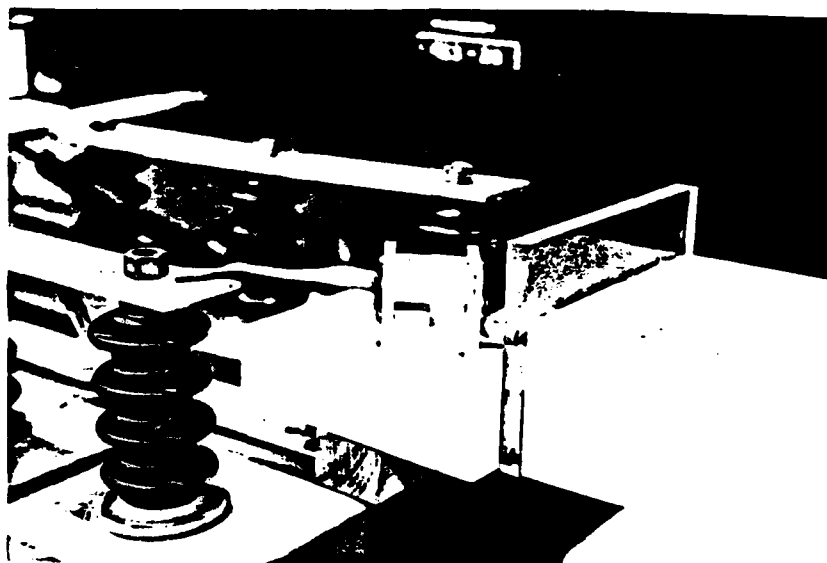
Fig. 6.5. Marx-Bank isolating spark gap
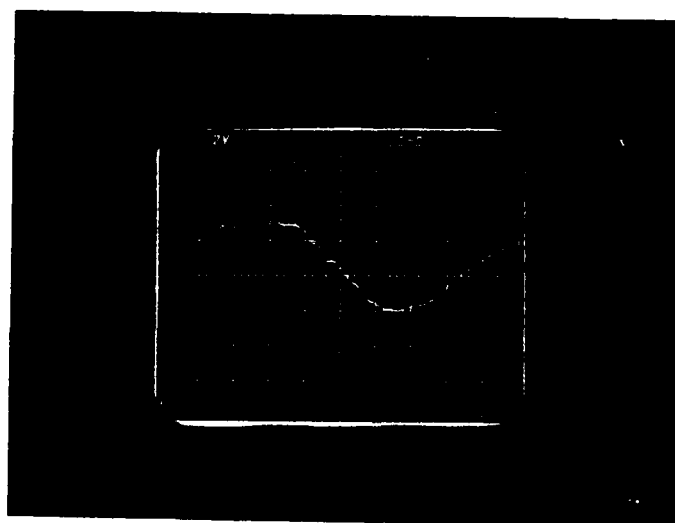
Fig. 6.6. TL charging voltage waveform (Anomalous breakdown)
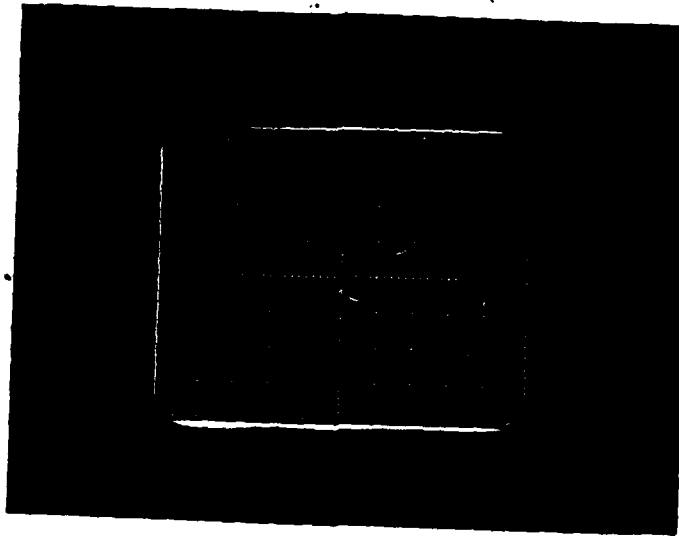
Fig. 6.7. TL charging voltage waveform
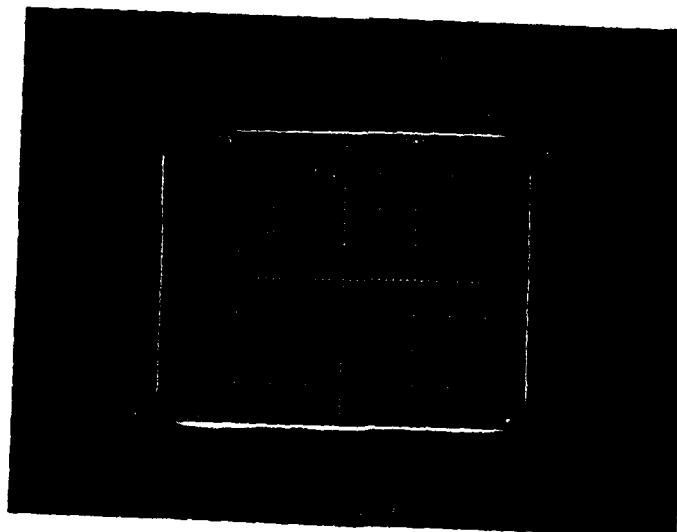
Fig. 6.8. TL charging voltage waveform
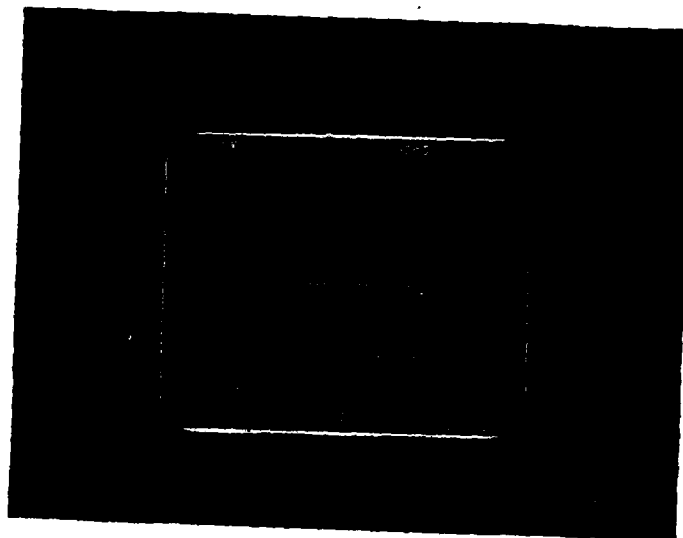
Fig. 6.9. TL charging voltage waveform
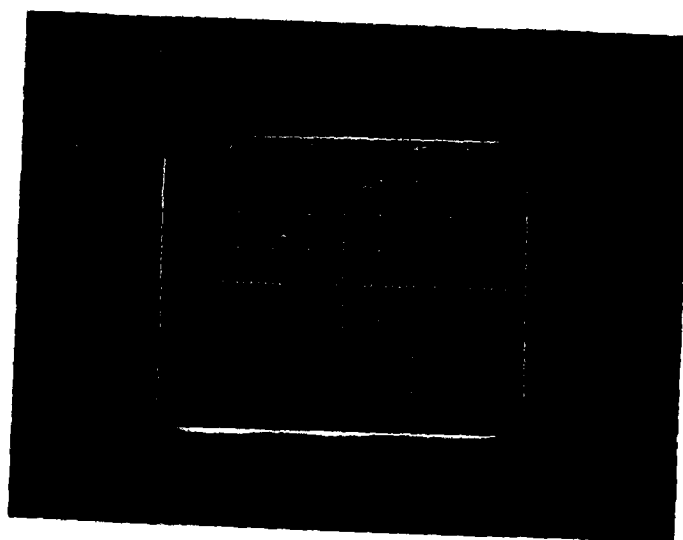
Fig. 6.10. TL charging voltage waveform

be modeled as a negative voltage wave appearing at the instant of breakdown and traveling in the opposite direction as the charging pulse. If the system voltage would have peaked out at the time of discharge the resulting waveform would show only a gradual decline toward zero potential and no step would have occurred (see Figure 6.9-6.11). But, if the voltage is still rising at the time of breakdown the negative voltage wave will encounter a rapidly changing positive wave and application of the principle of superposition will show that an intermediate voltage step can appear. As the gap separation is increased which corresponds to an increase in static breakdown strength, the waveforms start to assume the proper shape (see Figures 6.8 and 6.9). Notice how breakdown occurs on the rounded, slowly changing portion of the waveform. This indicates that peaking is occurring at the time of discharge. Pulse charging is inefficient enough without also operating in a premature breakdown mode. This type of operation can easily be avoided by proper adjustment of the input voltage. For any given electrode spacing, the input voltage should be slowly raised until a consistent sparking action results. This will ensure optimum use of the available energy in the pulse charging circuit.

At this point it should be stressed that even though over-voltaging is a common technique for causing uniform discharge breakdown along a laser channel, it is definitely not energy efficient in pulse charging circuits. The function of uniform discharge triggering has to be separated from the charging circuit in order to achieve both goals

of efficient energy use and uniform discharge triggering. On the average, the charging time for the TLs is about 250 msec. This is approximately equivalent to a 1 MHz charging signal. From Von Hipple,[23] the loss tangent (δ) for glycerine at 1 MHz is approximately $300 \times 10^{+4}$. Charging losses are therefore about 2%. Since the TLs do not always discharge exactly on the voltage peak, but are sometimes delayed, there are additional losses which occur by internal bleedoff. These latter losses may be determined by consideration of the RC decay constant for a DC signal. This constant has previously been given by $\eta\epsilon$, where η is the dielectric resistivity and ϵ the permittivity. The resistivity of glycerine is given by reference (24) to be 15.6 mΩ-cm and ϵ the permittivity is given by the same reference to be 3.9×10^{10} f/m.

Therefore $RC = \eta\epsilon = (15.6 \text{ m}\Omega\text{-cm})(3.9 \times 10^{-8} \text{ f/cm}) = 60.8$ usec

The magnitude of the internal energy loss will be equal to

$$\text{Loss} = [1-(V(t)/Vpk)]$$

with $V(t) = V_{pk} [1-e^{t/RC})]$ where t becomes the time lag interval. From Figure 6.10 this is determined to be no more than 100 nsec. Substituting this value into the time interval, the internal losses due to bleed-off are found to be much less than 1%. Therefore in this case, the major portion of the losses occur during the initial charging cycle and time lag decay losses are minimal.

In all the aforementioned cases, the Marx-Bank was the primary source for the pulse charging circuit. Later measurements with

the resonant charging scheme yielded somewhat better results. The busbar impedance between the discharge capacitor and the TLs was significantly reduced by decreasing the conductor separation, (Figure 6.11), thereby increasing the peak charging current of the circuit. This naturally led to a decrease in the voltage risetime on the TLs from 250 nsec to approximately 180 nsec (see the lower trace in Figure 6.20). This increased rate of charging will naturally reduce bleedoff losses, but it will also increase the skin losses associated with the higher discharge currents and charging frequency. From an efficiency standpoint, the shorter 180 nsec charging times are probably not much better than the longer 250 nsec ones for these reasons.

Capacitive Matching

The major difference in the two pulse charging circuits utilized is the output capacitance of each. The lower output capacitance of the resonant scheme (15 nf) as compared to the Marx network (53 nf) will enable it to be more closely matched to that of the transmission lines. It should be remembered that exact capacitive matching between source and load (TLs) will maximize the power transfer efficiency. Figures 6.12 and 6.13 show the source voltage of the capacitor as a function of time in the resonant case. Notice that the peak charging voltage is about 4.4 kv before discharge and about 2.2 kv after it has discharged and energized the TLs. These values of initial and final capacitor voltages reflect the fact that resonant transfer of the energy from the capacitor to the storage line is not occurring,
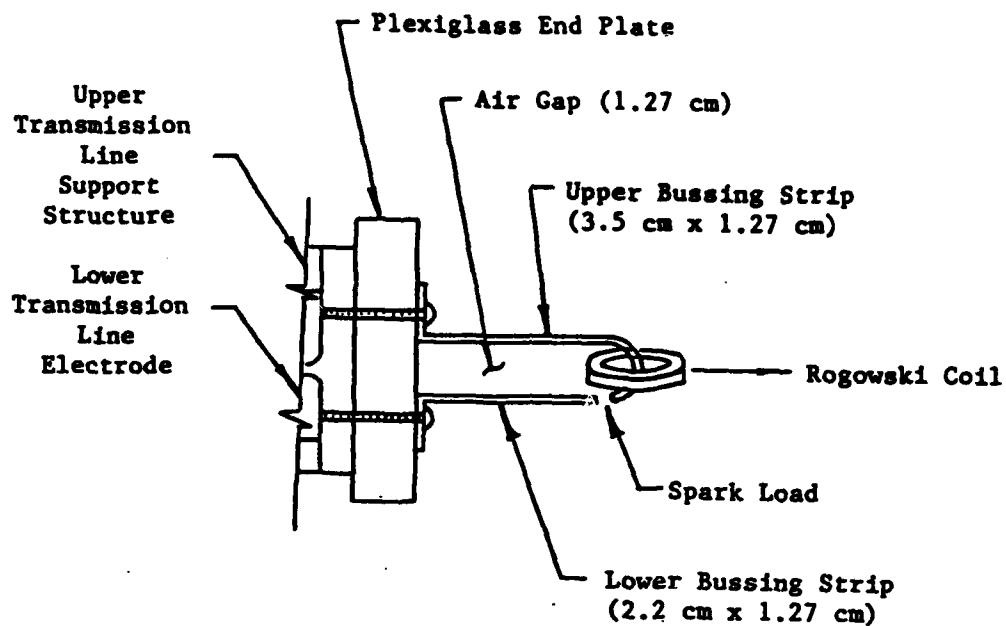
Fig. 6.11. New busbar configuration
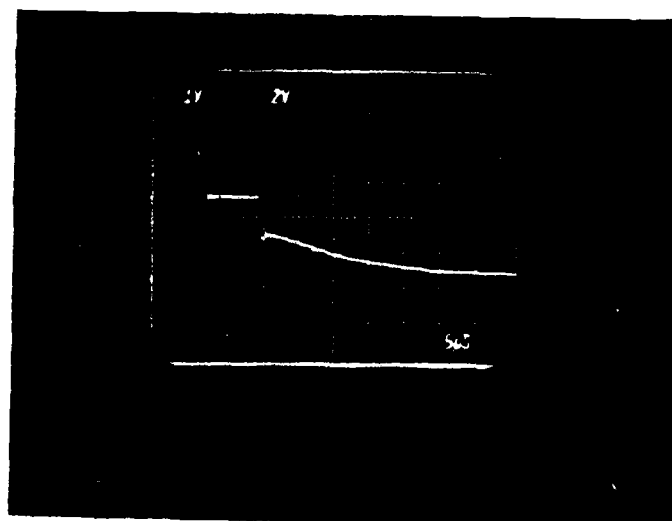
Fig. 6.12. Capacitor voltage, before and after breakdown

otherwise the capacitor voltage would be reduced to zero. Analysis of the waveforms for the capacitive matching experiments (Figures 6.18 and 6.19) show that at the charging frequency of 1.4 MHz the quality factor of the circuit is less than 3. From this value of the quality factor it can be determined from equation (50) that the transfer efficiency should be about 70 percent. This agrees well with the 25 percent of the total amount of initial system energy remaining on the capacitor as determined from the voltage on the capacitor (2.2 kv) after charging of the TLs. Another phenomenom that is apparently occurring at low repetition rates is bleed-off of the capacitor. Notice in Figure 6.12 that the voltage level at the time of discharge is significantly less than just after resonant recharging has occurred. The explanation for this phenomenom probably lies in the quality of the diode chain chosen to prevent this type of bleedoff. It appears that there is insufficient reverse blocking impedance for keeping the capacitor fully charged for more than a fraction of a second. It should be added that at higher repetition rates there is no bleed-off noticeable (Figure 6.14 through 6.15). This condition can probably be lived with or corrected by using a better quality diode. Capacitive matching between source and load is very important because it minimizes late and undesirable energy delivery. Figures 6.16 through 6.19 illustrate this behavior.

Figures 6.16 and 6.17 were taken with the Marx-Bank as the pulse charging source. Notice how both figures show the existence of two distinct oscillation frequencies. The higher frequency corresponds to the TL discharge while the one its superimposed on belongs to the

- 75 -
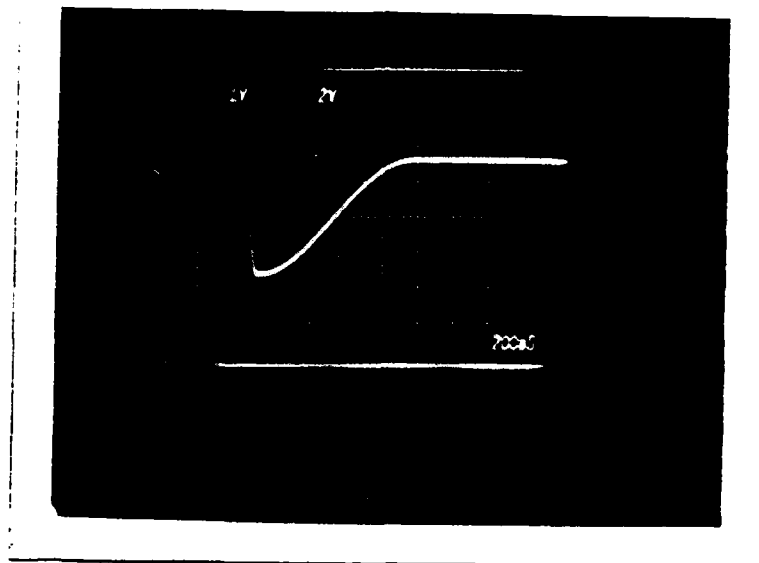
Fig. 6.13. Capacitor voltage, before and after breakdown
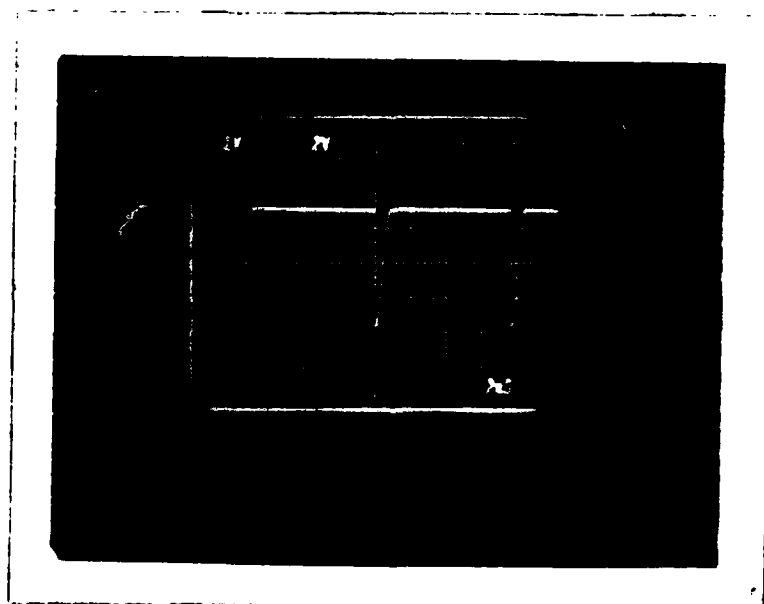
Fig. 6.14. Capacitor voltage (143 pps)

- 76 -

discharging Marx-Bank. The difference between these two photographs lies in the capacitance of the TL as compared to that of the Marx. Figure 6.18 has a much lower capacitance associated with it than Figure 6.19. It should also be remembered that the impedance of the TL is inversely proportional to its capacitance. Therefore, a lower capacitive TL should also have a higher output impedance which would reduce the first current peak it experiences for a given charging voltage. That is exactly what is borne out in Figures 6.18 and 6.19 These photographs were taken with a Tektronix 7504 single beam oscilloscope and a Physics International model 205 Rogowski coil. The coil was accidentally linked backwards by the discharge loop for these experiments, hence the need to have the voltage inverted on the scope. Later, the same experiment was repeated but with the resonant charging network and a Tektronix dual beam 7704 oscilloscope. The resonant charging scheme with its lower output capacitance allowed it to be exactly matched to the TL, while the dual beam capability allowed observation of both the current and the voltage simultaneously. Notice in Figure 6.20 how the envelope of the TL current and voltage oscillations decay rather uniformly to zero. On the other hand, in Figure 6.21 there is a distinct and appreciable driving force acting past the time at which the TL oscillations have died out. This clearly shows the need to operate pulse charging circuits in capacitive matched modes in order to make the best possible use of the available energy.
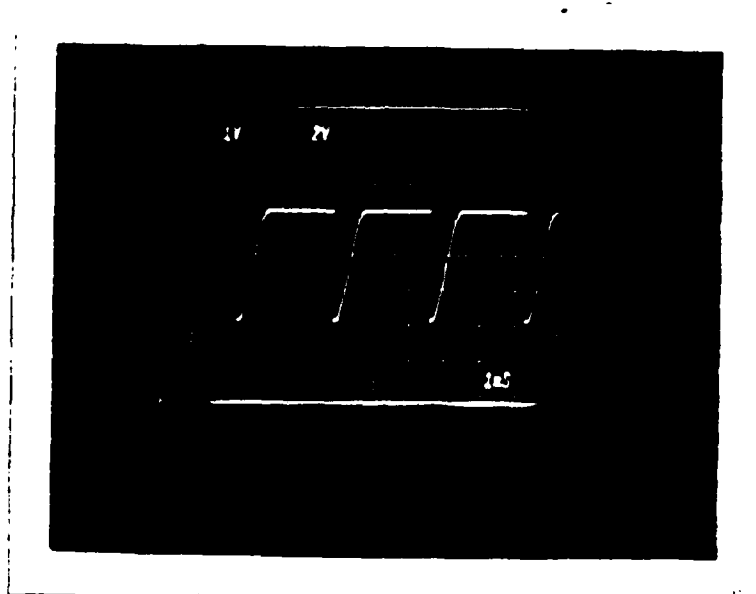
Fig. 6.15. Capacitor voltage (555 pps)
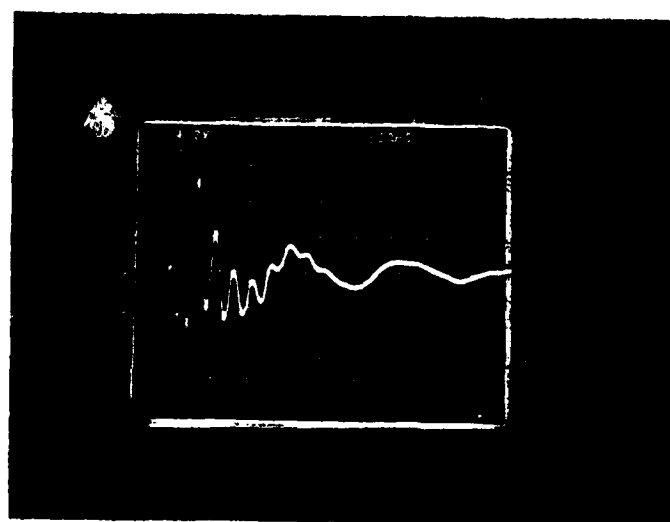
Fig. 6.16. TL current output waveform (source capacitance = 6TL capacitance)
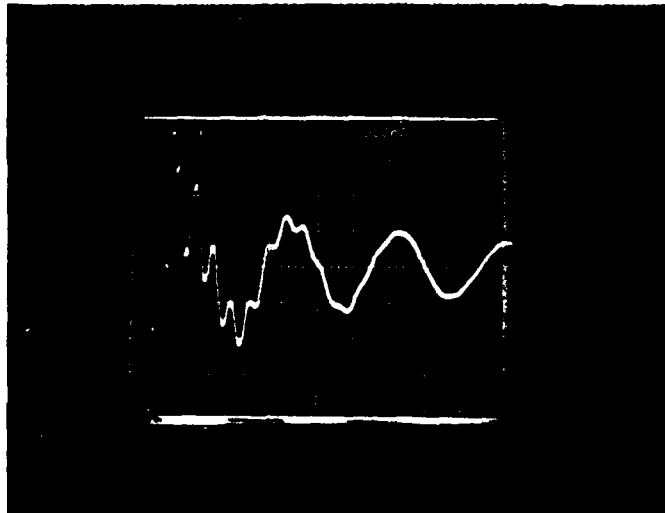
Fig. 6.17. TL current output waveform (source capacitance = 10 TL capacitance)
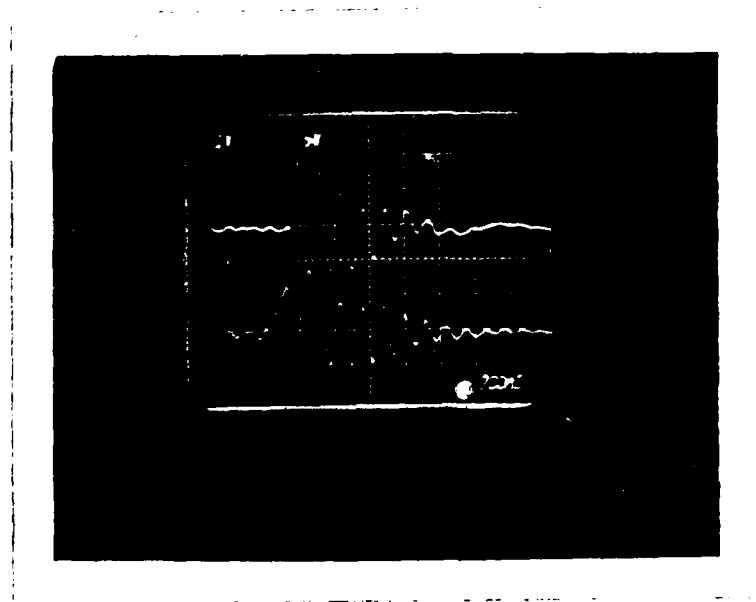
Fig. 6.18. TL current and voltage waveforms (source capacitance = TL capacitance)
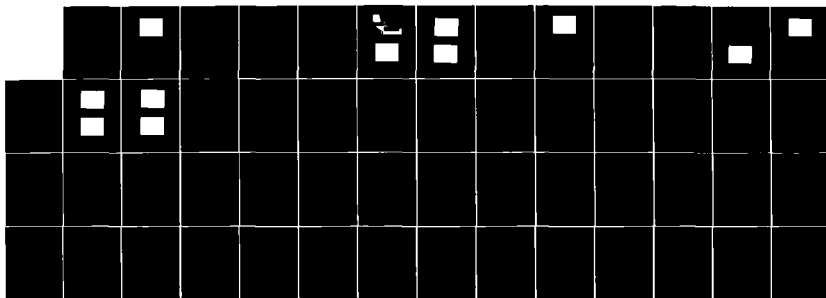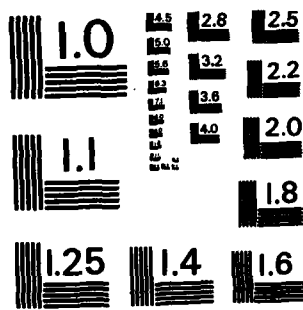
MICROCOPY RESOLUTION TEST CHART

NATIONAL BUREAU OF STANDARDS-1963-A
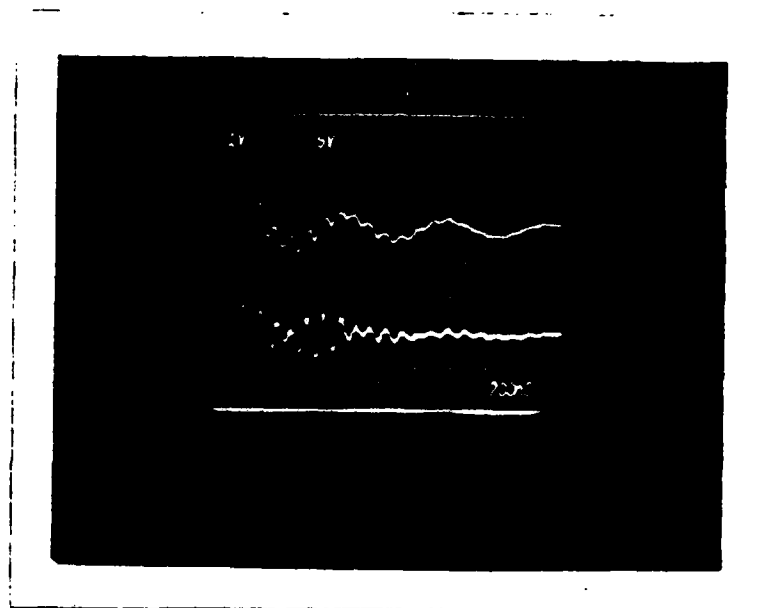
Fig. 6.19. TL current and voltage waveform (source capacitance >> TL capacitance)
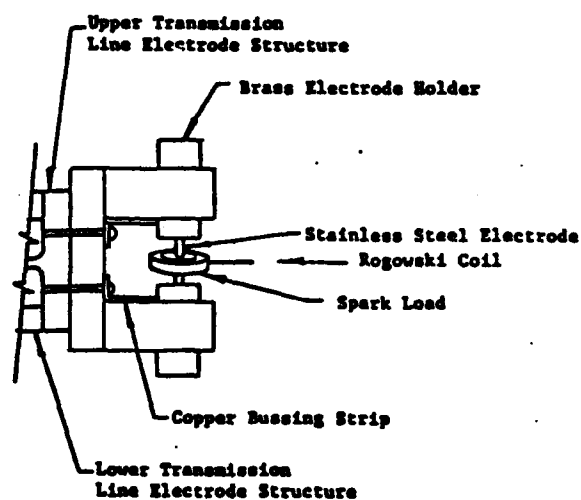
Fig. 6.20. Stainless steel pin electrode configuration

Current Risetime Experiments

One of the basic design criterion of the TL discharge circuit was that it generate a rectangular shaped output pulse. To achieve this criterion it is necessary to reduce the pulse risetime to much less than half the one way transit time of the TL (see the section on pulse shaping). Much experimental time and effort was therefore directed toward measurements of current pulse risetimes under varying conditions of output inductance and impedance. The two principal output configurations tested are illustrated in Figures 6.20 and 6.21. Figure 6.20 is of the first configuration tested. It consisted of a TL output busing network and a stainless steel electrode arrangement originally designed for use in a high intensity spark lamp array. The main geometrical variable in this configuration was the electrode spacing. Changing the electrode spacing varied both the arc inductance and the load impedance. This enabled observation of the effect of these two variables on both the risetime and the impedance matching characteristics between the load and the Tls. Table 2 in Appendix 3 lists the measured and calculated results for the entire series of experiments with certain test series being referenced here for analysis purposes.

The transmission lines were initially set at their designed spacing of 1 mm. and measurements of the charging voltage waveforms and current pulse outputs were made. The voltage was measured with a 6015 Tektronix hi-voltage probe while the discharge current was monitored with the PI Rogowski coil. Figure 6.22 is typical of the current waveforms observed. The results of the first set of experiment (Series

A) indicated that the current risetimes were too long to show the flat top characteristics of a discharging distributed parameter network. The next series of tests (Series B) were aimed at reducing the inductance of the output configuration by reducing the spark gap spacing of the load. In Reference (6) it was reported that in many instances the arc inductance was a major contributor to the total loop inductance of a discharge circuit. Therefore, by varying the arc length it should be possible to reduce its effect on the total loop inductance of the transmission line's output section. The spark electrode separation distance S_{SL} was varied from 1 mm to 2.88 mm and finally all the way up to 4.88 mm. Current and voltage measurements were made at each separation. The results are tabulated in Table 2. Figures 6.23 through 6.25 are representative of the photographs taken of the current pulse waveform during this series of experiments.

At first, it was very confusing because no matter what spacing was used all the risetimes were in the neighborhood of 50 nsec. In fact, closer inspection of the data made it even more confusing because one of the shorter risetimes observed was with the largest spacing (4.88 mm) and one of the longest risetimes with the smallest spacing (1 mm). The reason for these results was traced to the fact that all the experiments were not correlated with a single input voltage and peak current. In other words, a faster rising or sharper pulse can have a risetime much longer than a slower rising pulse if its peak value is much greater than in the latter case. Therefore, a much

TABLE 2

Tabulated Data and Results for the LTL Experiments

Test Series	S_{PL} (cm)	Z_{TL} (ohms)	S_{SL} (cm)	I_{pk} (kA)	I(10-90%) (kA)	T_R(10-90%) (nsec)	dI/dt (10-90%) (x10^{11} A/sec)	V_{pk} (kv)	S (nsec)	$Z=V_{pk}/I_{pk}$ (ohms)	V_o (kv)
A	1	1.3	2.8	13.0	10.6	34	3.1	21	180	1.6	10
		1.3	2.8	8.8	6.6	32	2.1	14	185	1.6	7.5
		1.3	2.8	13.8	11.1	42	2.6	22	190	1.6	10
	1	1.3	2.8	9				16	180	1.3	7.5
B		1.3		6.0	4.8	60	.8		100		5
		1.3		6.0	4.8	60	.8		110	.8	5
		1.3		6.5	5.2	50	1.1	5.2	100	1.00	5
		1.3	2.9	7.0	5.2	52	.9	6.8	225	1.00	5
		1.3	2.9	8.3	6.6	54	1.2	6.8	230	1.8	7.5
		1.3	4.9	7.5	6.0	36	1.1	13	250	2.3	7.5
		1.3	4.9	4.8	4.7	48	.8	13	250	2.9	7.5
	1	1.3	4.9	5.5	4.5	52	.9	14	250	2.3	7.5
C	.25	.4	.3	6.5	5.2	84	.7	4	125	.6	2.0
	.25	.4	.3	5.0	4.0	80	.6	4		.4	2.0
	.25	.4	.3	6.5	5.2	96	.4	4		.6	2.0
D		1.3	2.9	7.5	6.1	34	1.8	15	150	2.0	7.5
		1.3	2.9	7.0	5.6	40	1.4	15		2.1	7.5
		1.3	2.9	5.5	4.4	36	1.2	10	100	1.8	5.0
	1	1.3	2.9	7.5	6.1	36	1.7	15		2.0	7.5
E	2.4	3.6	>1	7.5	4.8	18	2.6				4.5
	2.4	3.6	>1	6.5	4.8	18	2.6				4.5
	2.4	3.6	>1	7.0	4.8	18	3.0				4.5
	2.4	3.6	>1	7.0	4.8	18	2.6				4.5
F	6	8.9	>1	1.6	1.3	44	2.2	15		9.1	3.9
	6	8.9	>1	1.6	1.3	44	3.2	15		9.1	3.9
	6	8.9	>1	1.6	1.3	44	3.2	15		9.1	3.9

* Adjusted risetimes T_R (adj) = $\left(T_R \text{(observed)}^2 - T_R \text{(scope + amp.)}^2 - T_R \text{(probe)}^2 \right)^{1/2}$
            6 nsec   4 nsec   2 nsec
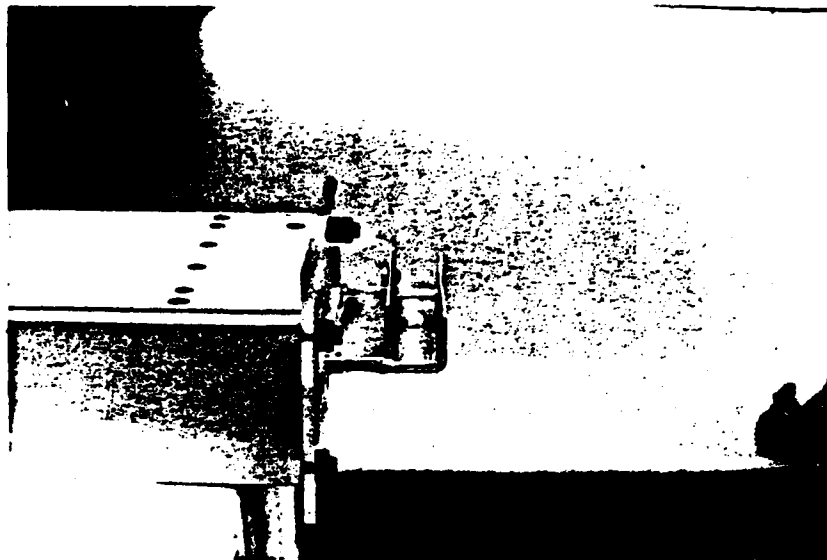
Fig. 6.21. Low inductance output configuration
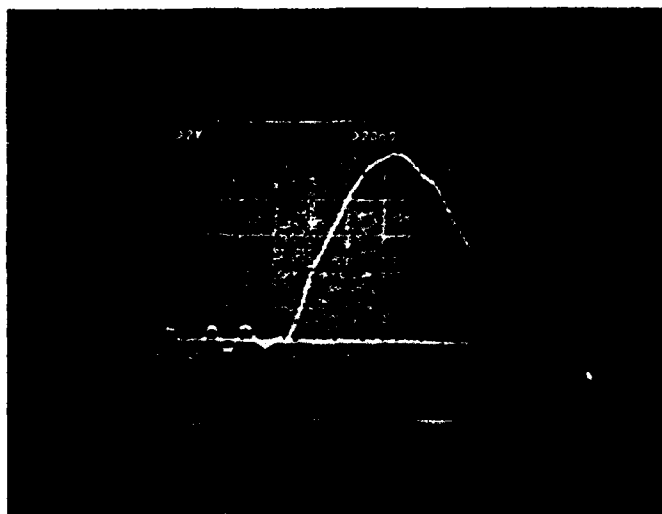
Fig. 6.22. TL current output waveform
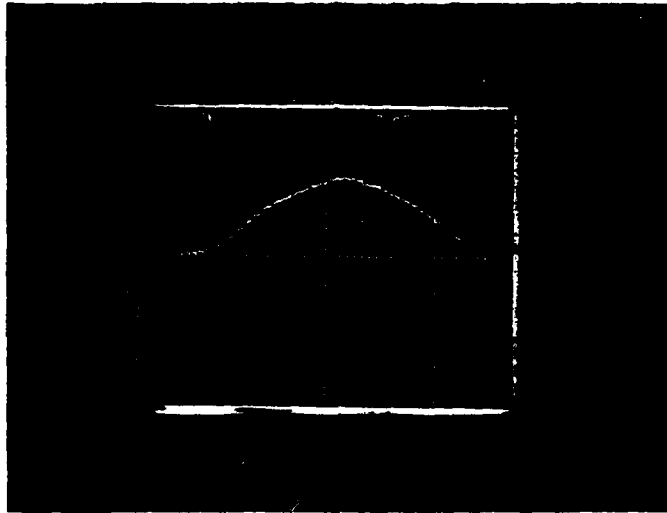
Fig. 6.23. TL current output waveform
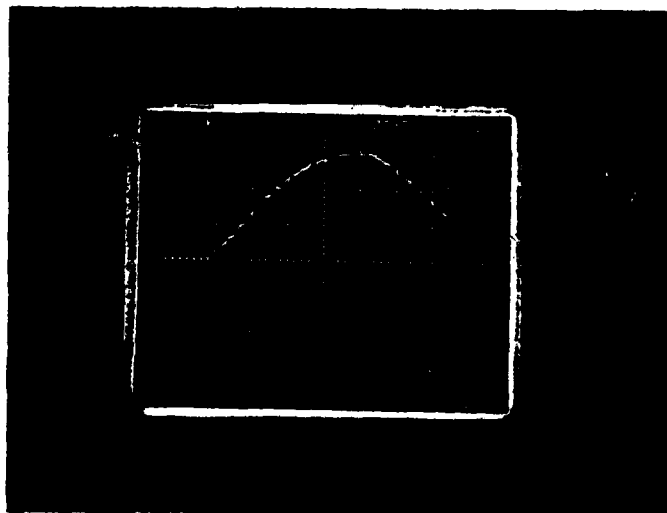
Fig. 6.24. TL current output waveform

better indicator of what is occurring as the arc inductance varies for a given input voltage would be dI/dt, the rate of change of the current on the pulse wavefront. Comparison of the rates of current change in the second set of experiments showed that the anticipated inverse relationship between output inductance and dI/dt did take place. Since the values for the 1 mm electrode spacing experiment were taken at only a 5 kv input voltage as compared to the 7.5 kv used in the other two cases it was necessary to correct these values of dI/dt by a factor of 1.5 (i.e. 7.5/5.0). This correction is necessary in order that any variation in dI/dt be only attributable to a change in output inductance and not output voltage. The results are plotted in Figure 6.26 It can be seen that as the arc length and its corresponding inductance is increased the rate of change of the current on the pulse wavefront goes down. This inverse relationship between output inductance and current rate of change is exactly what should occur.

It was also realized at this time that the reason the rise-times were not changing was because the peak values of the current pulses, I_{pk}, were changing at approximately the same rate as dI/dt was changing. The peak value of the current pulse is given by equation (22) to be

$$I_{pk} = V_{pk}/(Z_{TL} + R_L) \qquad (22)$$

For any given TL spacing, Z_{TL} is constant and for a given input voltage V_{pk} the only remaining variable is the load impedance R_L. The load impedance consists of a series combination of two components, R_L and L.
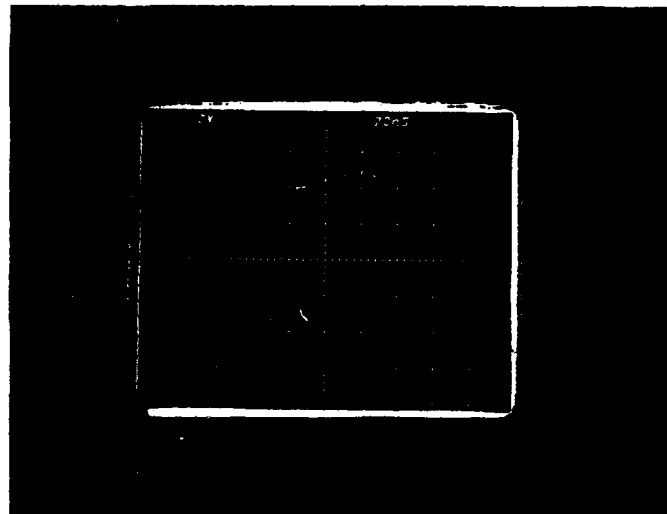
Fig. 6.25. TL current output waveform
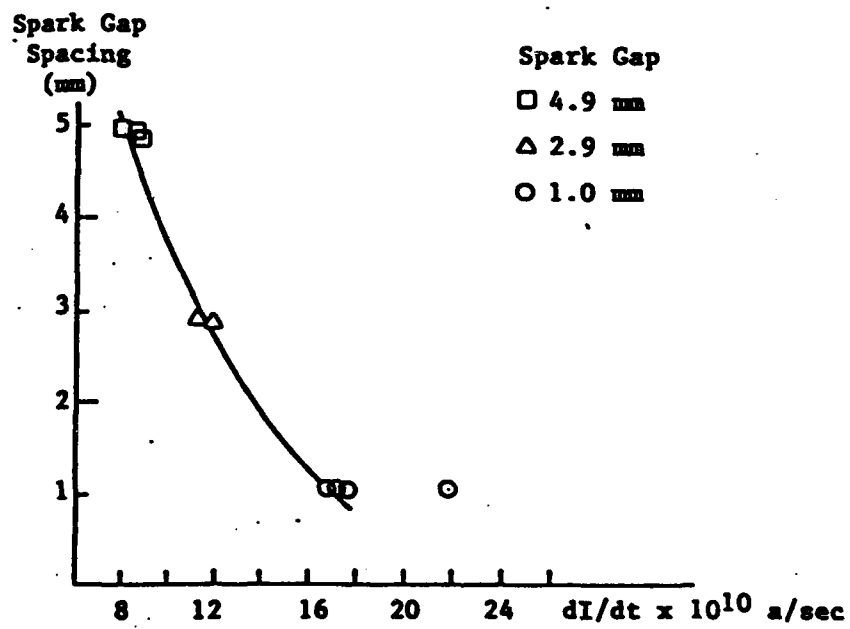
Fig. 6.26. Spark electrode spacing vs dI/dt

- 87 -

R_L is the resistive component of the output configuration. R_L includes skin resistances and all ohmic resistances in the spark itself. The inductive part of the load impedance L is composed of all the series inductances in the output configuration which includes all busing inductances and the inductance of the spark itself. As the spark electrode spacing is increased, both R_L and L will increase also. In the Series B experiments, the increase in the inductive component has reduced the dI/dt on the pulse wavefront, but it also in combination with the resistive part has limited the magnitude of the first current peak. These two effects occurring simultaneously were the reasons that the pulse risetimes were not changing. It is also the reason why increased damping of the TL discharge was not observed. Damping is dependent only upon the resistive component of the discharge loop and not the total impedance. While increasing the length of the discharge did increase the total load impedance, evidently the increased ohmic resistance of the spark was not of sufficient magnitude to manifest itself as an increase in the damping factor of the circuit. Figure 6.27 is a plot of the total load impedance versus the spark electrode spacing. The calculated load impedance values for the 1 mm spacing using equation (22) had to be adjusted because the peak voltage observed on the traces was much below the output of the Marx. If the observed value for the voltage was used to calculate the total ouput impedance, its value fell below the natural impedance of the TL which is theoretically impossible. It was determined that in cases of premature breakdown, the peak discharge current would depend upon the

voltage across the transmission line and not the breakdown voltage observed on the spark gap.

It was apparent after the first two series of experiments were completed that with the given output configuration and TL spacing no variation in the spark length would reduce the risetimes. It was then decided to check the inverse relationship between the risetime and the TL impedance (i.e., $T_R \propto TL^{-1}$). The TL was set at the lowest spacing possible (.25 mm) and the risetimes measured. The risetimes went up as expected to as much as 96 nsec (Figures 6.28 and 6.29). This clearly substantiated the inverse relationship and showed that shorter risetimes could be achieved for any given output configuration simply by increasing the TL impedance. The disadvantage in this type of operation has already previously been shown to be inefficient if the load impedance is much smaller than the impedance of the TL. For this reason, before the TL impedance was to be increased in order to reduce risetimes it was decided to try and reduce the ouput inductance of the busing network and associated electrode arrangement. To this end, several arrangements of short busing strips and electrodes were tested to see whether or not the risetimes could be reduced without changing the TL spacing and impedance. Figure 6.30 illustrates the configurations tested and Table 2, Section D lists the results.

The risetimes were still no better than obtained in the very first set of experiments. During the testing and measurement phases of these experiments it became clear that the need to insert the Rogowski coil in between current carrying conductors contributed significantly to the output inductance. This suggested that it was imperative to

- 89 -
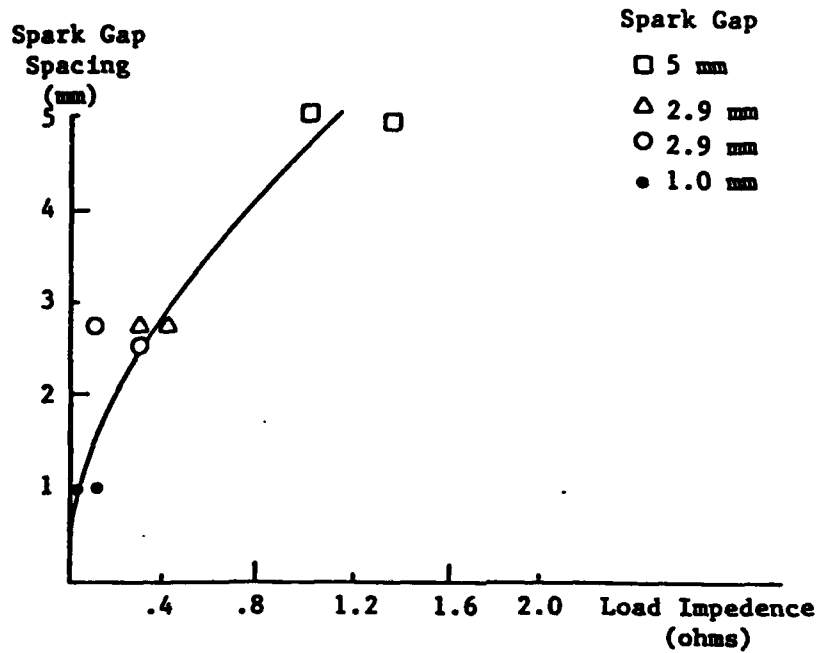
Fig. 6.27. Spark electrode spacing vs. load impedance
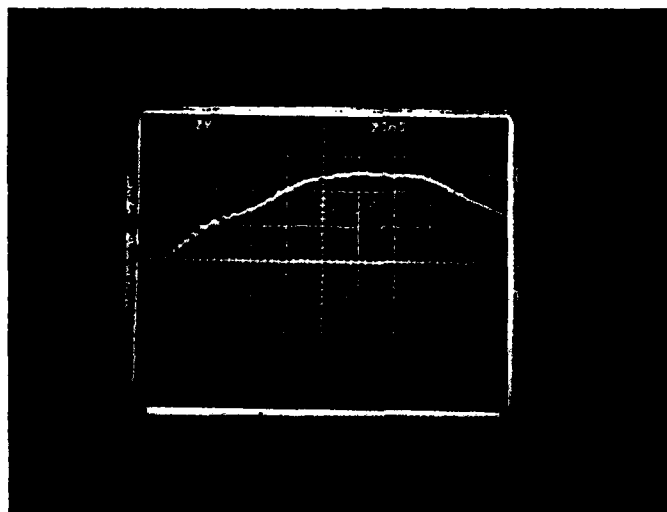
Fig. 6.28. TL current output waveform (Z_{TL} = .4 ohm)

- 90 -
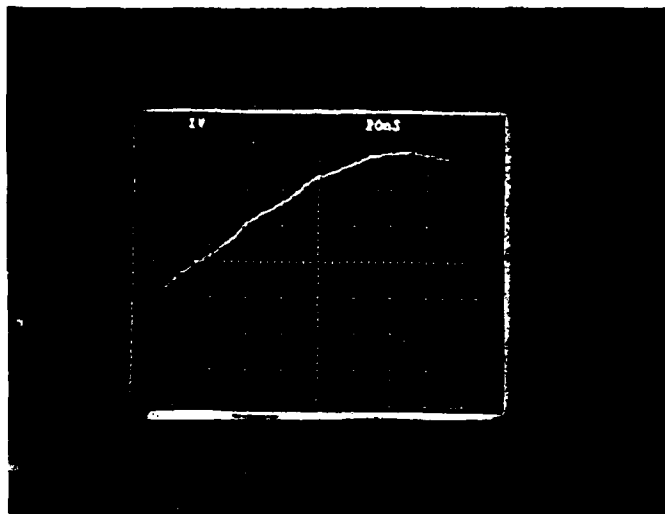
Fig. 6.29. TL current output waveform (Z_{TL} = .4 ohm)
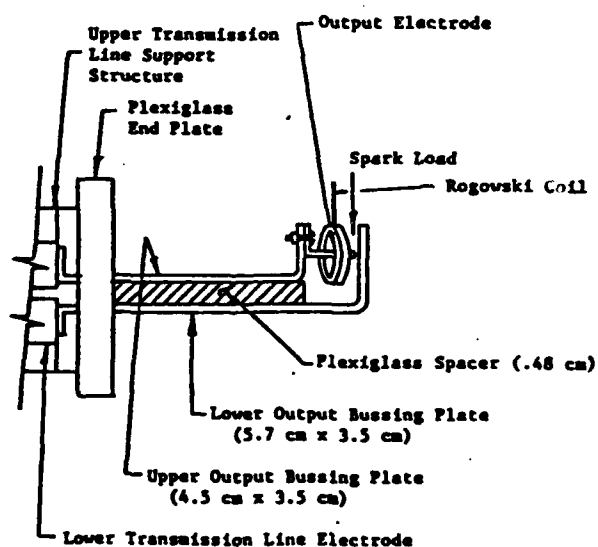
Fig. 6.30. Short busing strip output configuration

reduce all other contributions to the output inductance to an absolute minimum. Therefore, at the same time that the TL spacing was increased, a new output configuration was also used. This configuration is shown in Figure 6.21. The new configuration utilized the widest possible busing strip from the TL to the spark load, thereby minimizing busing inductance. At the load end it was decided to reduce the arc length to the shortest possible usable value. The arc length in all remaining series of experiments was set at no more than 3.2 mm. The fifth series of experiments (Series E) used this low inductance configuration and a 2.4 mm TL spacing ($Z_{TL} = 3.58 \,\Omega$). The risetimes were 16 to 18 nsec long and were characteristic of distributed parameter discharges (See Figures 6.31 through 6.32) Notice how the tops of the discharges are finally leveling out as compared to Figures 6.25 and 6.29. The inclined shape of the top of the pulse is probably the result of the high capacitance Marx-Bank trying to drive the transmission line voltage up during discharge.

The last two sets of experiments, Series F and G were performed after the Marx-Bank had been replaced by the resonant charging network. Micrometers were also added to the upper section of the transmission line which enabled the spacing and hence the TL impedance to be more easily varied to any desired value. The TL impedance was raised to 8.9 ohms and the associated risetimes observed. For the 8.9 ohm spacing, the current risetimes (10-90%) were no more than 6 nsec.*

---

*Unadjusted risetimes which did not account for instrumentation errors
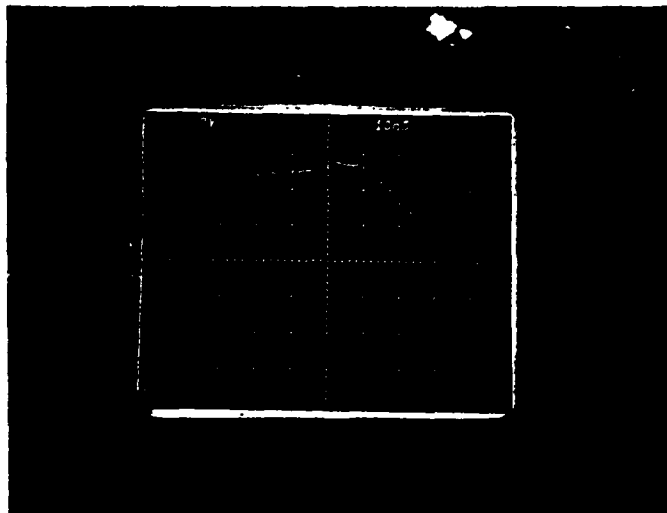
Fig. 6.31. TL current output waveform (Z_{TL} = 3.6 ohm)
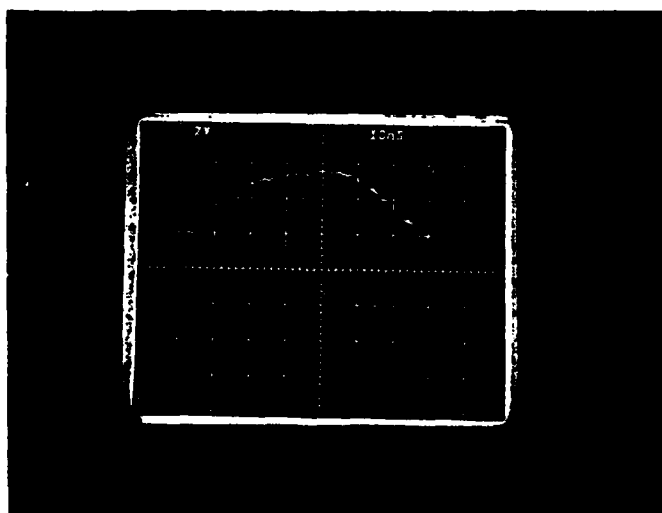
Fig. 6.32. TL current output waveform (Z_{TL} = 3.6 ohm)

- 93 -

Fig. 6.33. TL current and voltage output waveforms (Z_{TL} = 8.9 ohm)
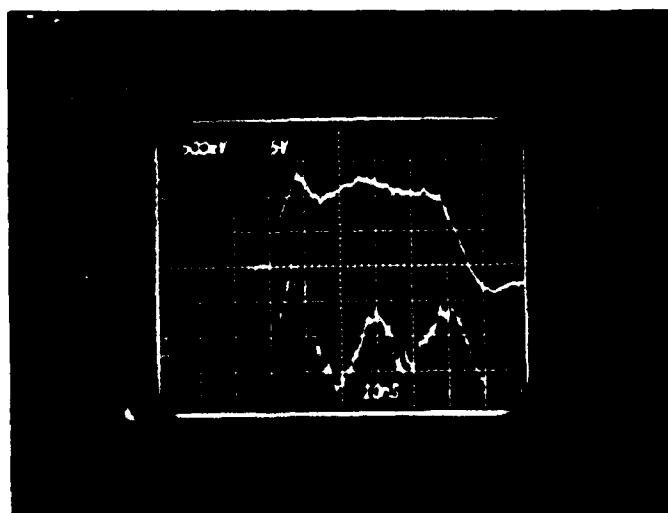
Fig. 6.34. TL current and voltage output waveforms (Z_{TL} = 8.9 ohm)

Figures 6.33 and 6.34 show some of the traces observed on a Tektronix 7844 dual beam oscilloscope. The upper trace is of the current, while the lower is of the voltage. Note that the voltage trace does not show the characteristic rectangular shape that the current trace does. This is in this time frame. Inspection of the traces show that the time period between the first voltage peak after breakdown and the first voltage minimum is about 8-10 nsec, substantiating the hypothesis that reflections are taking place. It is also very evident by the traces that the discharge is also highly underdamped. This was a result of trying to minimize the arc inductance and its effect on the risetimes. Unfortunately, this also reduces the load impedance and causes the ringing so noticeable in the traces. Figure 6.35 summarizes the entire series of risetime experiments by plotting risetimes versus the transmission line impedances.

Figure 6.35 shows the TL output current risetimes versus the TL impedence. It should be noted that the fastest risetime pulses were obtained with the highest impedence line tested (i.e., 8.9). The reason for this is that by equation 21 the output current risetime is proportional to the output inductance and inversely proportional to the TL impendence. Therefore, for a given output configuration and hence output inductance, a faster risetime current pulse can be obtained by increasing the TL impedence. Unfortunately, in this specific instance the desired square wave pulse shapes were achieved with a TL impendance much higher than the anticipated laser or flashlamp loads of approximately 1 ohm that this system could potentially drive. In order to improve on this mismatch, it would be necessary to reduce the output

- 95 -

inductance that the TL sees to an absolute minimum. The value of the output inductance can be determined by using equation 21 and the known TL impendance and measured current risetimes. This calculation for tests D through F shows that the output inductance varies from about 40 to 60 nhy. This range of output inductances results from having to vary the output bussing strips separation distances as the TL impendance is changed. The output inductance includes all electrical bussing strips between the TL and spark load and the inductance of the spark itself. It is estimated using equation 12 that the major portion of this inductance (25 to 35 nhy) results from having to introduce the Rogowski coil into the discharge circuit. If another method of current measurement, such as a current shunt, were used, the risetimes obtainable from the lower impendance settings of the TL could be reduced to *the 10 to 20 nsec region.*
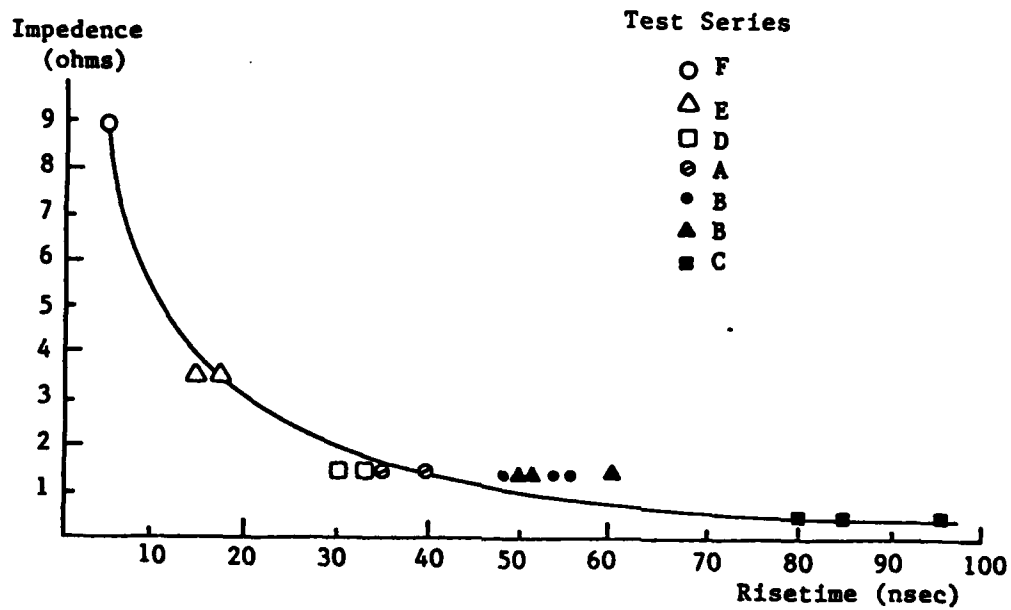
Fig. 6.35. TL output pulse risetime vs TL impedance

7. CONCLUSION

The purpose of this study was the investigation of methods for improving the lifetime and reliability of fast risetime electrical discharge circuit applicable to use in high repetition rate short-wavelength laser schemes. The deficiencies of conventional driving circuits has been shown to be centered around the use of low-inductance, high voltage capacitors whose lifetimes are extremely limited under high repetition rate conditions. One approach with potential promise for circumventing this problem is through the use of liquid dielectrics-most notably water and glycerine whose self-healing properties and stored energy density characteristics appear favorable for use in high repetition rate, fast risetime electrical discharge circuits.

In order to test the effectiveness of such circuits in potential laser applications, a prototype electrical energy storage device has been designed, constructed and laboratory tested. The device was built to operate as a short length hi-voltage transmission line utilizing liquid glycerine as its dielectric. The basic diffi-culty and expense incurred just building the structural element of the energy storage device suggests that significant reductions in the complexity and cost would have to be achieved for this aspect of the circuit before this type of approach would be acceptable in many applications other than just strictly research ones.

In summary of the set of experiments performed, much has been learned and substantiated concerning the fundamental operating charac-

teristics of distributed parameter networks (i.e., transmission line networks) for possible laser excitation. The transition region between distributed parameter and lumped parameter discharges (i.e., ordinary capacitor discharges) have been observed and measurements of current and voltage waveforms taken. The predicted inverse relationship between risetime and source impedance has been shown to hold true for varying conditions on the output network. It has also been proven that the current rate of change is definitely proportional to the output inductance which includes both busing and load inductance. During the course of these experiments, it was also found that the need to use a current transformer to measure the current risetimes adversely affected the very parameter that was to be measured. Use of the doughnut shaped Rogowski coil required a significant separation of the current carrying conductors on the load end of the TL. This required separation of the conductors resulted in an additional 25 to 35 nhy of inductance being introduced into the output load, thereby restricting current risetimes attainable at the lower TL impedence settings of the device. This definitely points out the need to use another method and/or probe for measuring the pulsed current output of the transmission lines. In this context it would be worth considering the use of some sort of current shunt or current viewing resistor which would not have such a deleterious effect on the parameter being measured.

The transmission line tested exhibited the square wave current pulse characteristic of this type of energy storage element. Current risetimes as short as 4 nsec were obtained at the 8.9 ohm

impedence setting of the TL. Pulse repetition rates of up to 2khz were achieved. Continuous firing of this system at repetition rates of 1 khz for periods of about five minutes duration (i.e. 300,000 shots) were also achieved without an internal fault occurring in the glycerine dielectric. Longer periods of continuous operation were not limited by the TL, but by the load spark discharge electrodes which became eroded and carbon coated by the high number of successive discharges. This caused the required breakdown voltage for the spark gap to increase and the system at some point would fail to fire reliably. The system had to be shut down and the electrodes cleaned and the spark gap spacing readjusted. Maximum power transfer experiments for optimizing the transfer of energy from the TL to a spark load were not attempted. The major emphasis on testing centered on studying only the TL and its busing network by minimizing the spark load including its inherent inductance. This was done with the knowledge that once the TL and its output busing strips electrical discharge characteristics were known, the optimum load in terms of resistance and inductance could be determined. As originally designed, the system would provide 1 joule of energy per shot from a 1 ohm TL operating into a matched load. The design criterion of only 1 joule per shot was necessitated by desire to also achieve khz repetition rates. The power supplies utilized in this study were a definite limitation to the maximum per pulse energy delivered at high repetition rates in this system.

In conclusion, the use of liquid dielectrics and their self-healing characteristics in reliable, high speed electrical dis-

charge circuits appear quite favorable as compared to conventional discharge circuitry. While liquids are almost invariably used in e-beam device, their use in simpler electrical discharge schemes has been highly limited. Further work with liquid dielectrics and their advantages and disadvantages could lead to the construction of devices not only for research type applications, but those pertaining to commercial use also.

RECOMMENDATIONS

It should be emphasized that even though the energy-storage device tested should have considerable promise for use in high repetition rate, fast discharge laser applications, further modification of the prototype device would be necessary before it could be used in laser driving circuits. The modifications are as follows:

1. Design and construct a simple energy storage device utilizing liquid dielectrics. A lightweight, multiple electrode transmission line structure weighing not more than 100 lbs and capable of delivering 10 to 20 joules of energy into a 1 ohm load at repetition rates of 1 khz would illustrate the competitiveness of this type of device as compared to the state-of-the-art solid state capacitors designed for similar application. The device tested in this study had considerably more structural mass than required, and it was limited by the available power supply to delivering only a single joule per shot.

2. Improve the electrical coupling on the input and output sections of the storage device. With proper design the input and output bussing networks self-inductance could be minimized thereby improving on the charging times of the transmission lines and minimizing the output current pulse's risetimes into the load.

3. Add a flow system and deionization scheme in order to utilize water as the dielectric. A flow system would allow for the cooling and deionization of the water dielectric under an extended periods of firing a high repetition rate. This would further test the longevity capabilities of this type of system.

4. Another area which would need improvement is the switch used to pulse charge the transmission line energy storage device. The present switch, an air blown spark gap, is susceptible to carbon buildup after periods of firing at high repetition rates. This leads to unreliable operation and therefore needs improvement. A high power thyraton or other switch of this type is suggested.

5. A fifth change that is necessary is to do away with the Rogowski coil that was used in the present study in favor of a stripline current monitoring device. The need to insert the doughnut-shaped Rogowski coil in the output loop of the discharge circuit greatly increased the output inductance of the loop, thereby restricting the current risetimes attainable with this particular arrangement.

The above suggested modifications could lead to an improved high repetition rate fast discharge circuit for use in laser excitation schemes. While the present study was aimed at those laser applications requiring direct discharge or flash-lamp excitation, one should not

overlook other possible applications such as small, high repetition rate electron beam devices. E-beam devices typically use TL energy storage elements in their excitation circuits. E-beam machines have the important attribute that once the beam exits from the device, its pulse energy, width and shape cannot be affected by the load upon which it impinges. This means that a high impedance e-beam machine can efficiently excite a much lower impedance load. It should be noted that e-beam devices have found wide-spread applications in the optics and semi-conductor industry and a high repetition rate machine could increase productivity significantly.

In addition to the proposed modifications and applications, it is important to continue the investigations for other liquid dielectrics which could be used in electrical energy storage applications. An in-depth literature search could reveal other liquids whose electrical properties suggest that they might show improved operational characteristics in fast discharge systems as compared to the liquids studied in this project. Liquids possessing high dielectric strengths or larger permittivities than the liquids studied in this project could increase the stored energy density presently attainable, thereby allowing construction of smaller and lighter structures which would have the same output pulse length and energy delivering capabilities as systems using the more conventional, aforementioned liquid dielectrics.

The next step in further determining the capabilities of liquid dielectric transmission lines for hi-power laser applications would be the construction of a new and much larger transmission line

system. This system should be capable of delivering 20 to 30 joules of energy into a matched 1 ohm load with current risetimes in the 10 to 20 nsec region. A cooling and recirculation system for the liquid dielectric would further demonstrate the advantages of liquid dielectrics as compared to solid dielectrics in hi-power applications. After successful completion of that follow-on phase, the device could be incorporated into a laser.

To find the maximum of the power transfer from a resistively charged capacitor to a load, equation (36) is to be first differentiated with respect to the capacitance C. The resulting equation is then set to zero and the relationship between C and R and T solved for. Following this procedure we have

$$E_L = 1/2 \ CV^2(1-e^{-t/RC})^2 \tag{36}$$

$$dE_L/dC = \frac{d[AC(1-e^{B/C})^2]}{dC}$$

where $A = V^2/2$ and $B = -t/R$

$$dE_L/dC = \frac{d}{dC}[(AC)(1-e^{B/C}+e^{2B/C})]$$

$$dE_L/dC = (AC)[(-e^{B/C})(-B/C^2) + (e^{2B/C})(-2B/C2)]$$
$$+ (A)[1-2e^{B/C} + e^{2B/C}]$$

Setting $dE_L/dC = 0$ and solving for C

$$0 = (AC)[(-2_e{}^{B/C})(-B/C2) + (e^{2B/C})(-2B/C2)]$$
$$+ (A)[1-2_e{}^{B/C} + e^{2B/C}]$$
$$0 = 1 + (-2 + 2B/C)e^{B/C} + (1 - 2B/C)e^{2B/C}$$

Letting $x = e^{B/C}$, $D = (-2 + 2B/C)$ and $H = (1 - 2B/C)$, we now have

$$0 = 1 + Dx + Hx^2$$

This equality may be solved by the use of the binomial theorem. If $x = 1$, then since $x = e^{B/C}$, this means that $B = 0$. Recalling

that $B = -t/r$, this requires that either $t = 0$ or $R = \infty$. Since neither of these cases is of practical interest, the only remaining solution is $x = 1-(2B/C)$.

$$x = [1 - 2B/C]-1$$
$$e^{B/C} = [1 - 2B/C]-1 \quad \text{or} \quad -t/RC = [1 + 2t/RC]^{-1}$$

It should be noted that the above expression is transcendental in nature and an exact solution in terms of C does not exist. Nevertheless an approximation can be made by a series expansion of $e^{B/C}$

$$e^{B/C} = 1 + B/C + \frac{(B/C)^2}{2!} + \frac{(B/C)^3}{3!} + \frac{(B/C)^4}{4!} +\ldots$$

Using only the first four terms in the series

$$e^{B/C} = 1 + \frac{B/C}{2!} + \frac{(B/C)^2}{6!}$$

$$e^{t/RC} = 1 + 2t/RC = 1 + t/RC + \frac{t^2/R^2C^2}{2} + \frac{t^3/R^3C^3}{6}$$

$$\frac{t^3/R^3C^3}{6} + \frac{t^2/R^2C^2}{2} - t/RC = 0$$

$$\frac{t^2/R^2C^2}{6} + \frac{t/RC}{2} - 1 = 0$$

Letting $x = t/RC$

$$\frac{x^2}{6} + \frac{x}{2} - 1 = 0$$

Again, we can solve this expression by application of the binomial theorem giving

$$x = -4.37 \text{ and } x = 1.37$$

Since a negative value of x can only correspond to a negative time period this case is of no interest. Therefore, the remaining solution can be used to obtain the desired result.

$$x = t/RC = 1.37 \text{ or } C = .73t/R$$

APPENDIX 2

The derivation of the expression for the RC decay constant of a TL is based on the product of the equations for the resistance and capacitance of parallel plate capacitor. These equations can be obtained from reference (11) and the derivation performed accordingly. From (11) we have

$$R = \eta s/A \text{ and } C = \epsilon A/s$$

Taking the product RC we find that the decay constant is independent of geometry and depends only upon the characteristics of the dielectric itself.

$$RC = (\eta s/A)(\epsilon A/s) = \eta \epsilon$$

References

1. Weast, R. C., 1964, "Persistant Lines of the Elements," Handbook of Chemistry and Physics, 45th Edition, p. E96-E99.

2. Reed, J. Jensen, 1976, "Prospects for Uranium Enrichment," Laser Focus, 12, p. 51-63.

3. Schalow, J. and Townes, C., 1958, "Optical Masers," Physics Review, 112, p. 1940.

4. Schafer, F.P., 1973, Dye Lasers, (New York: Springer-Verlag), p. 54

5. F. T. Arecchi and Schulz-Dubois, E.O., 1972, Laser Handbook (New York: North-Holland Publishing Co.), p. 327-368.

6. Marshall, I.S., 1962, "Strong-Current Pulse (spark) Discharges in Gas, Used in Pulsed Light Sources,", Soviet Physics Uspehi, 5, p. 475.

7. Reitz, J. R. 1967, Foundations of Electromagnetic Theory, (Reading, Mass.: Addison-Wesley), p. 250.

8. Johnson, G.E., 1971, Basics of Circuit Analysis for Practical Engineering (New York: Barnes and Noble), p. 140.

9. Frungel, F., 1965, High Speed Pulse Technology, (New York: Academic Press), p. 113.

10. Richter, P., Kimel J. D., and Moulton G.C., 1976, "Pulsed Uv Nitrogen laser: Dynamical Behavior," Applied Optics, 15, p. 756-760.

11. Sorokin, P.P., et al, 1968, "Flashlamp-Pumped Organic-Dye Lasers," Journal of Chemical Physics, 48, p. 4726-4741.

12. Aristov, A.V. et al, 1969, "Influence of Certain Quenchers of Fluorescence on the Threshold of the Laser Effect in Organic Phosphors," Optical Spectroscopy, 27, p. 548.

13. F. Emmett, et al., 1977, "ArF and keF lasers," Aplied Physics letters, 36, p. 418.

14. Booker, H.G., 1959, An Approach to Electrical Science, (New York: McGraw-Hill), p, 548.

15. Hoffman, P. and Ferrante, J. "Energy Storage Capacitors of High Energy Density," IEEE Transactions on Electrical Insulation, 17, p. 235-239.

16. Hayworth, B.R., 1968, "The Behavior of Polyester Film Energy Storage Capacitors," IEEE Transactions on Electrical Insulation, $\underline{3}$, p. 47

17. Capacitor Specialists, Inc., P.O. Box 2052, Escondido, Calif., CSI Data Sheet No. 0674-WM on HI-Voltage Energy Storage Capacitors.

18. J. C. Martin, 1970, "Nanosecond Pulse Techniques," Atomic Weapons Research Establishments Note No. SSWA/JCM/704/49 Aldemastion, England.

19. Olson, N.T., 1976, "The Power Behind the Pulse," Optical Spectra, $\underline{10}$, p. 42-46.

20. Weszak, L., 1969 "Power-Supply Design for Pulsed Lasers," Microwaves, $\underline{21}$, p. 38.

21. Glascoe, and Lebacqz, 1965, Pulse Generators, (New York: Dover)

22. D. G. Sutton, et al., 1976, "Fast-discharge-initiated KrF laser, "Applied Physics letters, $\underline{28}$, p. 522.

23. Von Hipple, E. 1954, Dielectric Materials and Applications (New York: Wiley), p. 361-368.

PART II

PULSER CIRCUIT COMPUTER MODELING

1.   Transmission Line Model

The transmission line, laser cavity characteristics and power supply circuitry can be modeled as shown in Fig. 1. The equations below follow directly from the model.

$$V_0 = \frac{1}{C_1} \int_0^t i(-\ell,t)\, dt + L_1 \frac{di(-\ell,t)}{dt} + R_1 i(-\ell,t) + v(-\ell,t)$$
$$\text{(Power supply)}$$

$$v(o,t) = L_2 \frac{di(o,t)}{dt} + R_2 i(o,t) \qquad \text{(Laser gap)}$$

$$C \frac{\partial v(x,t)}{\partial t} = -\frac{\partial i(x,t)}{\partial x}$$
$$L \frac{\partial i(x,t)}{\partial t} = -\frac{\partial v(x,t)}{\partial x} \qquad \text{(Transmission line)}$$

These equations can be solved using the Laplace transform method to yield voltage and currents during the time the initial pulse is discharging through the laser cavity. The follow-on currents occuring after the initial pulse cannot be conveniently modeled using this method because of the large number of terms due to transmisson line reflections. The equation can also be solved numerically using the Runge-Kutta method to evaluate the lumped elements. This method gives results for the initial discharge and later follow-on conditions. The primary usefulness of the Lapace transform method is as a check of the more general numerical method.

These two methods agree very closely over the valid range of the Laplace Transform method and diverge thereafter. This indicates that the computer code for the numerical method is correct since it uses the same procedure both for the initial pulse and the follow-on currents.

113

Fig. 1 Transmission Line Model
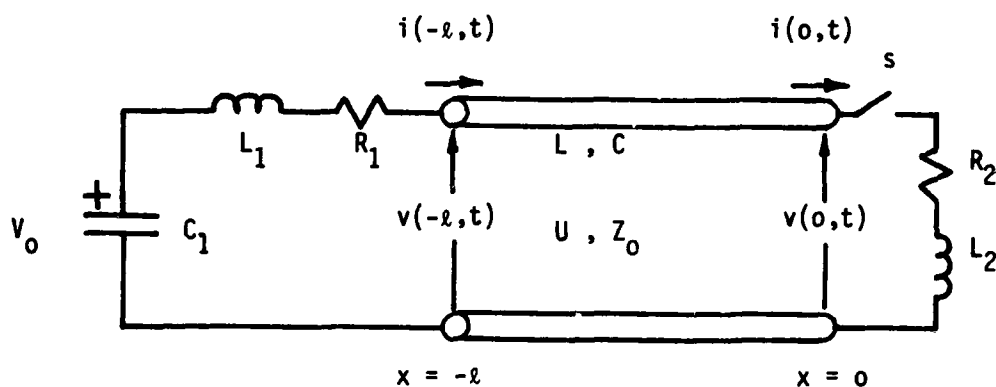
V_0 initial charge on capacitor

C_1 power supply capacitor

L_1 inductance of spark gap and leads

R_1 resistance of spark gap and leads

L_2 inductance of the laser cavity

R_2 resistance of laser cavity

ℓ transmission line length

U wave velocity on transmission line

Z_0 characteristic impedance of transmission line

S switch closes when gap potential is reached

114

2. Laplace Transform Solution

The equations that describe the transmission line can be transferred into the S-domain assuming the following initial conditions

$v(x,o) = V_0$ (transmission line initially charged)

$i(x,o) = 0$ (currents are small on the transmission

$i'(x,o) = 0$ line until the gap fires at $t = o$)

The transformed equations are:

$$\frac{V_0}{s} = (\frac{1}{SC_1} + SL_1 + R_1)\ I(-\ell,s) + V(-\ell,s)$$

$$V(o,s) = (SL_2 + R_2)\ I(o,s)$$

$$\frac{\partial^2 I(x,s)}{\partial x^2} - \frac{S^2}{U^2}\ I(x,s) = 0$$

and

$$SCV(x,s) - CV_0 = - \frac{\partial I(x,s)}{\partial x}$$

where

$$U = (LC)-1/2$$

The transmission line equation can be solved to obtain:

$$I(x,s) = A_1(s)\ e^{Sx/U} + A_2(s)\ e^{-Sx/U}$$

and

$$V(x,s) = \frac{V_0}{s} - Z_0 A_1(s)e^{Sx/U} + Z_0 A_2(s)\ e^{-Sx/U}$$

115

where

$$Z_0 = (L/c)^{1/2}$$

and

$$A_1(s) = \frac{V_0}{s\beta_1} \sum_{n=0}^{\infty} \left(\frac{\alpha_2 \beta_2}{\alpha_1 \beta_1}\right)^n e^{-2S\ell n/U}$$

$$A_2(s) = \frac{V_0}{s\beta_2} \sum_{n=0}^{\infty} \left(\frac{\alpha_2 \beta_2}{\alpha_1 \beta_1}\right)^n e^{-2S(n+1)/U}$$

where

$$\alpha_1 = \frac{1}{SC_1} + SL_1 + R_1 + Z_0$$

$$\alpha_2 = \frac{1}{SC_2} + SL_1 + R_1 - Z_0$$

$$\beta_1 = SL_2 + R_2 + Z_0$$

$$\beta_2 = SL_2 + R_2 - Z_0$$

The infinite series in A_1 and A_2 represents the reflections off the impedance discontinuities at the end of the transmission line.

In order to invert these equations into the time domain it is necessary to limit the infinite series to the zeroth and first terms. This limits the range of validity of the method, but it does give a good check for the numerical method.

The rising current wave in the gap is found to be:

116

$$i(o,t) = \frac{V_0}{R_2 + Z_0} \left(1 - e^{-(R_2+Z_0)t/L_2}\right)$$

The voltage across the driving capacitor is

$$v_c(t) = \frac{e^{-at}}{p} \left(a \sin px - p \cos px\right)$$

where

$$a = \frac{R_1 + Z_0}{2L} \quad \text{and} \quad p = \left(\frac{1}{LC} - \left(\frac{R_1 + Z_0}{2L}\right)^2\right)^{1/2}$$

3. Numerical Solution

The system equations can be solved numerically by dividing the transmission line into segments to represent the distance variation along the line and solving the boundry condition equations using Runge-Kutta. Two arrays, each 1024 segments long, model the transmission line. The arrays contain the forward and backward traveling voltage distribution X PLUS and X MINUS respectively. The time delay due to the transmission line is modeled by shifting the values in the array elements at each time increment. The voltage at any point along the line is the sum of the forward and backward waves. A block representation of the numerical method is shown below.

X PLUS →

```
┌──────────────┐   ┌─┐ ┌─┐ ┌─┐      ┌─┐  ┌─┐   ┌─┐   ┌──────────┐
│power supply  │ → │ │ │ │ │ │ ...  │ │  │ │   │ │ ← │Laser gap │
│equations     │   └─┘ └─┘ └─┘      └─┘  └─┘   └─┘   │equations │
│Runge-Kutta   │    1   2   3      1022 1023 1024   │Runge-Kutta│
│              │ ← │ │ │ │ │ │ ...  │ │  │ │   │ │ → │          │
└──────────────┘   └─┘ └─┘ └─┘      └─┘  └─┘   └─┘   └──────────┘
                  1024 1023 1022     3    2    1
```
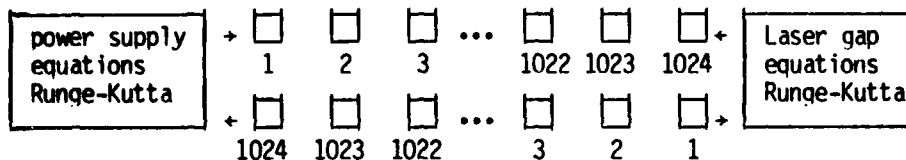
X MINUS ←

To initialize the system each element in X PLUS and X MINUS is set to V_0. At each time increment the values in X MINUS are shifted one cell left while X MINUS (1) is determined by the laser gap equations using X PLUS (1024) as an input voltage. X PLUS is determined similarly from the power supply equations.

To facilitate solutions state equations are generated from the boundary condition equations.

$$\dot{x}_1 = x_2$$

$$\dot{x}_2 = -\frac{1}{L_1 C_1} x_1 - \frac{R_1}{L_1} x_2 - \frac{V(\ell,t)}{L_1}$$

$$\dot{x}_3 = -\frac{R_2}{L_2} x_3 + \frac{V(o,t)}{L_2}$$

where

$$I(o,t) = x_3$$

$$I(\ell,t) = x_2$$

$$V_c(t) = \frac{x_1}{C_1} \qquad\qquad \text{(capacitor voltage)}$$

118

Standard first and second order Runge-Kutta methods are used to solve these
equations for each time increment or data shift on the transmission line.

4.   Numerical Results

Both the Laplace transform method and the numerical method results
were tabulated on a computer. A plot (Figure 2) comparing the current in
the gap computed by the two methods shows very good agreement for the time
interval when the Laplace method is valid. After that time the methods
diverge as they should. This comparison shows that the numerical method is
working properly since the same method of solution is used for the initial
pulse and the follow-on currents.

The two primary results that can be obtained from the numerical
method are the current in the laser gap and the voltage across the power
supply capacitor. The current in the gap is found to be a good current
pulse with fast rise and fall times during the initial phase of breakdown
(see Fig. 3). The follow-on currents are also large indicating a large
amount of energy is dissipated in the system after the initial pulse. This
limits the efficiency of the system. The capacitor voltage is found to
oscillate with large positive and negative peak voltages (see the computer
printout results). This indicates that the capacitor is highly stressed,
resulting in a short lifetime.

5.   Limitations of the Present Model

The transmission line model developed for analytically studying the
electrical characteristics of a liquid dielectric filled transmission line

119

is a useful, but somewhat limited computer tool. The model as it stands can very accurately predict output current and voltage waveform shapes for the circuit which is being modelled. Thus, it models well the circuit that was actually tested. Unfortunately other circuit configurations which include an additional switch between the source capacitance and the transmission line are more appropriate to the eventual practical application of this type of fast discharge circuitry. This additional switch would allow for decoupling the source capacitance from the transmission line, thereby eliminating any unwanted and late energy delivery from the source capacitance to the laser load once the transmission line has been discharged into the laser load. The present model was of course most useful in studying this problem. It should be possible to improve this model by applying the appropriate time constraints on the value of R_1, the resistance of the spark gap on the charging end of the transmission line circuit. If R_1 were to go to infinity at the same instant the the output switch S closes this would effectively decouple the source capacitor and transmission line. If the modification to the model and computer program were effected, it would be a much more powerful tool for use in analytical studies of this type of fast discharge circuitry. Modification of the model or of the laboratory was far beyond the scope of the study reported here.

Gap
Current
(10^3 amps)

1 - First reflection arrives at gap
2 - Laplace solution not valid after this time
    (only accounts for initial wave and first reflection)
3 - Third reflection

22.2 ns

Time, t
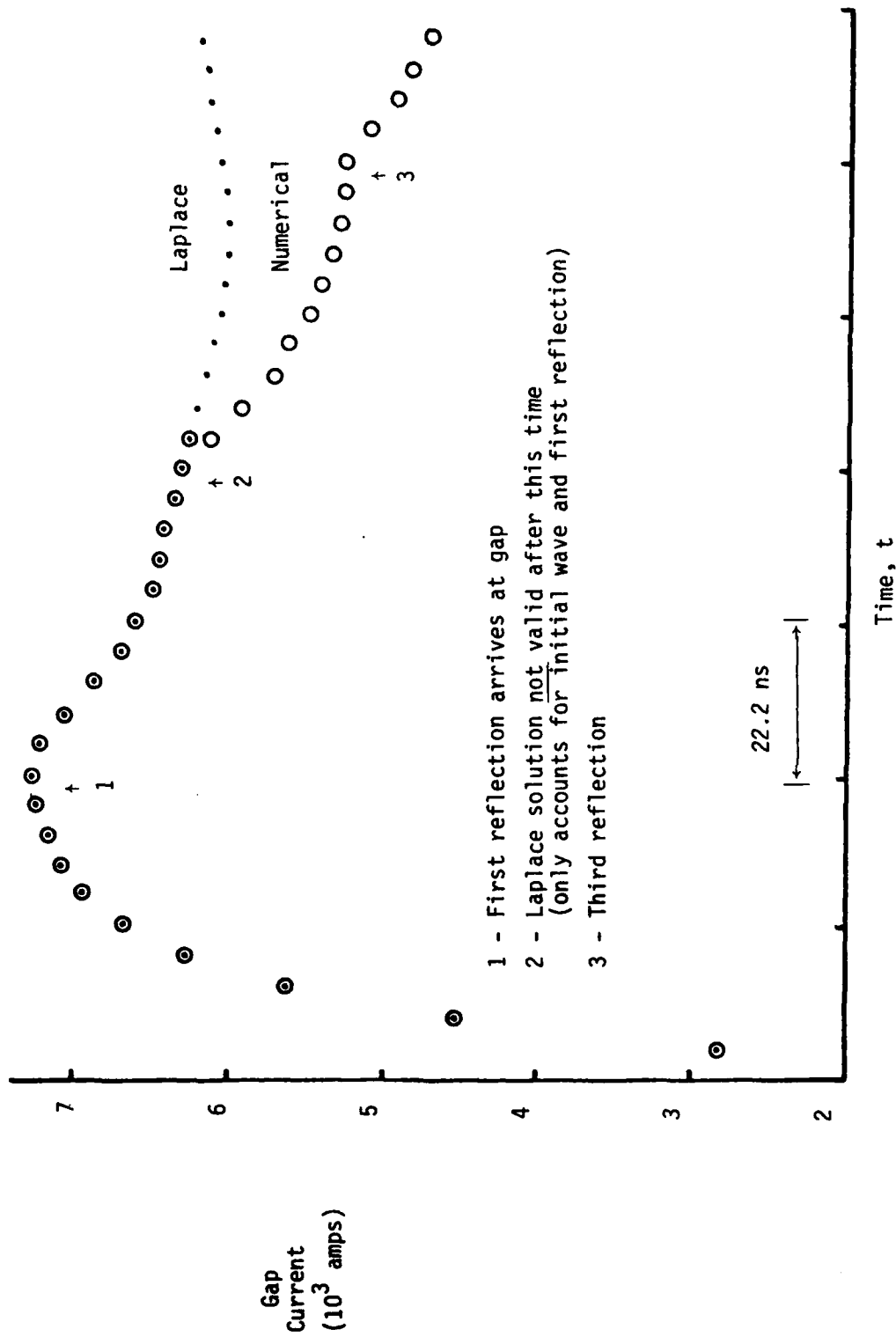
Fig. 2. Test cast comparison of Laplace and numerical solutions.

121
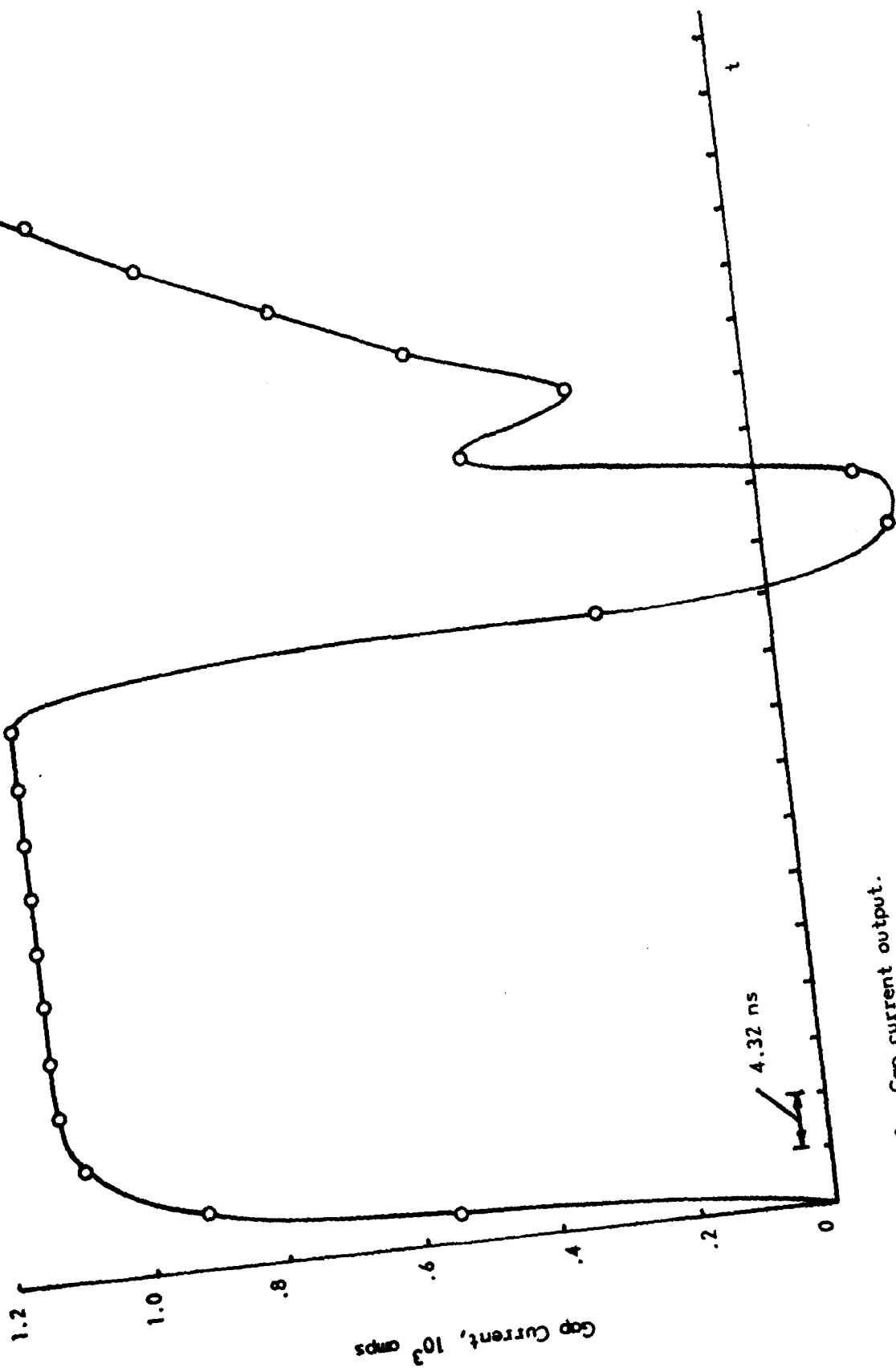
Fig. 3. Gap current output.

Gap Current, 10^3 amps

4.32 ns

t

122

```
1000C          THIS PROGRAM CALCULATES TRANSIENT CURRENTS AND
1010C          VOLTAGES ON A TRANSMISSION LINE.
1020C          MOD 1.0
1030C
1040C          INITIALIZATION
1050           DIMENSION FPLUS(1000),FMINUS(1000)
1060           REAL L1,L2,LENGTH,L0
1070           COMMON R1,L1,C1,R2,L2,VEND1,VEND2
1080           EXTERNAL F1,F2,F3
1090C
1100C          TERMINATION CIRCUIT PARAMETERS
1110           R1=.01
1120           L1=12.E-9            3X10^-7
1130           C1=.015E-6
1140           R2=1.
1150           L2=10.E-9      3X10^-2  ←  10~3
1160C
1170C          TRANSMISSION LINE PARAMETERS
1180           LENGTH =1.
1190           L0=1.97E-7       3.54X10^-9 → C0
1200           C0=2.5E-7        1.32X10^-7 → L0
1210           Z0=SQRT(L0/C0)
1220           VEL=1./SQRT(L0*C0)
1230C
1240C          TRANSMISSION LINE INITIALIZATION
1250           V0=8000.
1260           DO 10 I=1,1000
1270           FPLUS(I)=V0/2.
1280           FMINUS(I)=V0/2.
1290 10        CONTINUE
1300C
1310C          TIME AND INCREMENT SET
1320           PRINT,"NUMBER OF SEGMENTS"
1330           READ,ISEG
1340           PRINT,"OUTPUT EVERY NTH POINT.   N=?"
1350           READ, NN
1360           N=0
1370           PRINT,"MAXIMUM TIME"
1380           READ,TMAX
1390           TO=0.
1400           H=LENGTH/FLOAT(ISEG)/VEL
1410           TN=TO+H
1420C
1430C          INITIALIZE STATE VARIABLES
1440           X10=-V0*C1
1450           X20=0.
1460           X30=0.
1470C
1480C          PRINT HEADING
1490           WRITE(6,1000)
1500 1000      FORMAT(/////,6X,"TIME",9X,"CAP VOLTAGE",5X,"CURRENT 1",7X,"CURR
1510           VC=-X10/C1
1520           WRITE(6,1010) TO,VC,X20,X30
1530 1010      FORMAT(4E16.6)
1540C
1550C
1560C          CALCULATE TRANSMISSION LINE VOLTAGE
1570C          VEND1=VOLTAGE AT DRIVING END
1580C          VEND2=VOLTAGE AT LOAD
```

Good

Laplac

Runge-

```
1590 100     VEND1 = FPLUS(ISEG)+FMINUS(1)
1600         VEND2 = FMINUS(ISEG)+FPLUS(1)
1610C
1620C        CALCULATE CURRENTS IN TERMINATION CIRCUITS
1630C        DRIVING END (1)
1640C        X1=VOLTAGE ACROSS CAPACITOR
1650C        X2=CURRENT THROUGH CAPACITOR
1660         CALL RUKU2(X1N,X2N,X10,X20,F1,F2,TN,TO)
1670C        LOAD END (2)
1680C        X3=CURRENT IN LOAD
1690         CALL RUKU1(X3N,X30,F3,TN,TO)
1700C
1710C        PRINT RESULTS
1720         VC=-X1N/C1
1730         N=N+1
1740         NNN=MOD(N,NN)
1750         IF(NNN .EQ. 0) WRITE(6,1010) TN,VC,X2N,X3N
1760C
1770C        CALCULATE FPLUS AND FMINUS
1780         FINP=FMINUS(1)+Z0*X2N
1790         FINM=FPLUS(1)-Z0*X3N
1800C
1810C        SHIFT TRANSMISSION LINE
1820         DO 200 I=1,ISEG-1
1830         FPLUS(I)=FPLUS(I+1)
1840         FMINUS(I)=FMINUS(I+1)
1850 200     CONTINUE
1860         FPLUS(ISEG)=FINP
1870         FMINUS(ISEG)=FINM
1880C
1890C        ITERATE VOLTAGE, CURRENT, TIME
1900         X10=X1N
1910         X20=X2N
1920         X30=X3N
1930         TO=TN
1940         TN=TO+H
1950C
1960C        CHECK FOR TMAX
1970         IF(TN .LE. TMAX) GO TO 100
1980         STOP
1990         END
2000C
2010         FUNCTION F1(T,X1,X2)
2020         REAL L1,L2
2030         COMMON R1,L1,C1,R2,L2,VEND1,VEND2
2040         F1=X2
2050         RETURN
2060         END
2070         FUNCTION F2(T,X1,X2)
2080         REAL L1,L2
2090         COMMON R1,L1,C1,R2,L2,VEND1,VEND2
2100         F2 = -(X1/C1+R1*X2+VEND1)/L1
2110         RETURN
2120         END
2130         FUNCTION F3(T,X3)
2140         REAL L1,L2
2150         COMMON R1,L1,C1,R2,L2,VEND1,VEND2
2160         F3 = (-R2*X3+VEND2)/L2
2170         RETURN
2180         END
2190         SUBROUTINE RUKU1(WN,WO,F,TN,TO)
2200C        RUNGE-KUTTA FIRST ORDER EQUATION
2210         REAL K1,K2,K3,K4                      K2 = F(TO+H/2.,WO+K1/2.)*H
2220         H = TN-TO
2230         K1 = F(TO,WO)*H
```

```
2250        K3 = F(TO+H/2.,WO+K2/2.)*H
2260        K4 = F(TO+H,WO+K3)*H
2270        WN = WO+(K1+2.*K2+2.*K3+K4)/6.
2280        RETURN
2290        END
2300        SUBROUTINE RUKU2(W1N,W2N,W10,W20,F1,F2,TN,TO)
2310C       RUNGE-KUTTA   SECOND ORDER EQUATION
2320C
2330C       W1N AND W2N ARE THE NEW VALUES TO BE CALCULATED
2340C       W10 AND W20 ARE THE OLD VALUES
2350C       TN=TO+H
2360C       F1 AND F2 ARE THE FUNCTIONS FROM THE DEQ'S
2370C
2380        REAL K11,K12,K13,K14,K21,K22,K23,K24
2390        H=TN-TO
2400        K11 = F1(TO,W10,W20)*H
2410        K21 = F2(TO,W10,W20)*H
2420        K12 = F1(TO+H/2.,W10+K11/2.,W20+K21/2.)*H
2430        K22 = F2(TO+H/2.,W10+K11/2.,W20+K21/2.)*H
2440        K13 = F1(TO+H/2.,W10+K12/2.,W20+K22/2.)*H
2450        K23 = F2(TO+H/2.,W10+K12/2.,W20+K22/2.)*H
2460        K14 = F1(TO+H,W10+K13,W20+K23)*H
2470        K24 = F2(TO+H,W10+K13,W20+K23)*H
2480        W1N = W10 + (K11+2.*K12+2.*K13+K14)/6.
2490        W2N = W20 + (K21+2.*K22+2.*K23+K24)/6.
2500        RETURN
2510        END


*
```

```
1000C          THIS PROGRAM CALCULATES TRANSIENT CURRENTS AND
1010C          VOLTAGES ON A TRANSMISSION LINE USING LAPLACE TRANSFORM.
1020           REAL L1,L2,LENGTH,LO
1030           REAL I,IR,IF,I1,I21,I2,I31,I3,I41,I4
1040C
1050C          TERMINATION CIRCUIT PARAMETERS
1060           R1=.01
1070           L1=12.E-9
1080           C1=.015E-6
1090           R2=1.
1100           L2=10.E-9
1110C
1120C          TRANSMISSION LINE PARAMETERS
1130           LENGTH =1.
1140           LO=1.97E-9
1150           CO=2.5E-7
1160           ZO=SQRT(LO/CO)
1170           VEL=1./SQRT(LO*CO)
1180           TREF = LENGTH/VEL*2.
1190C
1200C          TRANSMISSION LINE INITIALIZATION
1210           VO=8000.
1220C
1230C          TIME AND INCREMENT SET
1240           PRINT,"NUMBER OF SEGMENTS".
1250           READ,ISEG
1260           PRINT,"OUTPUT EVERY NTH POINT.  N=?"
1270           READ, NN
1290           PRINT,"MAXIMUM TIME"
1300           READ,TMAX
1310           T = 0.
1320           H=LENGTH/FLOAT(ISEG)/VEL
1330C          CALCULATES RISE  AND FALL WAVEFORMS
1340 100           IR = VO/(R2+ZO)*(1.-EXP(-(R2+ZO)/L2*T))
1350           I=IR
1360           IF(T .LT. TREF) GO TO 400
1370           T=T-TREF
1380           A1=(R1-ZO)/L1
1390           AO=1./L1/C1
1400           C=(R2+ZO)/L2
1410           B=(R1+ZO)/2./L1
1420           W=SQRT(1./L1/C1-(R1+ZO)**2/(4.*L1*L1))
1460           D1=B*B+W*W
1470           D2=(B-C)*(B-C)+W*W
1475           D3=(B-C)*(B-C)-W*W
1480           I1 = AO/(C*C*D1)*(1.-EXP(-B*T)*(COS(W*T)+B/W*SIN(W*T)))
1490           I21 = (1.-AO/(C*C))/D2
1500           I2 = I21*(EXP(-C*T)-EXP(-B*T)*(COS(W*T)+(B-C)/W*SIN(W*T)))
1510           I31 = (C-A1+AO/C)*2.*(B-C)/(D2*D2)
1520           I3 = I31*(EXP(-C*T)-EXP(-B*T)*(COS(W*T)+D3/(2.*W*(B-C))*SIN(W*
1530           I4 = -(C-A1+AO/C)/D2*T*EXP(-C*T)
1540           IF=-2.*VO*ZO/(L2*L2)*(I1+I2+I3+I4)
1550           T=T+TREF
1560           I=I+IF
1590 400       WRITE(6,1000) T,I,IR,IF
1600 1000      FORMAT(4E16.6)
1610           T = T+H*NN
1620           IF(T .GT. TMAX) STOP
1630           GO TO 100
```

```
1000C               THIS PROGRAM CALCULATES TRANSIENT CURRENTS AND
1010C               VOLTAGES ON A TRANSMISSION LINE.
1020C               MOD 1.0
1030C
1040C               INITIALIZATION
1050                DIMENSION FPLUS(1000),FMINUS(1000)
1060                REAL L1,L2,LENGTH,LO
1070                COMMON R1,L1,C1,R2,L2,VEND1,VEND2
1080                EXTERNAL F1,F2,F3
1090C
1100C               TERMINATION CIRCUIT PARAMETERS
1110                R1=.01
1120                L1=3.E-7
1130                C1=.015E-6
1140                R2=1.
1150                L2=20.E-9
1160C
1170C               TRANSMISSION LINE PARAMETERS
1180                LENGTH =1.
1190                LO=1.32E-7
1200                CO=3.53E-9
1210                ZO=SQRT(LO/CO)
1220                VEL=1./SQRT(LO*CO)
1230C
1240C               TRANSMISSION LINE INITIALIZATION
1250                VO=8000.
1260                DO 10 I=1,1000
1270                FPLUS(I)=VO/2.
1280                FMINUS(I)=VO/2.
1290 10             CONTINUE
1300C
1310C               TIME AND INCREMENT SET
1320                PRINT,"NUMBER OF SEGMENTS"
1330                READ,ISEG
1340                PRINT,"OUTPUT EVERY NTH POINT.   N=?"
1350                READ, NN
1360                N=0
1370                PRINT,"MAXIMUM TIME"
1380                READ,TMAX
1390                TO=0.
1400                H=LENGTH/FLOAT(ISEG)/VEL
1410                TN=TO+H
1420C
1430C               INITIALIZE STATE VARIABLES
1440                X10=-VO*C1
1450                X20=0.
1460                X30=0.
1470C
1480C               PRINT HEADING
1490                WRITE(6,1000)
1500 1000          FORMAT(/////,6X,"TIME",9X,"CAP VOLTAGE",5X,"CURRENT 1",7X,"CURREN'
1510                VC=-X10/C1
1520                WRITE(6,1010) TO,VC,X20,X30
1530 1010          FORMAT(4E16.6)
1540C
1550C
1560C               CALCULATE TRANSMISSION LINE VOLTAGE
1570C               VEND1=VOLTAGE AT DRIVING END
1580C               VEND2=VOLTAGE AT LOAD
1590 100           VEND1 = FPLUS(ISEG)+FMINUS(1)
```

```
1600          VEND2 = FMINUS(ISEG)+FPLUS(1)
1610C
1620C        CALCULATE CURRENTS IN TERMINATION CIRCUITS
1630C        DRIVING END (1)
1640C        X1=VOLTAGE ACROSS CAPACITOR
1650C        X2=CURRENT THROUGH CAPACITOR
1660          CALL RUKU2(X1N,X2N,X10,X20,F1,F2,TN,TO)
1670C        LOAD END (2)
1680C        X3=CURRENT IN LOAD
1690          CALL RUKU1(X3N,X30,F3,TN,TO)
1700C
1710C        PRINT RESULTS
1720          VC=-X1N/C1
1730          N=N+1
1740          NNN=MOD(N,NN)
1750          IF(NNN .EQ. 0) WRITE(6,1010) TN,VC,X2N,X3N
1760C
1770C        CALCULATE FPLUS AND FMINUS
1780          FINP=FMINUS(1)+Z0*X2N
1790          FINM=FPLUS(1)-Z0*X3N
1800C
1810C        SHIFT TRANSMISSION LINE
1820          DO 200 I=1,ISEG-1
1830          FPLUS(I)=FPLUS(I+1)
1840          FMINUS(I)=FMINUS(I+1)
1850 200      CONTINUE
1860          FPLUS(ISEG)=FINP
1870          FMINUS(ISEG)=FINM
1880C
1890C        ITERATE VOLTAGE, CURRENT, TIME
1900          X10=X1N
1910          X20=X2N
1920          X30=X3N
1930          TO=TN
1940          TN=TO+H
1950C
1960C        CHECK FOR TMAX
1970          IF(TN .LE. TMAX) GO TO 100
1980          STOP
1990          END
2000C
2010          FUNCTION F1(T,X1,X2)
2020          REAL L1,L2
2030          COMMON R1,L1,C1,R2,L2,VEND1,VEND2
2040          F1=X2
2050          RETURN
2060          END
2070          FUNCTION F2(T,X1,X2)
2080          REAL L1,L2
2090          COMMON R1,L1,C1,R2,L2,VEND1,VEND2
2100          F2 = -(X1/C1+R1*X2+VEND1)/L1
2110          RETURN
2120          END
2130          FUNCTION F3(T,X3)
2140          REAL L1,L2
2150          COMMON R1,L1,C1,R2,L2,VEND1,VEND2
2160          F3 = (-R2*X3+VEND2)/L2
2170          RETURN
2180          END
2190          SUBROUTINE RUKU1(WN,WO,F,TN,TO)
2200C        RUNGE-KUTTA FIRST ORDER EQUATION
2210          REAL K1,K2,K3,K4
2220          H = TN-TO          2250          K3 = F(TO+H/2.,WO+K2/2.)*H
2230          K1 = F(TO,WO)*H
2240          K2 = F(TO+H/2.,WO+K1/2.)*H
```

```
2260        K4 = F(TO+H,WO+K3)*H
2270        WN = WO+(K1+2.*K2+2.*K3+K4)/6.
2280        RETURN
2290        END
2300        SUBROUTINE RUKU2(W1N,W2N,W1O,W2O,F1,F2,TN,TO)
2310C       RUNGE-KUTTA  SECOND ORDER EQUATION
2320C
2330C       W1N AND W2N ARE THE NEW VALUES TO BE CALCULATED
2340C       W1O AND W2O ARE THE OLD VALUES
2350C       TN=TO+H
2360C       F1 AND F2 ARE THE FUNCTIONS FROM THE DEQ'S
2370C
2380        REAL K11,K12,K13,K14,K21,K22,K23,K24
2390        H=TN-TO
2400        K11 = F1(TO,W1O,W2O)*H
2410        K21 = F2(TO,W1O,W2O)*H
2420        K12 = F1(TO+H/2.,W1O+K11/2.,W2O+K21/2.)*H
2430        K22 = F2(TO+H/2.,W1O+K11/2.,W2O+K21/2.)*H
2440        K13 = F1(TO+H/2.,W1O+K12/2.,W2O+K22/2.)*H
2450        K23 = F2(TO+H/2.,W1O+K12/2.,W2O+K22/2.)*H
2460        K14 = F1(TO+H,W1O+K13,W2O+K23)*H
2470        K24 = F2(TO+H,W1O+K13,W2O+K23)*H
2480        W1N = W1O + (K11+2.*K12+2.*K13+K14)/6.
2490        W2N = W2O + (K21+2.*K22+2.*K23+K24)/6.
2500        RETURN
2510        END
```

```
RUN
NUMBER OF SEGMENTS
=50
OUTPUT EVERY NTH POINT.   N=?
=10
MAXIMUM TIME
=1E-6
```

TIME	CAP VOLTAGE	CURRENT 1	CURRENT 2
0.	0.800000E 04	0.	0.
0.431722E-08	0.800000E 04	0.	0.908018E 03
0.863444E-08	0.800000E 04	0.	0.108274E 04
0.129517E-07	0.800000E 04	0.	0.111637E 04
0.172689E-07	0.800000E 04	0.	0.112284E 04
0.215861E-07	0.800000E 04	0.	0.112408E 04
0.259033E-07	0.798936E 04	0.978313E 02	0.112432E 04
0.302206E-07	0.793798E 04	0.261540E 03	0.112437E 04
0.345378E-07	0.783899E 04	0.424684E 03	0.112438E 04
0.388550E-07	0.769478E 04	0.575076E 03	0.112438E 04
0.431722E-07	0.750936E 04	0.710967E 03	0.112438E 04
0.474894E-07	0.728689E 04	0.832618E 03	0.249667E 03
0.518067E-07	0.703139E 04	0.940667E 03	-0.208696E 03
0.561239E-07	0.674666E 04	0.103582E 04	-0.163239E 03
0.604411E-07	0.643631E 04	0.111879E 04	0.428408E 02
0.647583E-07	0.610375E 04	0.119028E 04	0.275052E 03
0.690756E-07	0.574779E 04	0.127562E 04	0.495173E 03
0.733928E-07	0.537967E 04	0.126851E 04	0.694294E 03
0.777100E-07	0.502189E 04	0.121527E 04	0.871215E 03
0.820272E-07	0.467998E 04	0.116245E 04	0.102661E 04
0.863444E-07	0.435134E 04	0.112386E 04	0.116156E 04
0.906617E-07	0.403154E 04	0.110089E 04	0.114273E 04
0.949789E-07	0.371632E 04	0.109157E 04	0.187046E 04
0.992961E-07	0.340213E 04	0.109331E 04	0.223304E 04
0.103613E-06	0.308615E 04	0.110358E 04	0.219669E 04
0.107931E-06	0.276628E 04	0.112005E 04	0.200475E 04
0.112248E-06	0.243967E 04	0.113795E 04	0.178991E 04
0.116565E-06	0.211358E 04	0.113638E 04	0.159814E 04
0.120882E-06	0.177939E 04	0.119392E 04	0.143990E 04
0.125199E-06	0.142406E 04	0.127543E 04	0.131429E 04
0.129517E-06	0.104646E 04	0.134489E 04	0.121740E 04
0.133834E-06	0.652320E 03	0.138960E 04	0.124738E 04
0.138151E-06	0.249001E 03	0.140910E 04	0.123690E 04
0.142468E-06	-0.156717E 03	0.140697E 04	0.763430E 03
0.146786E-06	-0.559220E 03	0.138746E 04	0.546377E 03
0.151103E-06	-0.954090E 03	0.135453E 04	0.632379E 03
0.155420E-06	-0.133801E 04	0.130281E 04	0.840985E 03
0.159737E-06	-0.170636E 04	0.126528E 04	0.105076E 04
0.164054E-06	-0.206648E 04	0.123066E 04	0.121457E 04
0.168372E-06	-0.241028E 04	0.115224E 04	0.132307E 04
0.172689E-06	-0.272788E 04	0.105428E 04	0.138077E 04
0.177006E-06	-0.301803E 04	0.964620E 03	0.151735E 04
0.181323E-06	-0.328501E 04	0.893927E 03	0.124178E 04
0.185641E-06	-0.353439E 04	0.841744E 03	0.119673E 04
0.189958E-06	-0.377089E 04	0.803541E 03	0.144443E 04
0.194275E-06	-0.399779E 04	0.774221E 03	0.150820E 04
0.198592E-06	-0.421661E 04	0.742736E 03	0.133706E 04
0.202909E-06	-0.442946E 04	0.736744E 03	0.106663E 04
0.207227E-06	-0.463668E 04	0.696963E 03	0.803156E 03
0.211544E-06	-0.483019E 04	0.651247E 03	0.590860E 03

RUN
NUMBER OF SEGMENTS
=50
OUTPUT EVERY NTH POINT.   N=?
=2
MAXIMUM TIME
=1E-6

TIME	CAP VOLTAGE	CURRENT 1	CURRENT 2
0.	0.800000E 04	0.	0.
0.863444E-09	0.800000E 04	0.	0.315719E 03
0.172689E-08	0.800000E 04	0.	0.542787E 03
0.259033E-08	0.800000E 04	0.	0.706094E 03
0.345378E-08	0.800000E 04	0.	0.823546E 03
0.431722E-08	0.800000E 04	0.	0.908018E 03
0.518067E-08	0.800000E 04	0.	0.968771E 03
0.604411E-08	0.800000E 04	0.	0.101246E 04
0.690755E-08	0.800000E 04	0.	0.104389E 04
0.777100E-08	0.800000E 04	0.	0.106649E 04
0.863444E-08	0.800000E 04	0.	0.108274E 04
0.949789E-08	0.800000E 04	0.	0.109444E 04
0.103613E-07	0.800000E 04	0.	0.110284E 04
0.112248E-07	0.800000E 04	0.	0.110889E 04
0.120882E-07	0.800000E 04	0.	0.111324E 04
0.129517E-07	0.800000E 04	0.	0.111637E 04
0.138151E-07	0.800000E 04	0.	0.111862E 04
0.146786E-07	0.800000E 04	0.	0.112023E 04
0.155420E-07	0.800000E 04	0.	0.112140E 04
0.164054E-07	0.800000E 04	0.	0.112223E 04
0.172689E-07	0.800000E 04	0.	0.112284E 04
0.181323E-07	0.800000E 04	0.	0.112327E 04
0.189958E-07	0.800000E 04	0.	0.112358E 04
0.198592E-07	0.800000E 04	0.	0.112380E 04
0.207227E-07	0.800000E 04	0.	0.112397E 04
0.215861E-07	0.800000E 04	0.	0.112408E 04
0.224496E-07	0.799987E 04	0.577169E 01	0.112416E 04
0.233130E-07	0.799913E 04	0.208846E 02	0.112422E 04
0.241764E-07	0.799733E 04	0.425205E 02	0.112427E 04
0.250399E-07	0.799414E 04	0.686543E 02	0.112430E 04
0.259033E-07	0.798936E 04	0.978313E 02	0.112432E 04
0.267668E-07	0.798284E 04	0.129007E 03	0.112434E 04
0.276302E-07	0.797448E 04	0.161431E 03	0.112435E 04
0.284937E-07	0.796424E 04	0.194566E 03	0.112436E 04
0.293571E-07	0.795207E 04	0.228028E 03	0.112436E 04
0.302206E-07	0.793798E 04	0.261540E 03	0.112437E 04
0.310840E-07	0.792197E 04	0.294908E 03	0.112437E 04
0.319474E-07	0.790404E 04	0.327991E 03	0.112437E 04
0.328109E-07	0.788421E 04	0.360690E 03	0.112437E 04
0.336743E-07	0.786252E 04	0.392938E 03	0.112438E 04
0.345378E-07	0.783899E 04	0.424684E 03	0.112438E 04
0.354012E-07	0.781364E 04	0.455897E 03	0.112438E 04
0.362647E-07	0.778651E 04	0.486554E 03	0.112438E 04
0.371281E-07	0.775764E 04	0.516641E 03	0.112438E 04
0.379916E-07	0.772705E 04	0.546150E 03	0.112438E 04
0.388550E-07	0.769478E 04	0.575076E 03	0.112438E 04
0.397184E-07	0.766085E 04	0.603417E 03	0.112438E 04
0.405819E-07	0.762532E 04	0.631174E 03	0.112438E 04
0.414453E-07	0.758820E 04	0.658350E 03	0.112438E 04
0.423088E-07	0.754954E 04	0.684946E 03	0.112438E 04

0.431722E-07	0.750936E 04	0.710967E 03	0.112438E 04
0.440357E-07	0.746770E 04	0.736418E 03	0.104304E 04
0.448991E-07	0.742459E 04	0.761304E 03	0.860538E 03
0.457626E-07	0.738006E 04	0.785629E 03	0.645344E 03
0.466260E-07	0.733416E 04	0.809398E 03	0.435354E 03
0.474894E-07	0.728689E 04	0.832618E 03	0.249667E 03
0.483529E-07	0.723831E 04	0.855294E 03	0.961554E 02
0.492163E-07	0.718844E 04	0.877431E 03	-0.237389E 02
0.500798E-07	0.713731E 04	0.899035E 03	-0.112010E 03
0.509432E-07	0.708495E 04	0.920112E 03	-0.172274E 03
0.518067E-07	0.703139E 04	0.940667E 03	-0.208696E 03
0.526701E-07	0.697666E 04	0.960707E 03	-0.225401E 03
0.535336E-07	0.692080E 04	0.980236E 03	-0.226163E 03
0.543970E-07	0.686382E 04	0.999262E 03	-0.214279E 03
0.552604E-07	0.680577E 04	0.101779E 04	-0.192536E 03
0.561239E-07	0.674666E 04	0.103582E 04	-0.163239E 03
0.569873E-07	0.668653E 04	0.105337E 04	-0.128259E 03
0.578508E-07	0.662540E 04	0.107043E 04	-0.890956E 02
0.587142E-07	0.656330E 04	0.108702E 04	-0.469375E 02
0.595777E-07	0.650026E 04	0.110314E 04	-0.271671E 01
0.604411E-07	0.643631E 04	0.111879E 04	0.428408E 02
0.613046E-07	0.637147E 04	0.113399E 04	0.891741E 02
0.621680E-07	0.630577E 04	0.114873E 04	0.135853E 03
0.630314E-07	0.623923E 04	0.116302E 04	0.182547E 03
0.638949E-07	0.617189E 04	0.117687E 04	0.229010E 03
0.647583E-07	0.610375E 04	0.119028E 04	0.275052E 03
0.656218E-07	0.603476E 04	0.120785E 04	0.320535E 03
0.664852E-07	0.596462E 04	0.122916E 04	0.365354E 03
0.673487E-07	0.589328E 04	0.124896E 04	0.409434E 03
0.682121E-07	0.582092E 04	0.126474E 04	0.452720E 03
0.690756E-07	0.574779E 04	0.127562E 04	0.495173E 03
0.699390E-07	0.567417E 04	0.128161E 04	0.536767E 03
0.708024E-07	0.560033E 04	0.128320E 04	0.577484E 03
0.716659E-07	0.552652E 04	0.128107E 04	0.617313E 03
0.725293E-07	0.545291E 04	0.127594E 04	0.656250E 03
0.733928E-07	0.537967E 04	0.126851E 04	0.694294E 03
0.742562E-07	0.530691E 04	0.125939E 04	0.731444E 03
0.751197E-07	0.523471E 04	0.124912E 04	0.767706E 03
0.759831E-07	0.516312E 04	0.123811E 04	0.803084E 03
0.768466E-07	0.509218E 04	0.122674E 04	0.837584E 03
0.777100E-07	0.502189E 04	0.121527E 04	0.871215E 03
0.785734E-07	0.495227E 04	0.120392E 04	0.903983E 03
0.794369E-07	0.488328E 04	0.119286E 04	0.935898E 03
0.803003E-07	0.481493E 04	0.118220E 04	0.966967E 03
0.811638E-07	0.474717E 04	0.117205E 04	0.997201E 03
0.820272E-07	0.467998E 04	0.116245E 04	0.102661E 04
0.828907E-07	0.461333E 04	0.115346E 04	0.105520E 04
0.837541E-07	0.454717E 04	0.114510E 04	0.108298E 04
0.846176E-07	0.448148E 04	0.113737E 04	0.110996E 04
0.854810E-07	0.441622E 04	0.113030E 04	0.113615E 04
0.863444E-07	0.435134E 04	0.112386E 04	0.116156E 04

```
RUN
NUMBER OF SEGMENTS
=50
OUTPUT EVERY NTH POINT.  N=?
=100
MAXIMUM TIME
=1E-4
```

TIME	CAP VOLTAGE	CURRENT 1	CURRENT 2
0.	0.800000E 04	0.	0.
0.431722E-07	0.750936E 04	0.710967E 03	0.112438E 04
0.863444E-07	0.435134E 04	0.112386E 04	0.116156E 04
0.129517E-06	0.104646E 04	0.134489E 04	0.121740E 04
0.172689E-06	-0.272788E 04	0.105428E 04	0.138077E 04
0.215861E-06	-0.501412E 04	0.630366E 03	0.436748E 03
0.259033E-06	-0.610572E 04	0.173694E 02	0.303261E 03
0.302206E-06	-0.530489E 04	-0.462119E 03	-0.657417E 03
0.345378E-06	-0.339236E 04	-0.891772E 03	-0.774774E 03
0.388550E-06	-0.675616E 03	-0.919987E 03	-0.103161E 04
0.431722E-06	0.184440E 04	-0.817010E 03	-0.817310E 03
0.474894E-06	0.371878E 04	-0.435795E 03	-0.586612E 03
0.518066E-06	0.440342E 04	-0.485256E 02	0.508070E 02
0.561238E-06	0.393328E 04	0.364326E 03	0.266137E 03
0.604410E-06	0.248113E 04	0.606922E 03	0.653429E 03
0.647582E-06	0.552961E 03	0.706238E 03	0.718615E 03
0.690754E-06	-0.133428E 04	0.578777E 03	0.659834E 03
0.733926E-06	-0.268733E 04	0.346371E 03	0.347499E 03
0.777098E-06	-0.322447E 04	0.249725E 02	0.506553E 02
0.820269E-06	-0.288225E 04	-0.256102E 03	-0.261027E 03
0.863441E-06	-0.183783E 04	-0.452304E 03	-0.425414E 03
0.906613E-06	-0.428893E 03	-0.504323E 03	-0.540234E 03
0.949785E-06	0.951652E 03	-0.431084E 03	-0.470947E 03
0.992957E-06	0.195074E 04	-0.249266E 03	-0.284708E 03
0.103613E-05	0.235421E 04	-0.265587E 02	-0.354533E 02
0.107930E-05	0.211492E 04	0.184854E 03	0.185394E 03
0.112248E-05	0.136027E 04	0.324996E 03	0.341220E 03
0.116565E-05	0.331883E 03	0.369542E 03	0.380553E 03
0.120882E-05	-0.678159E 03	0.315438E 03	0.327674E 03
0.125199E-05	-0.141614E 04	0.187355E 03	0.202029E 03
0.129517E-05	-0.171844E 04	0.226744E 02	0.428442E 02
0.133834E-05	-0.155246E 04	-0.131272E 03	-0.118309E 03
0.138151E-05	-0.100582E 04	-0.236718E 03	-0.242399E 03
0.142468E-05	-0.256851E 03	-0.270981E 03	-0.291210E 03
0.146786E-05	0.483879E 03	-0.232639E 03	-0.253294E 03
0.151103E-05	0.102730E 04	-0.138782E 03	-0.153210E 03
0.155420E-05	0.125476E 04	-0.188232E 02	-0.249613E 02
0.159737E-05	0.113897E 04	0.941045E 02	0.969816E 02
0.164055E-05	0.743902E 03	0.172023E 03	0.180413E 03
0.168372E-05	0.197828E 03	0.198513E 03	0.207176E 03
0.172689E-05	-0.344643E 03	0.171599E 03	0.176949E 03
0.177006E-05	-0.745406E 03	0.103120E 03	0.106653E 03
0.181324E-05	-0.915970E 03	0.150277E 02	0.194513E 02
0.185641E-05	-0.835694E 03	-0.680381E 02	-0.625212E 02
0.189958E-05	-0.549891E 03	-0.125334E 03	-0.121785E 03
0.194275E-05	-0.151980E 03	-0.144995E 03	-0.146722E 03
0.198593E-05	0.245346E 03	-0.125759E 03	-0.134071E 03
0.202910E-05	0.540640E 03	-0.763631E 02	-0.880157E 02
0.207227E-05	0.668592E 03	-0.123134E 02	-

END

DATE
FILMED

5 83

DTI